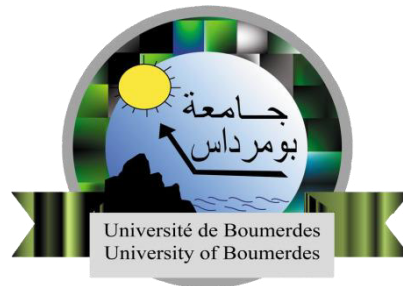
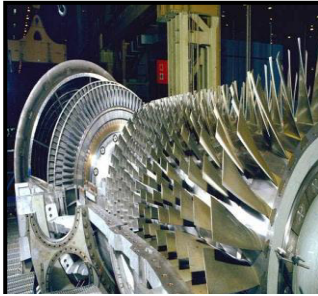


People's Democratic Republic of Algeria
Ministry of High Education and Scientific Research
University M'hamed Bougarra of Boumerdes

Faculty of Engineering

Department Of Industrial Maintenance

Engines' Dynamics and Vibroacoustics Laboratory



In Partial Fulfillment
of the Requirements for the Degree
Master in Mechanics and Systems Engineering

TOPIC

Effect of the compressor cooling on the blades mechanical strength

Realized by:

- **IBEN EL BOUSHAKI ZAKARIA**
- **BERCHACHE MOUAD**

Supervised by:

Mrs : F.BRAHIMI

2016/2017

Abstract

In this work, we will address to the study of the air flow simulation over a compressor blade and measuring the forces acting on them, so to analyze the Aerodynamic flow over the blade, computational fluid dynamics (CFD) is a powerful method for this simulation.

The flow around the compressor blade is studied and analyzed using three types of Materials (Steel, Titanium Alloy, Aluminum Alloy) with the profile NACA 65-10%, the same operating conditions are applied to compute the performance parameters ,i.e. Static pressure, Velocity and the aerodynamic coefficients which are the Lift and the drag, after that we conclude the forces according to these two parameters (Lift and Drag). Then we will address to study the effect of the aerodynamic forces which are by the air flow on the blade surface and its influence on the Von Mises stress and the total deformation to see which of these three materials is better for operating and more powerful and resistant than the two others while the forces are acting on them.

الملخص:

في هذا العمل، سوف نقوم بدراسة محاكاة تدفق الهواء على شفرة الضاغط و حساب القوى المؤثرة عليها، و لتحليل تدفق الهواء على الشفرة، ديناميات السوائل الحسابية هو وسيلة قوية لهذه المحاكاة.

تم دراسة وتحليل التدفق حول شفرة الضاغط وتحليلها باستخدام ثلاثة أنواع من المواد (الصلب وسبائك التيتانيوم وسبائك الألومنيوم) مع ناكا 65-10٪، يتم تطبيق نفس الظروف قصد استخراج عدة معايير ، أي ضغط ثابت، سرعة والمعاملات الهوائية التي هي رفع والسحب، وبعد ذلك نستنتج القوى وفقاً لهذين المعلمين (رفع وسحب). ثم سنقوم بدراسة تأثير القوى الهوائية التي هي عن طريق تدفق الهواء على سطح الشفرة وتأثيره على الإجهاد وتشوه الكلي لمعرفة أي من هذه المواد الثلاثة هو أفضل للتشغيل وأكثر قوة ومقاومة من الاثنين الآخرين.

Résumé

Dans ce travail, nous aborderons l'étude de la simulation de flux d'air sur une lame de mélangeur et de mesurer les forces qui agissent sur elles, afin d'analyser le flux aérodynamique sur la lame, la dynamique de fluide computationnelle (CFD) est une méthode puissante pour cette simulation.

Le flux autour de la lame du compresseur est étudié et analysé en utilisant trois types de matériaux (acier, alliage de titane, alliage d'aluminium) avec le profil NACA 65-10%, les mêmes conditions d'utilisation sont appliquées pour calculer les paramètres de performance, pour savoir la pression statique, la vitesse et les coefficients aérodynamiques qui sont l'Ascenseur et la traînée, après que nous concluons les forces selon ces deux paramètres (Ascenseur et la traînée). Ensuite, nous allons aborder pour étudier l'effet des forces aérodynamiques qui sont par le flux d'air sur la surface du lame et son influence sur le stress de Von Mises et la déformation totale pour voir lequel de ces trois matériaux est meilleur pour fonctionner et plus puissant et résistant que les deux autres pendant que les forces agissent sur eux.

Acknowledgements

This work has been done at Algeria airline company Workshop.

First of all we thank God almighty the most merciful for giving us the will, the patient and the courage to do this research.

Then we are grateful for the consistent guidance of our advisor **M. F.BRAHIMI** for giving us the possibility to do this research, who made also this experience enjoyable as well as challenging.

We express our sincere thanks to all the member of the aircraft maintenance and “El hadj” and Mr Azzeddine from workshop (H400) for all their support and helping us.

Above all we would like to thank our families for helping us and living with us each moment of insomnia we had and each difficulty helping us with the best they could.

We also want to extend our deepest gratitude to all the staff of the Laboratory LMDV (Dynamics motors and vibro-acoustics), president head of our Master’s studies, Professor **Abdelkader NOUR** and all the doctors for their support; it was a pleasure to work with them during all these years.

Finally we wish to thank all those who supported us and helped us to make this work especially my friends and colleagues on mechanics and engineering systems.

Summary

Abstract	II
List of figures	IV
List of tables	V
Nomenclature	VI
General Introduction	2

Chapter I: Presentation of CFM

I. INTRODUCTION

II. Types of jet engines	5
II.1 Turbojet	5
II.2 Turbofan	6
II.3 Ramjet.....	6
II.4 Scramjet	7
III. CFM evolution	7
IV. Components of CFM65.....	10
IV.1 Air intake (inlet/Fan).....	10
IV.2 COMPRESSOR (low pressure and high pressure compressor).....	10
IV.3 COMBUSTER (combustion chambers)	10
IV.4 TURBINE (low and high pressure)	11
IV.5 Nozzle and Exhaust.....	11
VI. Working Principal of the Turbojet	11
VI. Aircraft Engines requirements	14
VI.1 Fuel Economy	14
VI.2 Durability and Reliability.....	14
VI.3 Operating Flexibility	14
VI.4 Compactness	15
VI.5 Power plant selection	15

Chapter II: Overview on Compressors, Fluid and Blades

Introduction:	17
I. Compressor types.....	17
I.1 Centrifugal compressor.....	17
I.2. Axial compressor	20
II. Compressor flow modeling :	21
III. The basic equations of conservation	21
III.1 Mass conservation	21
III.2 Newton's second law or Navier-Stokes Equations	22
III.3 Energy equation.....	22
III.4 Ideal gas law.....	23
IV. Axial compressor blades	23
IV.1. Blades geometry.....	24
IV.2. Blades manufacturing process:	25
IV.3 Properties of Blades Materials:	26
V. Aerodynamic Forces:	27
VI. Compressor blades cooling	30
VI.1 Cooling techniques.....	30
VI.1.1 Forced internal convection.....	30
VI.1.2 Film-cooling:.....	31
VI.1.3 Impact of jets:.....	32
VI.1.4 Couplings of cooling methods :	32
VI.2 Film Cooling:	33
Conclusion :	34

Chapter III: Numerical simulation

Introduction:	40
I. The Gambit software:	40
II. Geometry Model:.....	40
The profile used is: NACA 65-10% - airfoil.....	40
II.1 First step: Isolated compressor blade:	41
II.2 Second step: The fluid domain	41
III. Fluent simulation software:	42
III.1 2D simulation:	42
III.1.1 first step Meshing the Geometry:	42
III.1.2 Flow properties:.....	43
III.1.3 Boundary conditions:	44
III.2 Calculation of drag and lift forces:.....	44
IV.3D Part:	47
IV.1 SOLIDWORKS Software:	47
IV.2 Static structure ANSYS Analysis:	47
IV.3 Structural steel Analysis:	48
V. The different effects on Blade Materials	49
V.1 The number of holes effect.....	49
V.2 The diameter of holes effect:.....	54
V.3. The Position of the holes effect:.....	57
V.4 The effect of the blade materials:	60
Conclusion:.....	69

List of figures

Chapter I

Figure I.1 Turbojet Engine	3
Figure I.2 Turbofan Engine.....	3
Figure I.3 Ramjet engine.....	4
Figure I.4 Scramjet engine.....	4
Figure I.5 CFM56 core.....	5
Figure I.6 CFM56 Evolution	6
Figure I.7 CFM56-7B.	6
Figure I.8 Components of Jet engine	7
Figure I.9 A comparison between the working cycle of a turbojet engine and a piston engine.....	9
Figure I.10 Working cycle on a pressure volume and enthalpy temperature diagrams.....	9
Figure I.11 Airflow through (a) divergent duct and (b) convergent duct.	10

Chapter II

Figure II.1 Main types of gas compressors	13
Figure II.2 Centrifugal compressor	14
Figure II.3 Centrifugal compressor working principle.....	14
Figure II.4 Axial compressor	15
Figure II.5 Working principle of axial flow compressor	15
Figure II.6 Axial compressor Blades.....	18
Figure II.7 Blade Geometry.	19
Figure II.8 Compressor Blades (NACA 65 series).	19
Figure II.9 Blade Forging Method.	20
Figure II.10 Airflow around and airfoil	22

List of figures

Figure II.11 Forces acting on an airfoil.	22
Figure II.12 Forces Applied on the upper and lower surfaces of a body.	23
Figure II.13 Forced internal convection cooling.....	25
Figure II.14 Film Cooling.....	25
Figure II.15 Jet impact cooling	26
Figure II.16 Representation of a blade and its cooling systems.....	26
Figure II.17 Coolant mass flow rate effect on the Ambient temperature.....	27
Figure II.18 (a) Idealized two-dimensional film cooling; (b) typical film cooled turbine inlet guide vane. 28	

Chapter III

Figure III.1 Blade structure with the coordinates.....	30
Figure III.2 Blade geometry	30
Figure III.3 Fluid zone surface without the blade surface.....	31
Figure III.4 Meshed Geometry.	32
Figure III.5 Scaled residuals.....	34
Figure III.6 Pressure coefficient around the profile.	34
Figure III.7 Pressure contour.	35
Figure III.8 Pressure contour of the Airfoil wall.	35
Figure III.9 Velocity contour.	36
Figure III.10 Importing the geometry of the profile.	37
Figure III.11 Meshing the profile.	37
Figure III.12 The fixed support and the force applied.	38
Figure III.13 Total deformation for different number of holes.	40
Figure III.14 Total deformation for number of holes on the blade.....	40
Figure III.15 Equivalent Von-Mises stress for Different number of holes..	42
Figure III.16 Equivalent Von Mises stress for number of holes on the blade..	42
Figure III.17 Total deformation for different Diameters of holes.....	44

List of figures

Figure III.18 Total Deformation for holes diameter..	44
Figure III.19 Equivalent Von-Mises stress For different diameters of hole.....	45
Figure III.20 Equivalent Von Mises Stress for holes diameter.....	46
Figure III.21 Total deformation for the different position of the holes.....	47
Figure III.22 Total Deformation for holes position on the blade.....	47
Figure III.23 Equivalent Von Mises stress for the different position of Holes.....	48
Figure III.24 Equivalent Von Mises Stress for holes position on the blade..	49
Figure III.25 Total deformation of the three materials Without Holes.....	50
Figure III.26 Total deformation of the three materials Without Holes.....	51
Figure III.27 Equivalent Von Mises Stress of the Three Materials Without holes.....	52
Figure III.28 Equivalent Von Mises Stress for the materials Without Holes.....	52
Figure III.29 Total deformation of the three Materials With holes.....	52
Figure III.30 Equivalent Stress of the three Materials With holes.....	53
Figure III.31 Total deformation with and without the holes for the steel ..	54
Figure III.32 Deformation for different number of holes of the structural steel.....	54
Figure III.33 Total deformation with and without holes for the Aluminum Alloy.....	55
Figure III.34 Maximum deformation for different number of holes for the Aluminum Alloy..	55
Figure III.35 Total deformation with and without holes for the Titanium Alloy..	56
Figure III.36 Maximum deformation for different number of holes of the Titanium Alloy.....	56
Figure III.37 Equivalent Von Mises Stress of the Steel.....	57
Figure III.38 Equivalent Von Mises Stress of the Steel with five holes..	57
Figure III.39 Equivalent Von Mises Stress of the Aluminum Alloy without holes.....	57
Figure III.40 Equivalent Von Mises Stress of the Aluminum Alloy with five holes..	58
Figure III.41 Equivalent Von Mises Stress of the Titanium Alloy without holes..	58
Figure III.42 Equivalent Von Mises Stress of the Titanium Alloy with five holes..	58
Figure III.43 Equivalent Von Mises Stress for different number of holes for eachMaterial.	59

List of Tables

Chapter II

Table II.1: Mach number regimes and compressibility effect.....	16
--	----

Chapter III

Table III.1: Mesh Information	32
Table III.2: Names of the Edges of the Geometry.	32
Table III.3: Boundary conditions of the geometry.	33
Table III.4: Input and output conditions for the simulation.....	33
Table III.5: Modal analysis boundary condition of the structural steel.....	37
Table III.6: The three materials properties.....	38
Table III. Results of stress, deformation with different number of holes.	39
Table III.8: Results of stress, deformation with different Diameter of holes.....	43
Table III.9: Results of stress, deformation with different position of holes.	46
Table III.10: Results of stress, deformation with different Materials.....	49

Nomenclature

Nomenclature

A :	Axial force in 2D	[N]
A_l :	Axial lower force in 2D	[N]
A_u :	Axial upper force in 2D	[N]
c :	Chord line	[m]
C_p :	Pressure coefficient	
C_l :	Lift coefficient in 2D	
C_d :	Drag coefficient in 2D	
C_n :	Normal force coefficient in 2D	
C_a :	Axial force coefficient in 2D	
C_m :	Moment coefficient in 2D	
C_L :	Lift coefficient in 3D	
C_D :	Drag coefficient in 3D	
C_N :	Normal force coefficient in 3D	
C_A :	Axial force coefficient in 3D	
C_M :	Moment coefficient in 3D	
D :	Drag	[N]
L :	Characteristic linear dimension	[m]
L :	Lift	[N]
LE :	Leading edge	
m :	Maximum camber	[m]
M :	Mach number	
M :	Moment	[N.m]
M :	Moment in 2D	[Nm]

Nomenclature

N :	Normal force in 2D	[N]
N_l :	Lower normal force in 2D	[N]
N_u :	Upper normal force in 2D	[N]
n :	Matter quantity	[mole]
θ :	Angle of pressure and shear orientation	[°]
ρ :	Density	[Kg/m ³]
P :	Gas pressure	[Pa]
P_u :	Upper surface distribution	[Pa]
P_l :	Lower pressure distribution	[Pa]
p :	Position of the maximum camber	[m]
p :	Pressure force	[N/m ²]
Q_∞ :	Free stream Dynamic pressure	[Pa]
Re :	Reynolds number	
R :	Specific gas constant	[J/Kg/k]
R :	Resultant force	[N]
S_u :	Upper surface	[m ²]
S_l :	Lower surface	[m ²]
S :	Area	[m ²]
T :	Temperature	[K]
TE :	Trailing edge	
t :	Maximum thickness	[m]
μ :	Dynamic viscosity	[Pa.s]
V :	Maximum velocity of the object	[m/s]
ϑ :	Kinetic viscosity	[m ² /s]

Nomenclature

$V :$	Gas volume	[m ³]
$V_{\infty} :$	Flow velocity	[m/s]
$X_u, Y_u :$	Airfoil upper surface coordinates	[m]
$X_l, Y_l :$	Airfoil lower surface coordinates	[m]
$x :$	Coordinates along the length of the airfoil	[m]
$x_{cp} :$	Center of pressure	[m]
$y :$	Coordinates above and below the line	[m]
$Y_c :$	Mean camber line coordinates	[m]
$Y_t :$	Thickness distribution	[m]
$\gamma :$	Specific heat ratio	
$\tau :$	Shear force	[N/m ²]
$\tau_u :$	Upper Shear stress distribution	[Pa]
$\tau_l :$	Lower shear stress distribution	[Pa]
$\alpha :$	Speed of sound	[m/s]

General introduction

General Introduction

In engineering, any invention is in fact a copy of an element obtained from the nature, which is the case for the aircraft compressors where the earliest air compressor was the human lung. People were using their breath to stoke fires. Once the power of the compressed air was discovered, our ancestors began seeking to adopt and control this new energy.

In 1500B.C, the first type of air compressor was invented, called Bellows, this device was a hand-held flexible bag that produced a concentrated blast of air, since that day human continued improving this technology until the actual days, where the air compressor is highly used in the aeronautic and spatial engineering either military or civilian.

Compressors fall into the category of machinery that is “all around us” but of which we are little aware. We find them in our houses, workplaces, and in most forms of transportation we use. Compressors serve in refrigeration, engines, chemical processes, gas transmission, manufacturing, and in just about every place where there is a need to move or compress gas. Many engineering disciplines (e.g. fluid dynamics, thermodynamics, tribology, and stress analysis) involved in designing and manufacturing compressors.

Compressor blades are one of the most critical and sensible components in turbojets. Understanding and control of steady phenomena inevitably present in compressor is one of the key points to improve their performances.

It is well-known that the compression of air elevates the temperature of the compressed air to high values. The friction losses also heat the air with the net result that a several hundred degree temperature difference exists between the inlet and discharge ends of the compressor.

Therefore, blade cooling is necessary to reduce the blade metal temperature to acceptable levels for the materials increasing the thermal capability of the engine. A wide range of internal and external cooling arrangements has been applied; however, the aim in both cases is to keep the entire blade cool enough and also to ensure that temperature gradients within the blade (which might lead to thermal stresses) are kept to an acceptable level.

GENERAL INTRODUCTION

Then compressor blades are subjected to very strenuous environments inside a turbojet. They face high temperatures, high stresses because of the unsteady fluid-mechanical forces, and a potential environment of high vibration. All three of these factors can lead to blade failures which are detrimental both for the structural integrity of the blade and consequently of the engine and the overall machine performances. Therefore compressor blades are carefully designed to resist to these conditions.

We are interested here to an important part of a turbojet compressor which needs to be protected from any phenomenon can threats its stability or minimize its efficiency.

Because of the film cooling system, we have to make some holes around the blade by material removal.

The purpose of this work is to highlight the effect of this cooling system based on the material removal on the blade strength. More precisely we will show the effect of the number, the diameter and the position of the holes. the material will be resistant and at the same time, more functioning to make the efficiency of the compressor raises, for that we are also interested to show the effect of the blade material type to choose the best one.

To achieve our purpose the report is organized in three chapters.

- The first one describes some generalities on the turbojets.
- The second chapter is a review on the compressors, fluid flows, blades and the cooling systems
- The Third chapter includes the numerical simulation steps and the different results obtained. This chapter is divided into two parts, the first part is reserved to fluid flow simulation to find the aerodynamic forces exerted by air on the blades, however in the second part some simulations are carry out to know the response of the compressor blade to these forces for two working conditions with and without film cooling system.
- Finally, the report ends with an overall conclusion.

Chapter I

Presentation of CFM

**Presentation of Algeria Airline company :**

Air Algérie is the national airline of Algeria, with its head office in the Immeuble El-Djazair in Algiers. With flights operating from Houari Boumedienne Airport, Air Algérie operates scheduled international services to 39 destinations in 28 countries in Europe, North America, Africa, Asia, and the Middle East, as well as domestic services to 32 airports. The airline is a member of the International Air Transport Association, the Arab Air Carriers Organization, and of the African Airlines Association (AFRAA) since 1968. As of December 2013, Air Algérie was 100% owned by the government of Algeria.



I. INTRODUCTION

The turbojet is an airbreathing jet engine, usually used in aircraft. It consists of a gas turbine with a propelling nozzle. The gas turbine has an air inlet, a compressor, a combustion chamber, and a turbine (that drives the compressor). The compressed air from the compressor is heated by the fuel in the combustion chamber and then allowed to expand through the turbine. The turbine exhaust is then expanded in the propelling nozzle where it is accelerated to high speed to provide thrust. Two engineers, Frank Whittle in the United Kingdom and Hans von Ohain in Germany, developed the concept independently into practical engines during the late 1930s.

Turbojets have been replaced in slower aircraft by turboprops because they have better range-specific fuel consumption. At medium speeds, where the propeller is no longer efficient, turboprops have been replaced by turbofans. The turbofan is quieter and has better range-specific fuel consumption than the turbojet. Turbojets are still common in medium range cruise missiles, due to their high exhaust speed, small frontal area, and relative simplicity.

Turbojets have poor efficiency at low vehicle speeds, which limits their usefulness in vehicles other than aircraft. Turbojet engines have been used in isolated cases to power vehicles other than aircraft, typically for attempts on land speed records. Where vehicles are 'turbine powered' this is more commonly by use of a turboshaft engine, a development of the gas turbine engine where an additional turbine is used to drive a rotating output shaft. These are common in helicopters and hovercraft.

II. Types of jet engines

Aircraft engines can be classified by several methods. They can be classed by operating cycles, cylinder arrangement, or the method of thrust production. All are heat engines that convert fuel into heat energy that is converted to mechanical energy to produce thrust. Most of the current aircraft engines are of the internal combustion type because the combustion process takes place inside the engine. Aircraft engines come in many different types, such as gas turbine based, reciprocating piston, rotary, two or four cycle, spark ignition, diesel, and air or water cooled. Reciprocating and gas turbine engines also have subdivisions based on the type of cylinder arrangement (piston) and speed range (gas turbine). Many types of reciprocating engines have been designed [1].

II.1 Turbojet

Turbojets are the oldest and most general purpose jet engines, finding use in a large variety of applications. They are most efficient at supersonic velocities, and are capable of speeds around Mach 3. Turbojets are found on all military fighters. They were also found on the Concorde and the Tupolev Tu-144 [1].

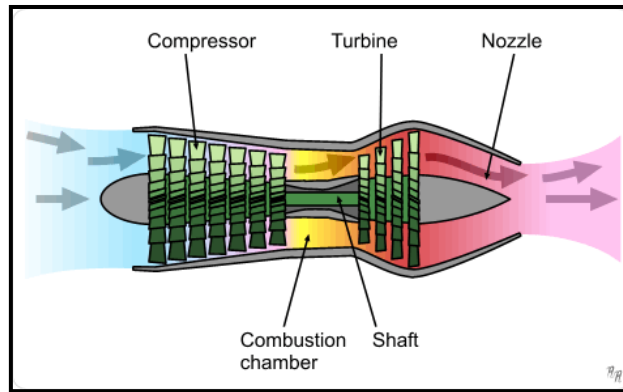


Figure I.1: Turbojet Engine

II.2 Turbofan

A turbofan is essentially a turbojet but with a large ducted fan that provides additional thrust by moving large amount of low velocity air around the main engine. This type of engine is more efficient than turbojets at subsonic speeds [1].

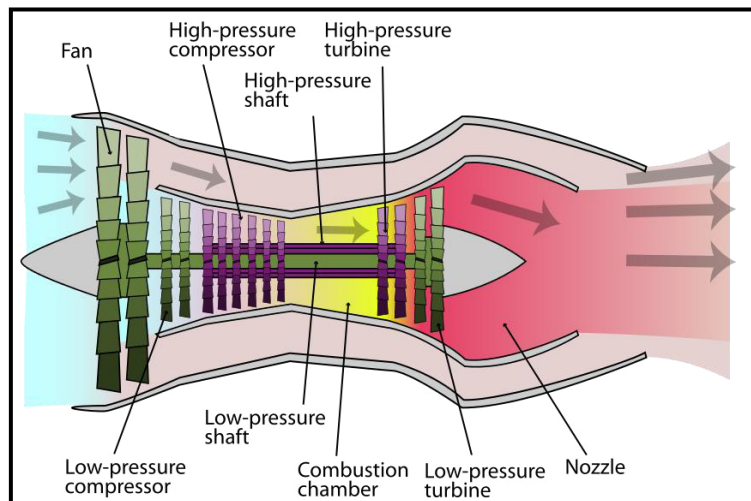


Figure I.2: Turbofan Engine.

Turbofans, being more efficient at subsonic velocities, are found on virtually all large commercial aircraft, such as the Boeing 747.

II.3 Ramjet

A ramjet is nothing more than a turbojet with all of the rotating parts removed. The engine's forward velocity compresses the air for combustion, making it necessary for some other form of propulsion to initially accelerate the engine. Ramjets are primarily used with missiles, due to their simple, small, and high-velocity design [1].

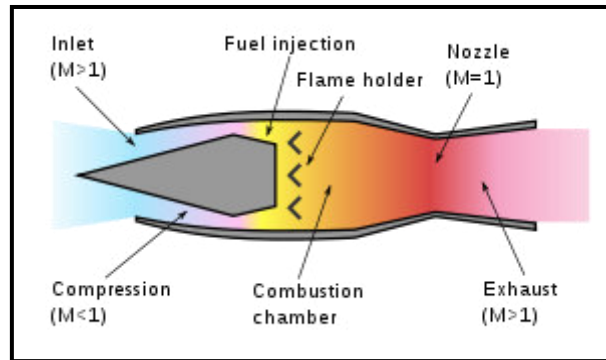


Figure I.3: Ramjet engine.

II.4 Scramjet

A scramjet is identical to a ramjet, but with one difference: combustion occurs with the air moving at supersonic velocities. As a result, scramjets are estimated not to work well below Mach 5, but could possibly reach speeds of Mach 24 (18000 mph). Scramjets are a relatively undeveloped technology, but currently much research is being done to explore their potential. Currently, there are no scramjets in use. However, there is a large military and civilian potential for their use [1].

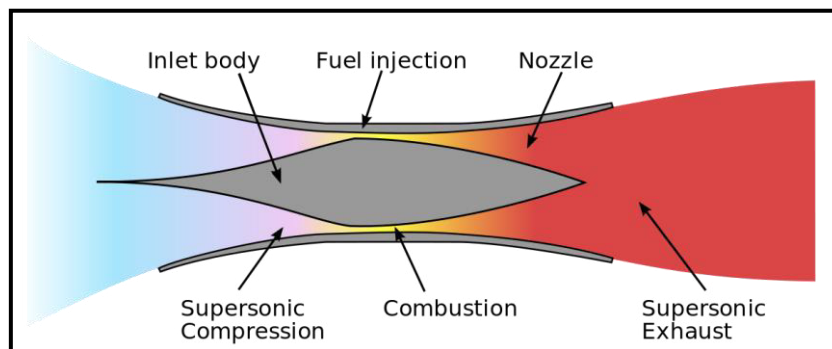


Figure I.4: Scramjet engine.

III. CFM evolution

The CFM international CFM56 (US Military designation F108) series is a family of High-bypass Turbofan aircraft engines made by CFM International (CFMI), with a thrust range of 18,000 to 34,000 pounds-force (80 to 150 kN). CFMI is a 50_50 joint-owned company of SNECMA, France and GE Aviation (GE), USA. Both companies are responsible for producing components and each has its own final assembly line. GE produces the high-pressure compressor, combustor, and high-pressure turbine, while some components are made by Avio of Italy. The engines are assembled by GE in Evendale, Ohio, and by SNECMA in Villaroche, France. The completed engines are marketed by CFMI [2].

The CFM56 first ran in 1974 and despite initial export restrictions, is now one of the most common turbofan aircraft engines in the world, with more than 20,000 having been built in four major variants. It is most widely used on Boeing 737 airliner, and under military designation F108, replaced the Pratt & Whitney JT3D engines on many KC-135 Stratotanker in the 1980s, creating the KC-135R variant of this aircraft. It is also the only engine (CFM56-5c) used to power the Airbus A340-200 and 300 series. The engine (CFM56-5A and 5b) is also fitted to Airbus A320 series Aircraft [3].

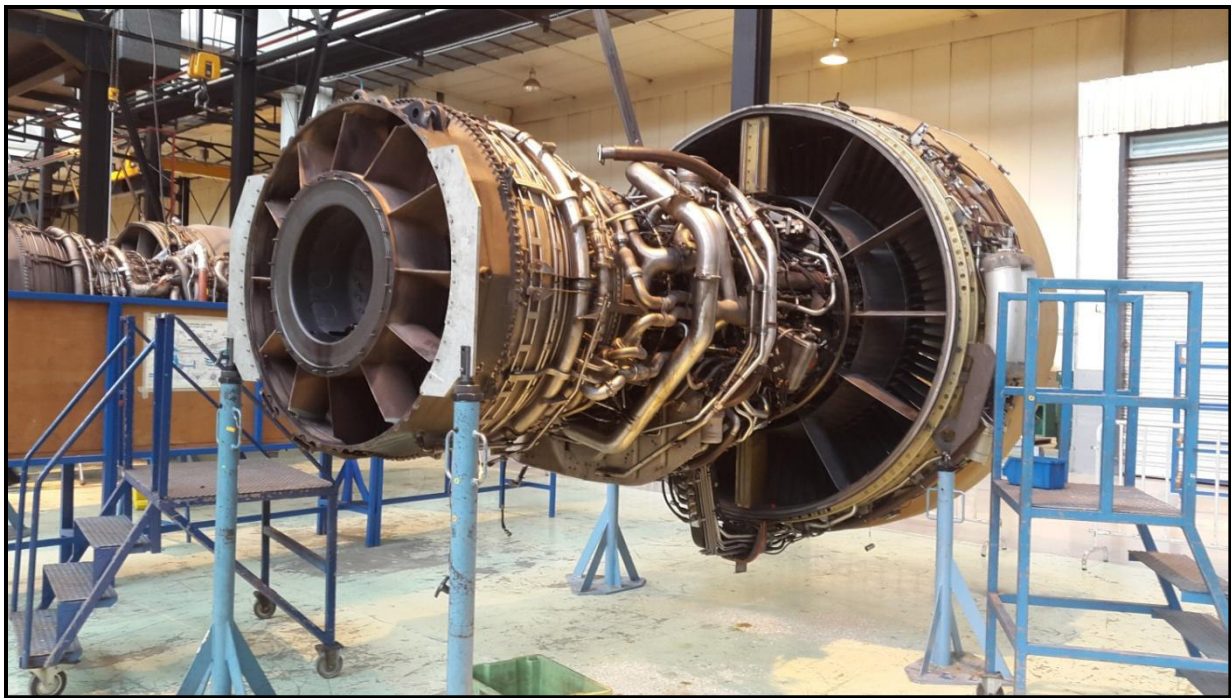


Figure I.5: CFM56 core.

The CFM56 core is based on the GE F101 engine (developed for the B-1 Bomber) and employs a single-stage high-pressure turbine to drive a nine stage compressor. Correspondingly, a SNECMA advanced four- or five- stage low pressure turbine, drives the SNECMA fan and booster.

In 2009, CFMI announced the latest upgrade to the CFM56 engine, the “CFM56-7B Evolution”, or CFM56-7BE. This upgrade, announced alongside Boeing’s newest 737 variant, further enhances the high- and low- pressure turbines with better aerodynamics, as well as improving engine cooling, and aims to reduce overall part count. CFMI expected the changes to result in a 4% reduction in maintenance costs and a 1% improvement in fuel consumption (2% improvement including the airframe changes for the new 737); However, flight and ground tests completed in May 2010 revealed that the fuel burn improvement was better than expected at 1.6%. Following 450 hours of testing, the CFM56-7BE engine was certified by FAA and EASA on July 30, 2010 and delivered since mid-2011 [3].

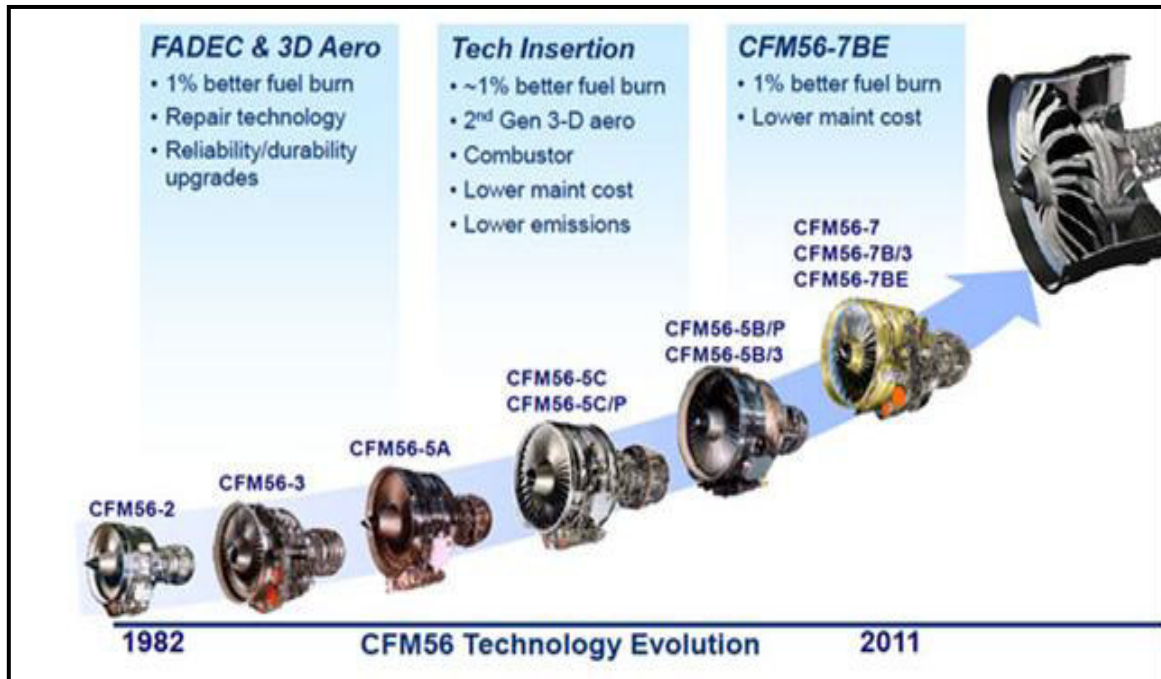


Figure I.6: CFM56 Evolution

The CFM56-5B/3 PIP (Performance Improvement Package) engine include these new technologies and hardware changes to lower fuel burn and lower maintenance cost. Airbus A320s were to use this engine version starting in late 2011.



Figure I.7: The CFM56-7B

IV. Components of CFM65

Major components of turbojet including references to turbofans, turboprops and turboshafts:

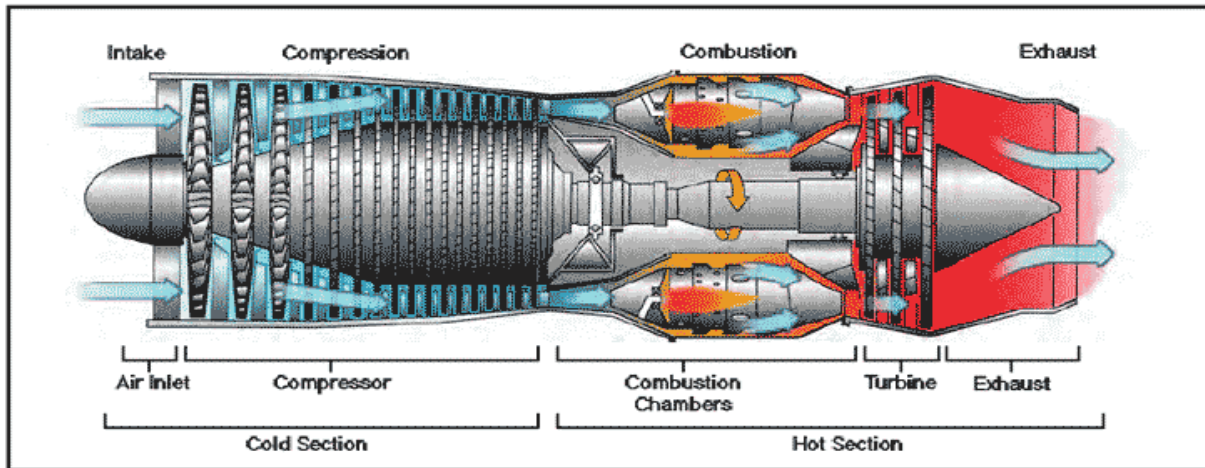


Figure I.8: components of Jet engine

IV.1 Air intake (inlet/Fan)

The fan is first component in a turbojet engine. This is the part which is also called AIR INLET section. The large spinning fan sucks in large quantity of air. Mostly blades of fan are made up of titanium. After sucking it speeds up the air and splits it into two parts. One part continues through core part or through the centre of jet engine where it is acted upon other jet engine components. The other part is “bypass” around the core. It goes through a duct that surrounds the core through the jet engine where it produces much of the force that propels the airplane forward. This cooler air helps to quiet the jet engine as well as adding thrust to the jet engine [4].

IV.2 COMPRESSOR (low pressure and high pressure compressor)

The Compressor is the first component in the jet engine core. The compressor is made up of fans with many blades attached to the shaft. It is of different stages. Each stage consists of vanes which rotates and stators which remains stationary. As air is drawn deeper through the compressor, its heat and pressure increases. Energy is derived from the turbine, passed along the shaft. The squashed air is then forced into the combustion chamber [4].

IV.3 COMBUSTER (combustion chambers)

In the combustor the air is mixed with fuel and then ignited. There are as many as 20 nozzles to spray fuel into the airstream. The mixture of air and fuel catches fire. This provides a high temperature, high-energy airflow. The fuel burns with the oxygen in the compressed air, producing hot expanding gases. The inside of the combustor is often made of ceramic materials to provide a heat-resistant chamber. The heat can reach 2700° [4].

IV.4 TURBINE (low and high pressure)

The high-energy airflow coming out of the combustor goes into the turbine, causing the turbine blades to rotate. The turbines are linked by a shaft to turn the blades in the compressor and to spin the intake fan at the front. This rotation takes some energy from the high-energy flow that is used to drive the fan and the compressor. The gases produced in the combustion chamber move through the turbine and spin its blades. The turbines of the jet spin around thousands of times. They are fixed on shafts which have several sets of ball-bearing in between them [4].

IV.5 Nozzle and Exhaust

The nozzle is the exhaust duct of the engine. This is the engine part which actually produces the thrust for the plane. The energy depleted airflow that passed the turbine, in addition to the colder air that bypassed the engine core, produces a force when exiting the nozzle that acts to propel the engine, and therefore the airplane, forward. The combination of the hot air and cold air are expelled and produce an exhaust, which causes a forward thrust. The nozzle may be preceded by a **mixer**, which combines the high temperature air coming from the engine core with the lower temperature air that was bypassed in the fan. The mixer helps to make the engine quieter [4].

VI. Working Principal of the Turbojet

All jet engines, which are also called gas turbines, work on the same principle. The engine sucks air in at the front with a fan. A compressor raises the pressure of the air. The compressor is made up of fans with many blades and attached to a shaft. The blades compress the air. The compressed air is then sprayed with fuel and an electric spark lights the mixture. The burning gases expand and blast out through the nozzle, at the back of the engine. As the jets of gas shoot backward, the engine and the aircraft are thrust forward.

The air goes through the core of the engine as well as around the core. This causes some of the air to be very hot and some to be cooler. The cooler air then mixes with the hot air at the engine exit area. A jet engine operates on the application of Sir Isaac Newton's third law of physics:

For every action there is an equal and opposite reaction. This is called thrust. This law is demonstrated in simple terms by releasing an inflated balloon and watching the escaping air propel the balloon in the opposite direction. In the basic turbojet engine, air enters the front intake and is compressed, then forced into combustion chambers where fuel is sprayed into it and the mixture is ignited. Gases which then expand rapidly and are exhausted through the rear of the combustion chambers. These gases exert equal force in all directions, providing forward thrust as they escape to the rear. As the gases leave the engine, they pass through a fan-like set of blades (turbine) which rotates the turbine shaft. This shaft, in turn, rotates the compressor, thereby bringing in a fresh supply of air through the intake. Engine thrust may be increased by the addition of an afterburner section in which extra fuel is sprayed into the exhausting gases which burn to give the added thrust [5].

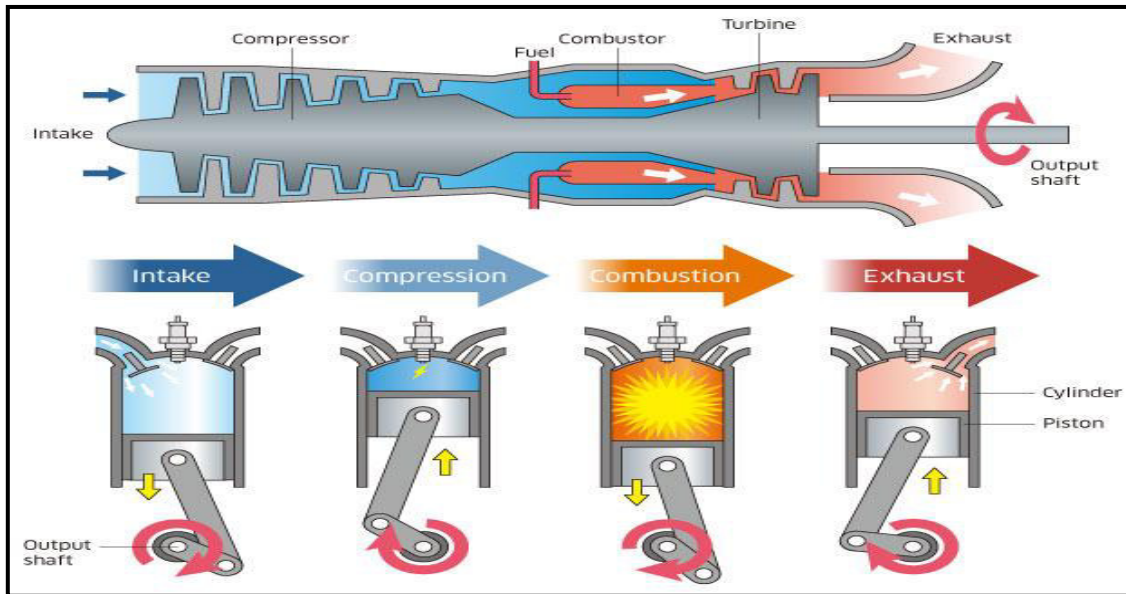


Figure I.9: a comparison between the working cycle of a turbojet engine and a piston engine.

The working cycle, upon which the gas turbine engine function is, in its simplest form, represented by the cycle shown on the entropy-temperature diagram in fig 7. Point A represents atmospheric pressure that is compressed along the line AB. From B to C heat is added to the air by introducing and burning fuel at constant pressure, thereby considerably increasing the volume of air. Pressure losses in the combustion chambers (Part 4) are indicated by the drop between B and C. From C to D the gases resulting from combustion expand through the turbine and jet pipe back to atmosphere. During this part of the cycle, Some of the energy in the expanding gases is turned into mechanical power by the turbine; the remainder, on its discharge to atmosphere, provides a propulsive jet. Because the turbo-jet engine is a heat engine, the higher the temperature of combustion the greater is the expansion of the gases [6].

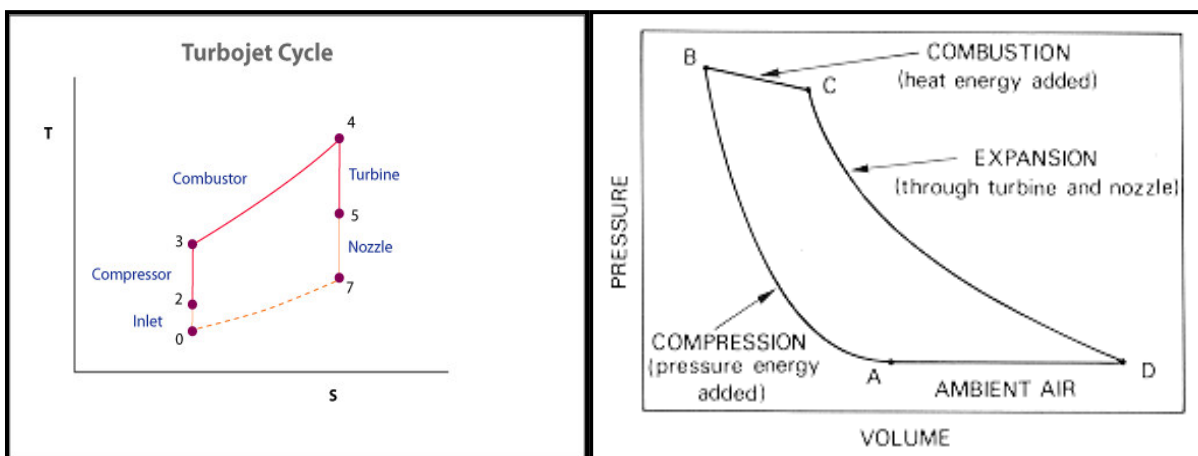
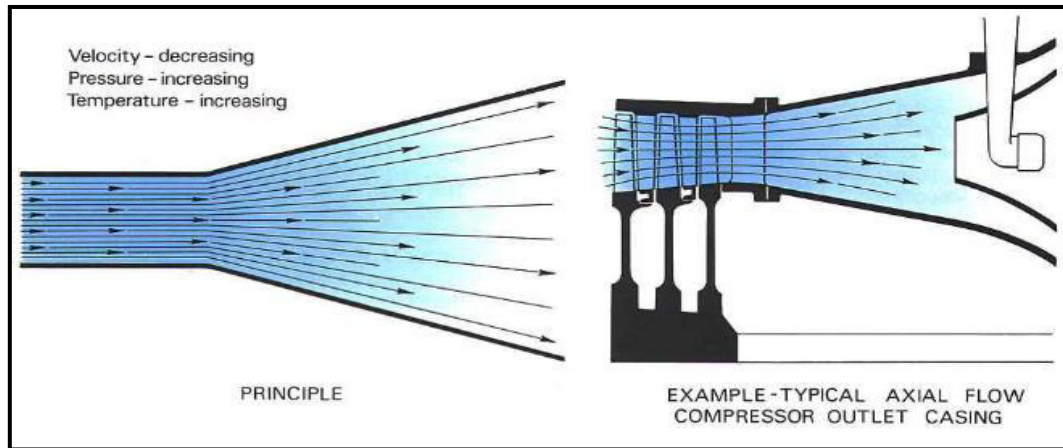


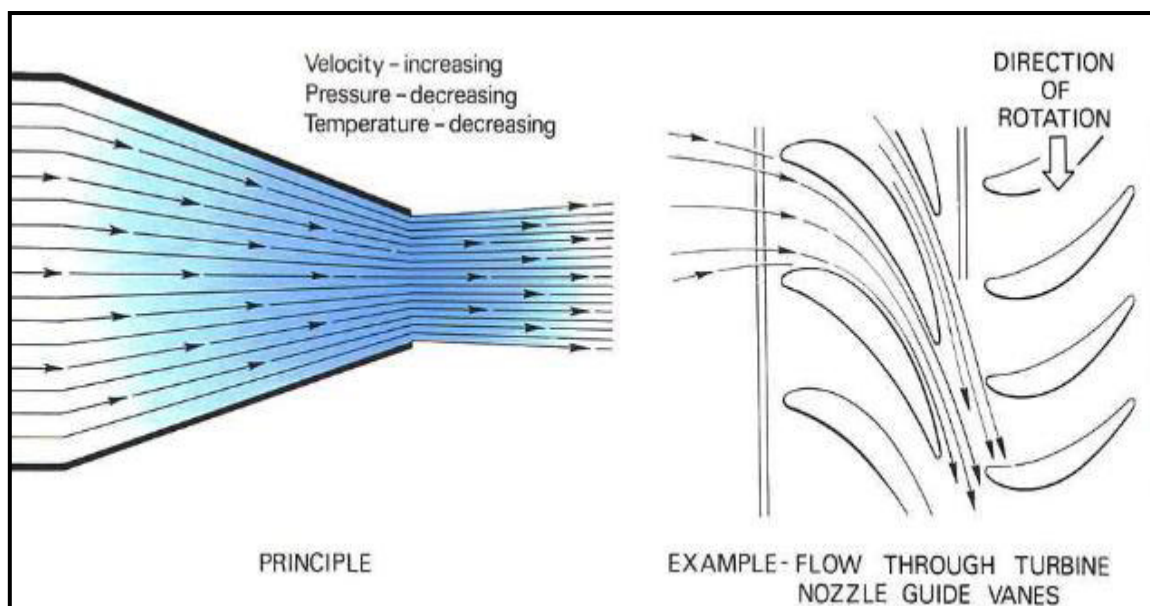
Figure I.10: Working cycle on a pressure volume and enthalpy temperature diagrams.

The combustion temperature, however, must not exceed a value that gives a turbine gas entry temperature suitable for the design and materials of the turbine assembly. The use of air-cooled blades in the turbine assembly permits a higher gas temperature and a consequently higher thermal efficiency.



(a)

The various components named above have constraints on how they are put together to generate the most efficiency of performance. The performance and efficiency of an engine can never be taken in isolation [6].



(b)

Figure I.11: Airflow through (a) divergent duct and (b) convergent duct.

VI. Aircraft Engines requirements

Aircraft Require Thrust to produce enough speed for the wings to provide lift or enough thrust to overcome the weight of the aircraft for vertical takeoff .For an aircraft to remain in level flight , thrust must be provide that is equal to and in the opposite direction of air craft drag . This thrust or propulsive force is provided by a suitable type of aircraft heat engine. All heat engines have in common the ability to convert heat energy into mechanical energy by the flow of some fluids mass (generally air) through the engine. In all cases, the heat energy is realised at a point in the cycle where the working pressure is high relative to atmospheric pressure.

All aircraft engines must meet certain general requirements of efficiency, economy, and reliability. Besides being economical in fuel consumption, an aircraft engine must be economical in the cost of original procurement and the cost of maintenance; and it must meet exacting requirements of efficiency and low weight-to-horsepower ratio. It must be capable of sustained high-power output with no sacrifice in reliability; it must also have the durability to operate for long periods of time between overhauls. It needs to be as compact as possible, yet have easy accessibility for maintenance. It is required to be as vibration free as possible and be able to cover a wide range of power output at various speeds and altitudes [7].

VI.1 Fuel Economy

The basic parameter for describing the fuel economy of aircraft engines is usually specific fuel consumption. Specific fuel consumption for gas turbines is the fuel flow measured in (lb/hr) divided by thrust (lb), and for reciprocating engines the fuel flow (lb/hr) divided by brake horsepower.

These are called thrust-specific fuel consumption and brake specific fuel consumption, respectively. Equivalent specific fuel consumption is used for the turboprop engine and is the fuel flow in pounds per hour divided by a turboprop's equivalent shaft horsepower. Comparisons can be made between the various engines on a specific fuel consumption basis. At low speed, the reciprocating and turboprop engines have better economy than the pure turbojet or turbofan engines. However, at high speed, because of losses in propeller efficiency, the reciprocating or turboprop engine's efficiency becomes limited above 400 mph less than that of the turbofan. Equivalent specific fuel consumption is used for the turboprop engine and is the fuel flow in pounds per hour divided by a turboprop's equivalent shaft horsepower. Comparisons can be made between the various engines on a specific fuel consumption basis [7].

VI.2 Durability and Reliability

Durability and reliability are usually considered identical factors since it is difficult to mention one without including the other. An aircraft engine is reliable when it can perform at the specified ratings in widely varying flight attitudes and in extreme weather conditions. Standards of power plant reliability are agreed upon by the Federal Aviation Administration (FAA), the engine manufacturer, and the airframe manufacturer. The engine manufacturer ensures the reliability of the product by design, research, and testing. Close control of manufacturing and assembly procedures is maintained, and each engine is tested before it leaves the factory.

Durability is the amount of engine life obtained while maintaining the desired reliability. The fact that an engine has successfully completed its type or proof test indicates that it can be operated in a normal manner over a long period before requiring overhaul. However, no definite time interval between overhauls is specified or implied in the engine rating. The time between overhauls (TBO) varies with the operating conditions, such as

engine temperatures, amount of time the engine is operated at high-power settings, and the maintenance received. Recommended TBOs are specified by the engine manufacturer.

Reliability and durability are built into the engine by the manufacturer, but the continued reliability of the engine is determined by the maintenance, overhaul, and operating personnel. Careful maintenance and overhaul methods, thorough periodical and pre-flight inspections, and strict observance of the operating limits established by the engine manufacturer make engine failure a rare occurrence [7].

VI.3 Operating Flexibility

Operating flexibility is the ability of an engine to run smoothly and give desired performance at all speeds from idling to full-power output. The aircraft engine must also function efficiently through all the variations in atmospheric conditions encountered in widespread operations [7].

VI.4 Compactness

To affect proper streamlining and balancing of an aircraft, the shape and size of the engine must be as compact as possible. In single-engine aircraft, the shape and size of the engine also affect the view of the pilot, making a smaller engine better from this standpoint, in addition to reducing the drag created by a large frontal area.

Weight limitations, naturally, are closely related to the compactness requirement. The more elongated and spread out an engine is, the more difficult it becomes to keep the specific weight within the allowable limits [7].

VI.5 Power plant selection

Engine specific weight and specific fuel consumption were discussed in the previous paragraphs, but for certain design requirements, the final power plant selection may be based on factors other than those that can be discussed from an analytical point of view. For that reason, a general discussion of power plant selection follows.

For aircraft whose cruising speed does not exceed 250 mph, the reciprocating engine is the usual choice of power plant.

When economy is required in the low speed range, the conventional reciprocating engine is chosen because of its excellent efficiency and relatively low cost. When high altitude performance is required, the turbo-supercharged reciprocating engine may be chosen because it is capable of maintaining rated power to a high altitude (above 30,000 feet). Gas turbine engines operate most economically at high altitudes. Although in most cases the gas turbine engine provides superior performance, the cost of gas turbine engines is a limiting factor. In the range of cruising speed

of 180 to 350 mph, the turboprop engine performs very well. It develops more power per pound of weight than does the reciprocating engine, thus allowing a greater fuel load or payload for engines of a given power. From 350 mph up to Mach .8–.9, turbofan engines are generally used for airline operations. Aircraft intended to operate at Mach 1 or higher are powered by pure turbojet engines/afterburning (augmented) engines, or low-bypass turbofan engines [7].

Chapter II

Overview on Compressors, Fluid and Blades

Introduction:

Compressors are mechanical devices which draw air and discharge it at higher pressure, usually into a piping system or tank. These machines can be used to compress room air into a high pressure distribution system to draw the air from a tank and discharge it into the atmosphere thereby causing a vacuum in the tank. Positive displacement compressors use pistons or rotors to compress the gas and dynamic compressors use impellers or blades for compression [8].

The primary purpose of the compressor is to increase the pressure of the air through the gas turbine core. It then delivers this compressed air to the combustion system. The compressor comprises the fan and alternating stages of rotating blades and static vanes. Rotors and stators embody an aerodynamic design to maximize the efficiency of the compression process [9].

I. Compressor types

Several types of compressors are used in the process industries. The most common, however, are:

- positive displacement compressor
- dynamic compressor

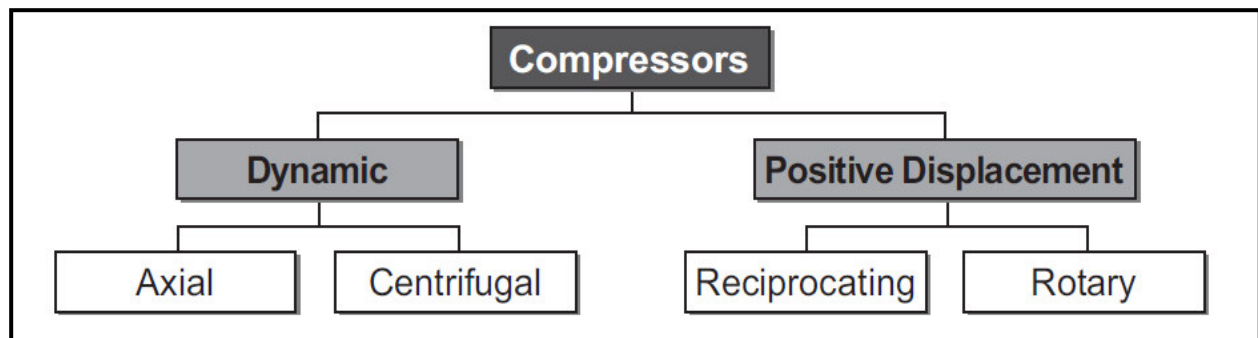


Figure II.1: Main types of gas compressors

Positive displacement compressors deliver a fixed volume of air at high pressures; it commonly can be divided into two types: rotary compressors and reciprocating compressors [10].

Dynamic compressors are non positive displacement compressors that use centrifugal or axial force to accelerate and convert the velocity of the gas to pressure. These compressors are divided into two types centrifugal and axial.

I.1 Centrifugal compressor

In the centrifugal compressors the gas flows from the inlet located near the suction eye to the outer tip of the impeller blade. The gas enters at the low pressure end and is forced through the impellers by the rotation of the shaft. As the gas moves from the center of the impeller toward the outer tip, the velocity is greatly increased. When the gas leaves the impeller and enters the volute, the velocity is converted to pressure due to the slowing down of the molecules. They are used throughout industry because they have few moving parts, are very energy efficient, and provide higher flows than similarly sized reciprocating compressors [11].



Figure II.2: Centrifugal compressor

Centrifugal compressors are also popular because their seals allow them to operate nearly oil-free, and they have a very high reliability. They are also effective in toxic gas service when the proper seals are used, and they can compress high volumes at low pressures. The primary drawback is that centrifugal compressors cannot achieve the high compression ratio of reciprocating compressors without multiple stages. The main components of a centrifugal compressor include bearings, a housing (casing), an impeller, an inlet and outlet, a shaft, shaft couplings, and shaft seals [11].

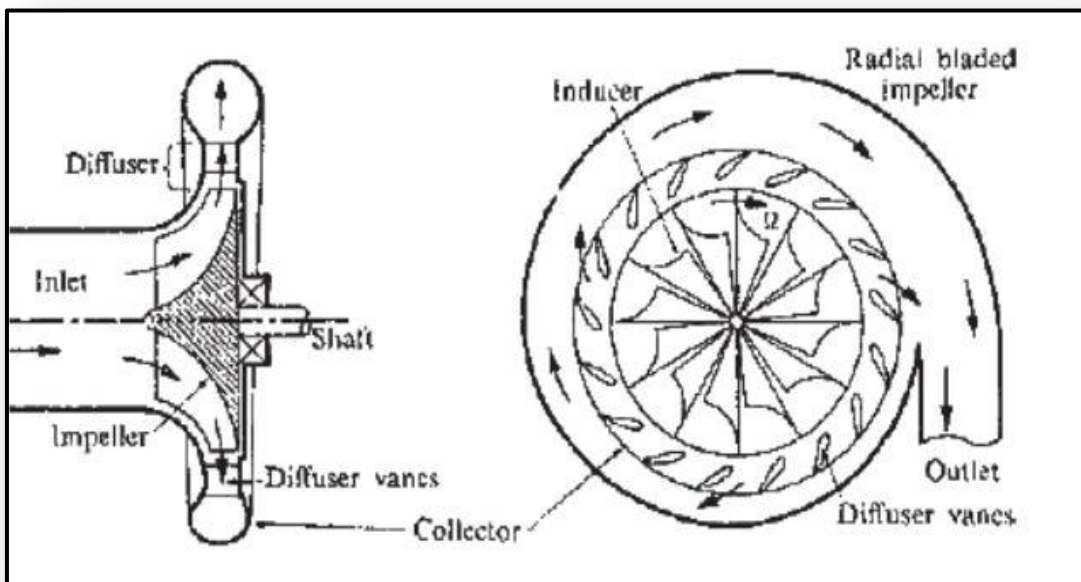


Figure II.3: Centrifugal compressor working principles.

I.2. Axial compressor

In the axial compressors the flow of gas is axial (in a straight line along the shaft). The main components of an axial compressor include the housing (casing), inlet and outlet, rotor and stator blades, shaft, and inlet guide vanes [4]. Rotor blades attached to the shaft spin and send the gas over stator blades, which are attached to the internal walls of the compressor casing. Rotation of the shaft and its attached rotor blades causes flow to be directed axially along the shaft, building higher pressure toward the discharge of the unit. Each pair of rotors and stators is referred to as a stage. Most axial compressors have a number of such stages placed in a row along a common power shaft in the center [11].

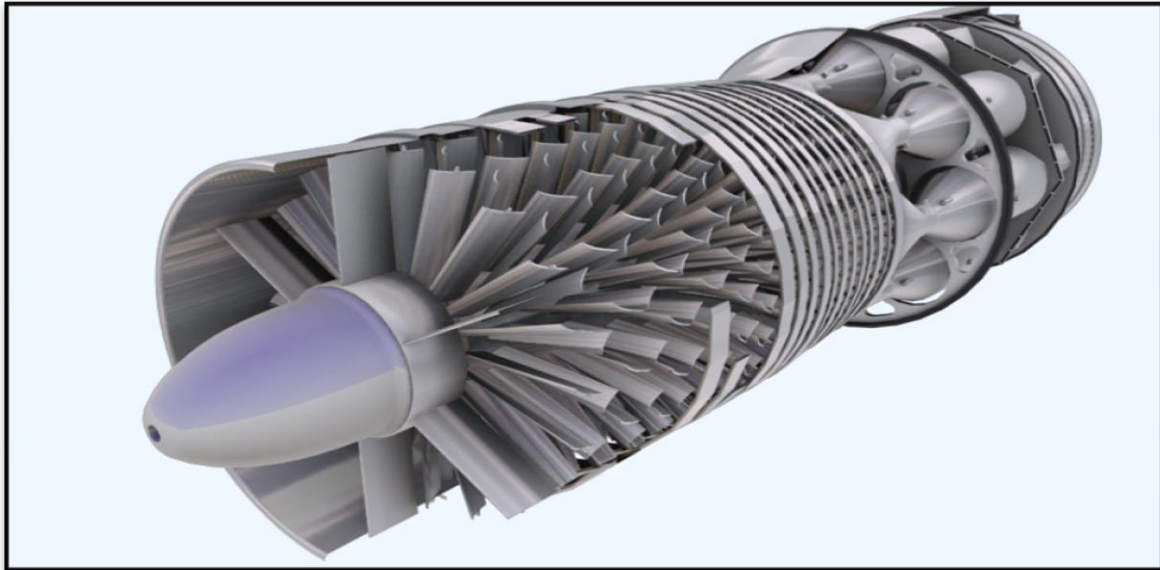


Figure II.4: Axial compressor

The stator blades are required to ensure efficiency. Without these stator blades, the gas would rotate with the rotor blades, resulting in a large drop in efficiency. One rotor and one stator make up a stage in a compressor. The axial flow compressor produces low pressure increase, thus the multiple stages are generally used to permit overall pressure increase up to 30:1 for some industrial applications [10].

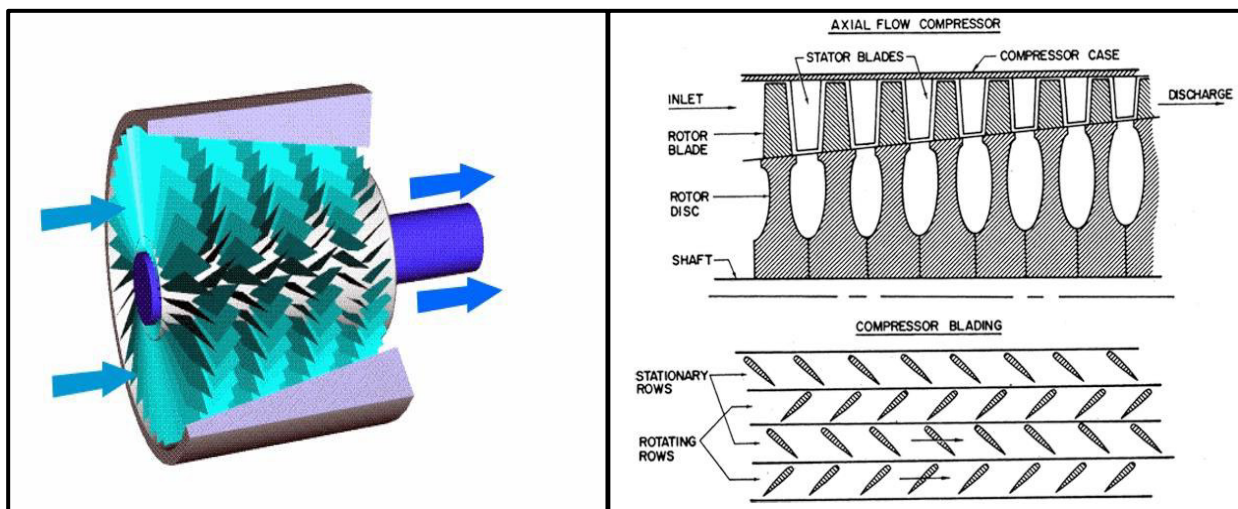


Figure II.5: Working principle of axial flow compressor.

II. Compressor flow modeling:

The motion of fluids can be predicted using the fundamental laws of physics together with the physical properties of the fluid, the real flow in turbo machines (Compressor/turbine) is three dimensional, unsteady, viscous and compressible [18].

The table II.1 presents the compressibility effect according to the Mach number regimes :

Table II.1: Mach number regimes and compressibility effect.

Mach Number regimes	Mach number range	Compressibility effect
Subsonic	Conditions occur for Mach numbers less than one M<1	For the lowest subsonic conditions, compressibility can be ignored
Transonic	Conditions occur when the speed of the object approaches the sound speed M=1	Compressibility effects are most important in transonic flows and lead to the early belief in a sound barrier the (increase in the drag near sonic conditions).
Supersonic	Conditions occur for Mach numbers greater than one M>1	Compressibility effects are important, and shock waves are generated by the surface of the object
Hypersonic	For this case the Mach number is greater than five M>5	-

III. The basic equations of conservation

III.1 Mass conservation

Basic fluid mechanics laws dictate that mass is conserved within a control volume for constant density fluids. Thus the total mass entering the control volume must equal the total mass exiting the control volume plus the mass accumulating within the control volume. for compressible viscous flow The continuity equations in conservation form is giving by[28] :

$$\frac{\partial \rho}{\partial t} + \Delta \cdot (\rho V) = 0 \quad (1)$$

III.2 Newton's second law or Navier-Stokes Equations

Newton's second law is simply the Law of conservation of momentum. It states that the time rate of change of momentum of a system of particles is equal to the sum of external forces acting on that body.

For compressible viscous flow the Navier-Stokes (Momentum equations) in conservation form are giving by:

$$x\text{-component : } \frac{\partial(\rho u)}{\partial t} + \Delta.(\rho u V) = -\frac{\partial p}{\partial x} + \partial f_x + (F_x)_{viscous} \quad (2)$$

$$y\text{-component : } \frac{\partial(\rho v)}{\partial t} + \Delta.(\rho v V) = -\frac{\partial p}{\partial y} + \partial f_y + (F_y)_{viscous} \quad (3)$$

$$z\text{-component : } \frac{\partial(\rho w)}{\partial t} + \Delta.(\rho w V) = -\frac{\partial p}{\partial z} + \partial f_z + (F_z)_{viscous} \quad (4)$$

III.3 Energy equation

The energy can neither be created nor destroyed which means the total amount of energy is fixed; the energy equation is a statement of the first law of thermodynamics involving energy, heat transfer and work. For compressible viscous flow, the energy equation in conservative form is written as follow:

$$\frac{\partial}{\partial t} \left[\rho \left(e + \frac{v^2}{2} \right) \right] + \nabla. \left[\rho \left(e + \frac{v^2}{2} \right) \mathbf{V} \right] = e. \dot{q} - \nabla.(\rho. \mathbf{V}) + \rho(f. \mathbf{V}) + \dot{Q}_{viscous} + \dot{W}_{viscous} \quad (5)$$

III.4 Ideal gas law

The ideal gas law is an equation that relates the volume, temperature, pressure and amount of gas particles to a constant. The ideal gas law can be used when three of the four gas variables are known.

$$P.V = n. R. T \quad (6)$$

- **P:** pressure of the gas.
- **V:** volume of the gas.
- **n:** number of moles.
- **R:** gas universal constant.
- **T:** temperature of the gas.

These equations are the heart of the fluid flow modeling. Solving them, for a particular set of boundary conditions (such as inlets, outlets, and walls), predicts the fluid velocity and its pressure in a given geometry.

IV. Axial compressor blades

The main parts of gas compressor are the rotor and stator parts which themselves are made by blades.

A blade is a type of fin with a surface that produces aerodynamic forces facilitating movement through air and other gases. As such, blades have an airfoil shape, a streamlined cross sectional shape producing lift.

design specification of the compressor blade is of major importance in the overall compressor design. The blade must be design not to fail due to gross over stressing or high cycle fatigue, hence a dovetail which is precise in size and position are used to keep the blades in their desired position and locations on the wheel. Both the stator and rotor blade is mounted in similar dovetail arrangement.

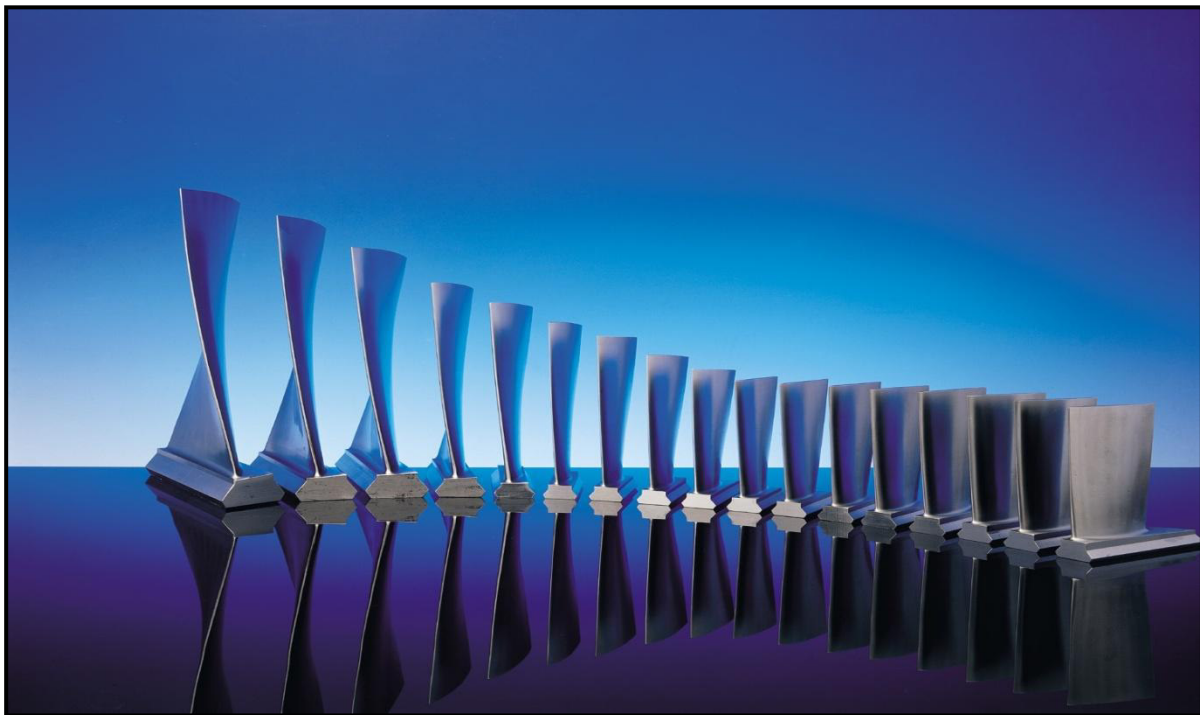


Figure II.6: Axial compressor Blades.

IV.1. Blades geometry

Blades are designed with specific geometry that adapts them to the varying conditions of flight. Cross-section shapes of most rotor blades are not the same throughout the span. Shapes are varied along the blade radius to take advantage of the particular airspeed range experienced at each point on the blade, and to help balance the load between the root and tip. The blade may be built with a twist, so an airfoil section near the root has a larger pitch angle than a section near the tip [12]. The main geometrical parameters of the airfoil are (figure II.7): the chord line, chord, mean camber line, maximum camber and thickness.

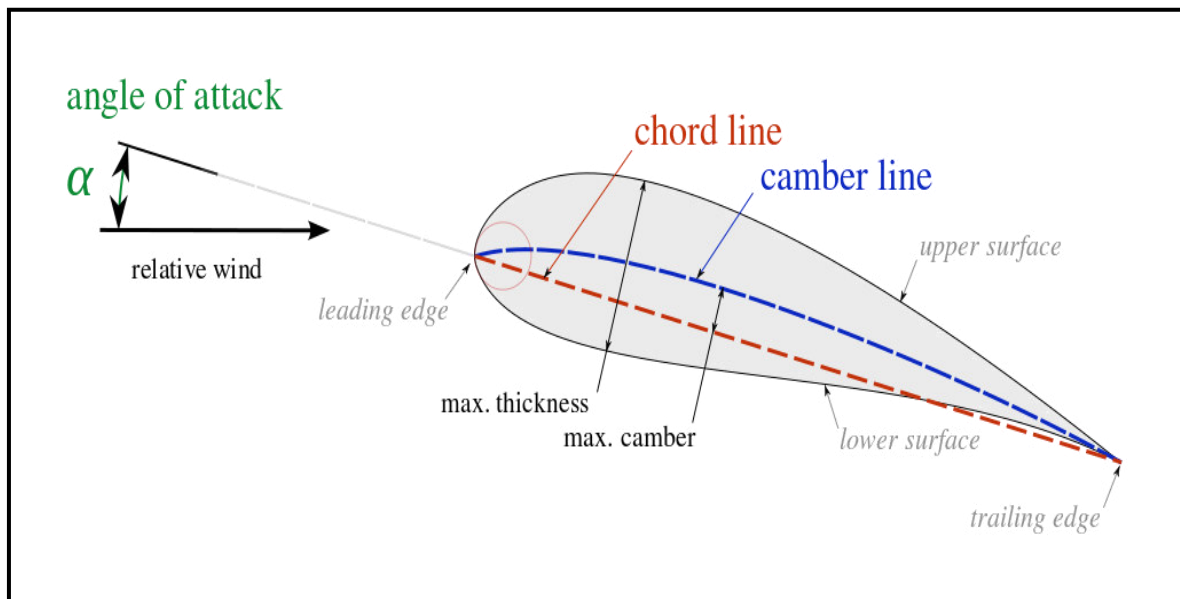


Figure II.7: Blade Geometry.

American practice was based on various families defined by the National Advisory Committee for Aeronautics (NACA), the most popular being the 65-series family. The shape of the NACA airfoils is described using a series of digits following the word "NACA". The parameters in the numerical code can be entered into equations to precisely generate the cross-section of the airfoil and calculate its properties [13].



Figure II.8: Compressor Blades (NACA 65 series).

The empirical component of the NACA design method was based primarily on a huge number of cascade performance tests of NACA 65-Series airfoils carried out at Langley.... These data allowed designers first to select preferred airfoil shapes along a blade to achieve a given design performance, including thermodynamic loss requirements, and then to predict the performance of the airfoils at specified off-design operating conditions. In large part because of the availability of this data-base, NACA 65-Series airfoils became the most widely used airfoils in axial compressors [17].

IV.2. Blades manufacturing process:

The development of directionally solidified airfoils was a significant advancement in aircraft engines. It provided for increases in operating temperatures and higher rotor speeds. In the conventional casting technique, the molten metal is poured into a ceramic mould. By controlling metal pouring and surrounding conditions, the molten metal solidifies from the surface to the centre of the mould, creating an equiaxed structure. In Directional Solidification, planar solidification occurs in the blade and the part is solidified by moving the planar front longitudinally. This produces a blade with an oriented grain structure that runs along the major axis and devoid of transverse grain boundaries unlike the former. The elimination of transverse grain boundaries adds on to the creep resistance and rupture strength of the alloy and the orientation provides a favorable modulus of elasticity to enhance fatigue life.

There are plenty of methods to manufacture compressor components:

- Castings are used to manufacture the more complex static components.
- Forging are typically used for the rotating components.

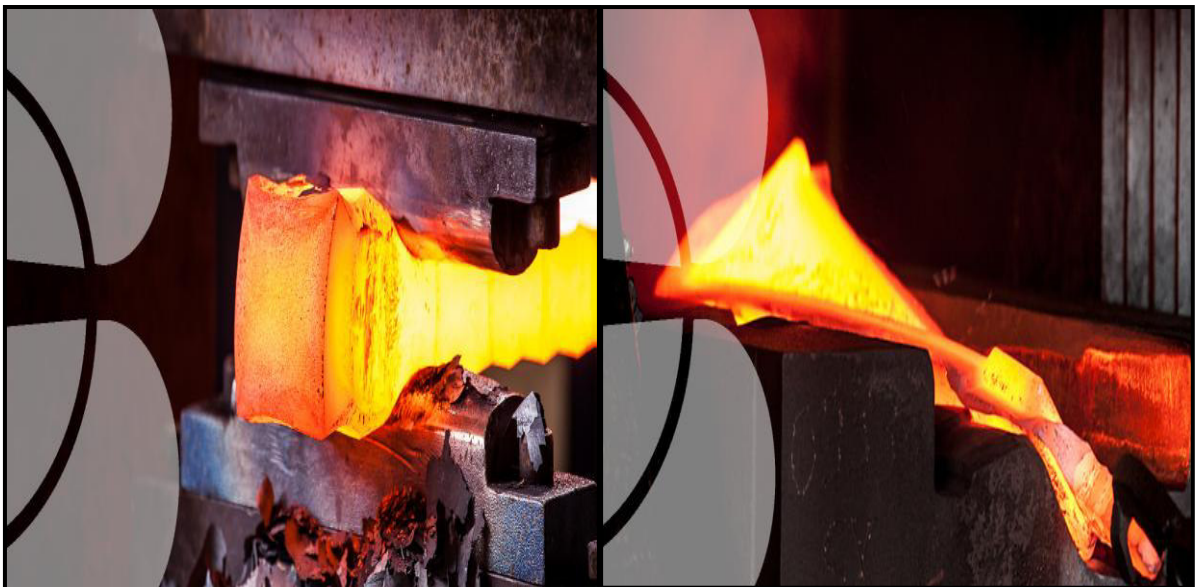


Figure II.9: Blade Forging Method.

In addition to the above, these blades possess more thermal fatigue resistance when compared to equiaxed blades. Later developments included single crystal blades which eliminate all grain boundaries (longitudinal and transverse). A single crystal with controlled orientation is produced in an airfoil shape. A substantial increase in the melting point of the alloy and an increase in high-temperature strength can be achieved by eliminating the grain boundaries. The transverse creep resistance and fatigue strengths of a single crystal blade are higher when compared to equiaxed and Directionally Solidified blades [14].

IV.3 Properties of Blades Materials:

The compressor blades Materials must have some requirement to avoid failure during operations, high strength (static, fatigue), high stiffness and low weight, so to achieve those requirement in the blades construction, industrials use Titanium Alloys, Aluminum Alloys and Nickel alloys.

- **Aluminum Alloys :**

An aluminum alloy is a chemical composition where other elements are added to pure aluminum in order to enhance its properties, primarily to increase its strength. These other elements include iron, silicon, copper, magnesium, manganese and zinc at levels that combined may make up as much as 15% of the alloy by weight. Alloying requires the thorough mixing of aluminum with these other elements while the aluminum is in molten liquid form.

- **Titanium**

Titanium Alloys has some attributes of prime importance to the design engineer which are[15]:

- ✓ Outstanding corrosion resistance
- ✓ Excellent erosion resistance
- ✓ High heat transfer capability

And it has also some secondary characteristics which are equally important:

- ✓ Low thermal expansion coefficient
- ✓ Non-magnetic character
- ✓ Fire resistance
- ✓ Short radioactive half-life

- **Nickel**

Nickel is a versatile element and will alloy with most metals. Complete solid solubility exists between nickel and copper. Wide solubility ranges between iron, chromium, and nickel make possible many alloy combinations. Nickel and nickel alloys are used for a wide variety of applications, the majority of which involve corrosion resistance and/or heat resistance. Some of these include:

- ❖ Aircraft gas turbines
- ❖ Steam turbine power plants
- ❖ Medical applications
- ❖ Nuclear power systems
- ❖ Chemical and petrochemical industries [16]

V. Aerodynamic Forces:

When a stream of air flows over and under an airfoil a total aerodynamic force is generated.

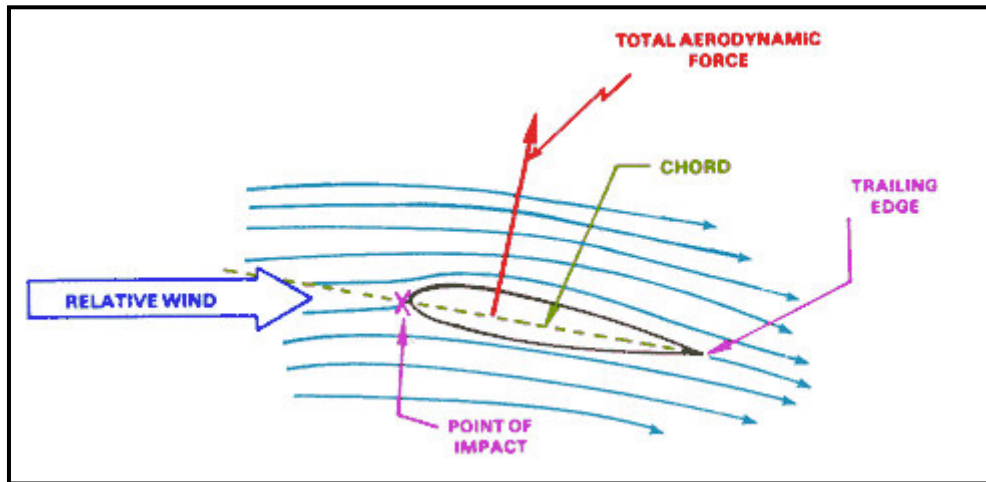


Figure II.10: Airflow around and airfoil

The Figure II.10 also shows airflow lines that illustrate how the air moves about the airfoil section. Air passing over the top of the airfoil produces aerodynamic force in another way the shape of the airfoil causes a low pressure area above the airfoil according to Bernoulli's Principle, and the decrease in pressure on top of the airfoil exerts an upward aerodynamic force. Pressure differential between the upper and lower surface of the airfoil is quite small - in the vicinity of 1 percent. Even a small pressure differential produces substantial force when applied to the large area of a rotor blade. The aerodynamic forces and moments on the body are due to only two basic sources:

- ✓ Pressure distribution over the body surface.
- ✓ Shear stress distribution over the body surface.

The total aerodynamic force, sometimes called the resultant force, may be divided into two components called lift and drag. Lift acts on the airfoil in a direction perpendicular to the relative wind. Drag is the resistance or force that opposes the motion of the airfoil through the air. It acts on the airfoil in a direction parallel to the relative wind.

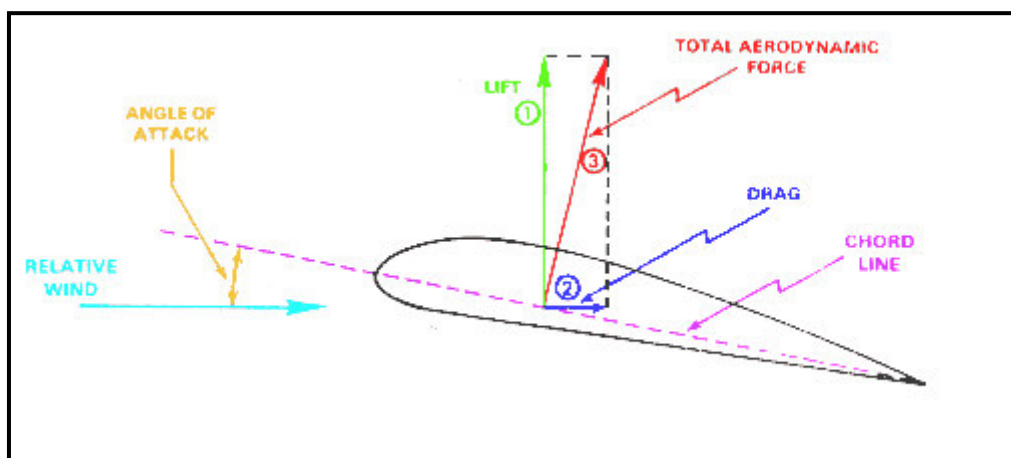


Figure II.11: Forces acting on an airfoil.

These forces are given by equation:

$$L = N \cdot \cos(\alpha) - A \cdot \sin(\alpha) \tag{7}$$

$$D = N \cdot \sin(\alpha) + A \cdot \cos(\alpha) \tag{8}$$

Where:

$$\begin{cases} N = - \int_{LE}^{TE} (p_u \cos(\theta) + \tau_u \sin(\theta)) dS_u + \int_{LE}^{TE} (p_l \cos(\theta) + \tau_l \sin(\theta)) dS_l \\ A = \int_{LE}^{TE} (-p_u \sin(\theta) + \tau_u \cos(\theta)) dS_u + \int_{LE}^{TE} (p_l \sin(\theta) + \tau_l \cos(\theta)) dS_l \end{cases} \tag{10}$$

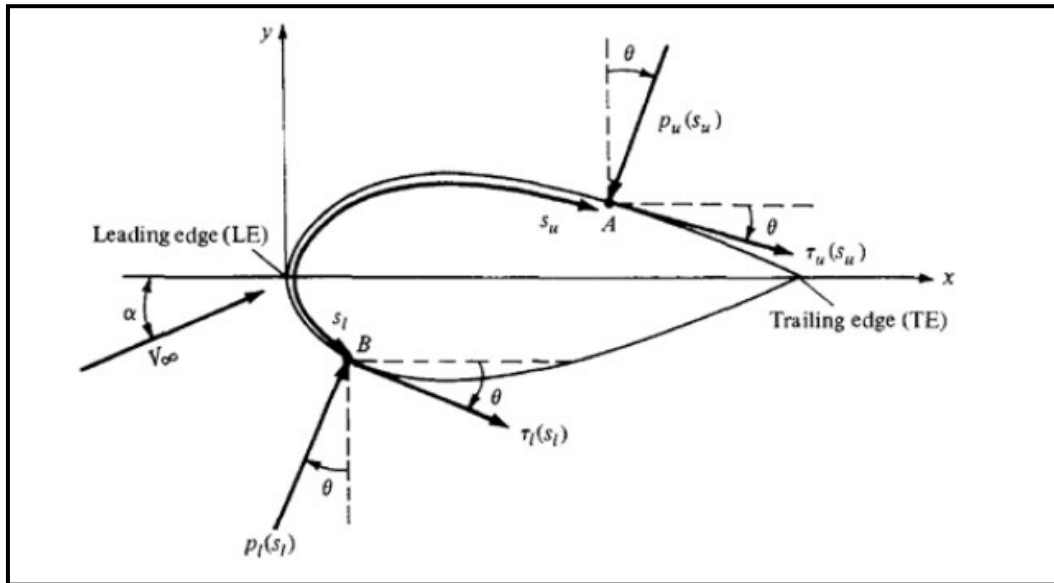


Figure II.12: Forces Applied on the upper and lower surfaces of a body.

The forces and moment depend on a large number of geometry and flow parameters. It is often advantageous to work with non dimensionalized forces and moment, for which most of these parameter dependencies are scaled out. For this purpose we define the following reference parameters [20]:

- ❖ Reference area: **S**
- ❖ Reference length: **L**
- ❖ Free stream dynamic pressure: $q_\infty = 1/2 \cdot \rho_\infty V_\infty^2$

- The lift coefficient : $C_L = \frac{L}{q_\infty S}$
- The drag coefficient : $C_D = \frac{D}{q_\infty S}$

For two dimensional bodies such as airfoils, the appropriate reference area/span is simply the chord C , and the reference length is the chord as well. The local coefficients are then defined as follows:

- The lift coefficient : $C_l = \frac{L'}{q_\infty \cdot C}$
- The drag coefficient: : $C_d = \frac{D'}{q_\infty \cdot C}$

VI. Compressor blades cooling

In order to improve the performances of the compressor many techniques of cooling were adopted to decrease the temperature of the compressor blades and to improve the resistance of the alloys used.

The technology of cooling the compressor components, primarily via internal convective flows of single-phase gases and external surface film cooling with air, has developed over the years into very complex geometries involving many differing surfaces, architectures, and fluid surface interactions. The fundamental aim of this technology area is to obtain the highest overall cooling effectiveness with the lowest possible penalty on the thermodynamic cycle performance. As a thermodynamic Brayton cycle, the efficiency of the compressor can be raised substantially by increasing the firing temperature. Modern compressors are fired at temperatures far in excess of the material melting temperature limits. This is made possible by the aggressive cooling of the hot gas path components using a portion of the compressor discharge air. Cooling is necessary to reduce the blade metal temperature to acceptable levels for the materials increasing the thermal capability of the engine.

A wide range of internal and external cooling arrangements has been applied in the past; however, the aim in both cases is to keep the entire blade cool enough and also to ensure that temperature gradients within the blade (which might lead to thermal stresses) are kept to an acceptable level [21].

VI.1 Cooling techniques

VI.1.1 Forced internal convection

This is the oldest cooling techniques. The aim is to the fresh air through channels inside the blade .This technique has gradually evolved into multi-pass systems, equipped with devices such as awnings, disturbances or spikes in order to generate thermal pumping and to improve transfers by increasing turbulence[23].

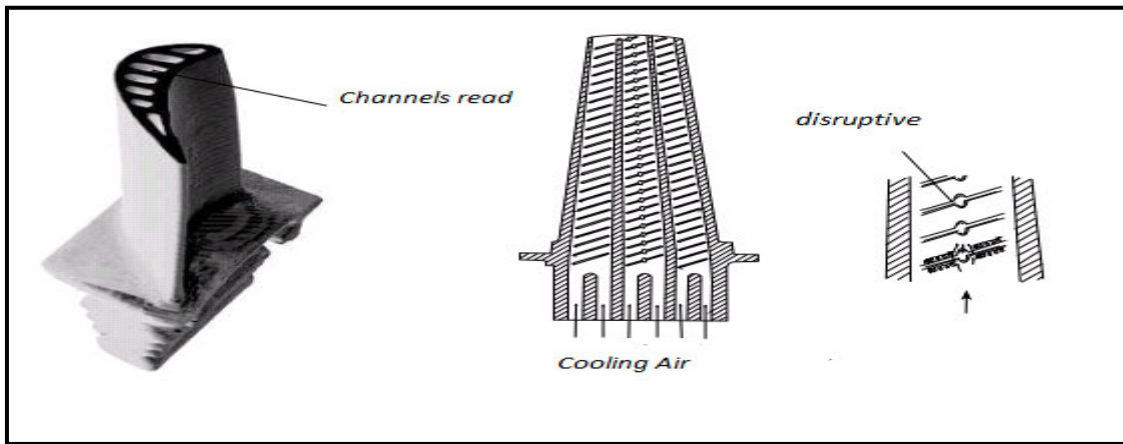


Figure II.13: Forced internal convection cooling.

VI.1.2 Film-cooling:

This involves creating a film of fresh air that protects the outer wall of the blade. The creation of this film is generally carried out by injecting air through several rows of orifices of small diameter and inclined in the direction of flow.

There are also films created by perspiration through porous materials and by effusion through several multi perforated wall layers. The major disadvantage of the film-cooling is that it is strongly degraded by the deposition of the soot particles and combustion residues that obstruct perforations and compromise efficiency of the cooling. This technique, while offering good thermal protection, is penalizing in terms of aerodynamic efficiency because it is highly disruptive the external flow around the blades and remains the subject of numerous studies [23].

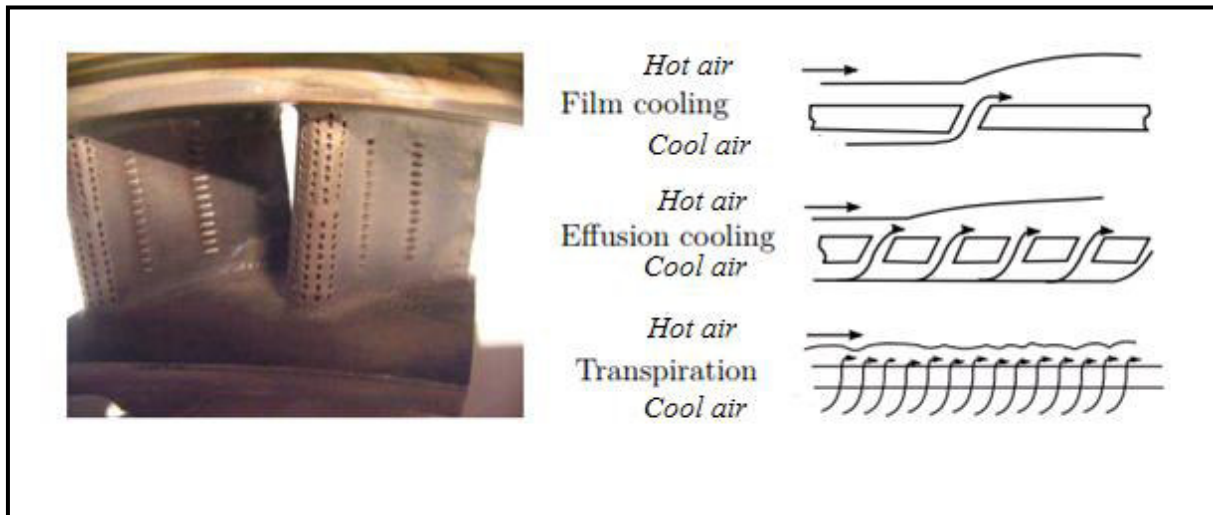
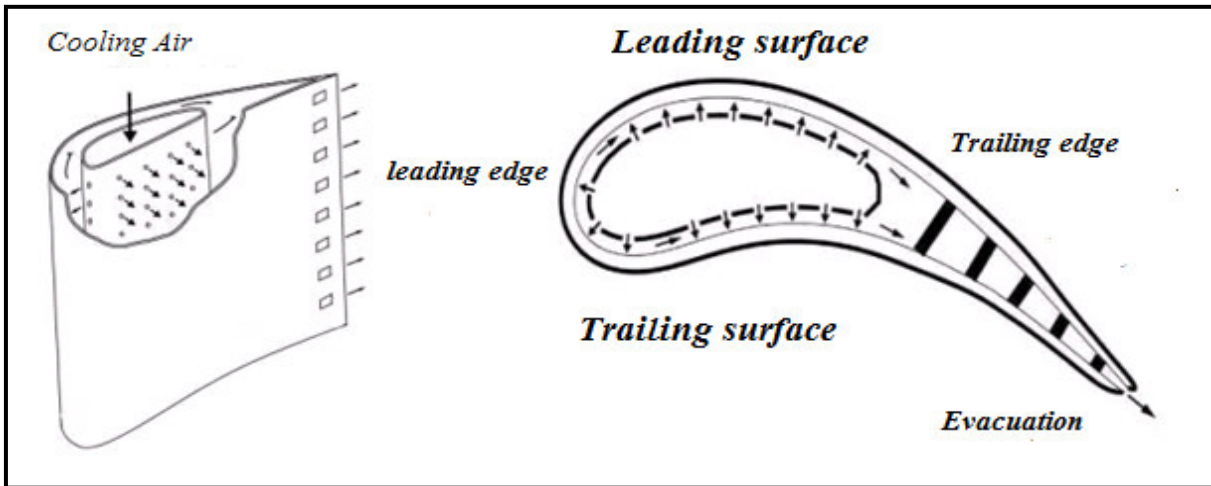


Figure II.14: Film Cooling.

VI.1.3 Impact of jets:

The technique of jet impact consists in shuffling the blade and drilling several orifices in this shirt. The jacket is supplied with fresh air and jets of air are formed at the outlet of the orifices and cool the inner wall of the turbine blades. The exchange coefficients obtained with this method are very high, which makes it very effective. This is why it is used in particular on the leading edge of the blades, In concentrated impact, because this part is particularly exposed to the heat flux outside. A distributed impact (jets matrix) is often introduced on the part Upstream of the intrados and the extrados of the dawn [23].



FigureII.15: Impact of jet cooling

VI.1.4 Couplings of cooling methods:

Often these methods are coupled to optimize the cooling of the compressor blades. This makes the design of these elements complex and geometric and aerodynamic parameters are then taken into account. The monkey-Those responsible for designing these elements must therefore find the best compromise between manufacturing cost, thermal protection, aerodynamic efficiency, resistance mechanical and lifetime [23].

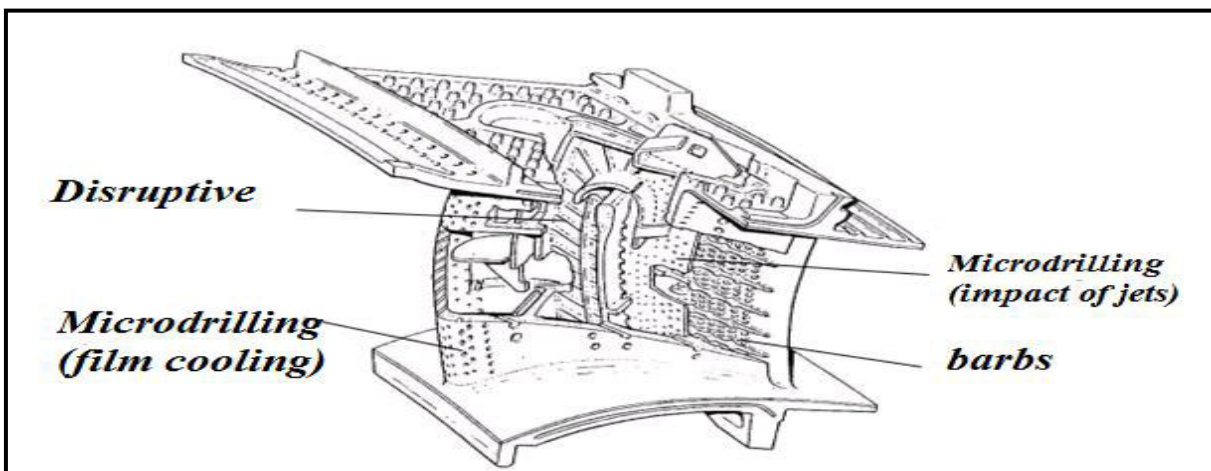


Figure II.16: Representation of a blade and its cooling systems.

VI.2 Film Cooling:

The primary process by which film cooling reduces the heat transfer to the wall is by reducing the gas temperature near the wall, reducing the driving temperature potential for heat transfer to the wall. As the coolant flows from the coolant holes, it mixes with the mainstream gas resulting in an increase in coolant temperature.

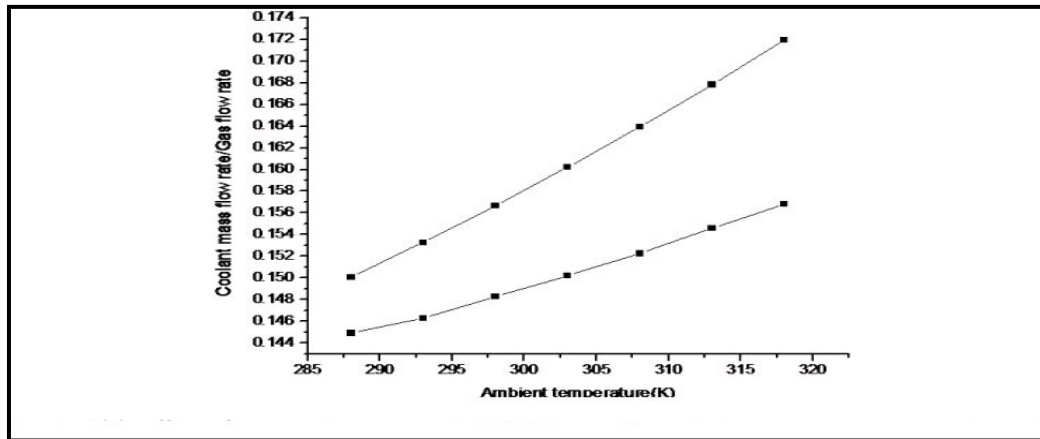


Figure II.17: coolant mass flow rate effect on the ambient temperature.

Film cooling is one of the major technologies allowing today's compressors blades to obtain extremely high firing temperatures, subsequent high efficiencies, and longer life parts. The art and science of film cooling concerns the bleeding of internal component cooling air through the external walls to form a protective layer of cooling between the hot gases and the component external surfaces. The application of effective film cooling techniques provides the first and best line of defense for hot gas path surfaces against the onslaught of extreme heat fluxes, serving to directly reduce the incident convective heat flux on the surface. Fundamental early research concentrated on nearly ideal film cooling formed by a two-dimensional layer.

Goldstein provides a thorough summary of the theory, modeling, and experimental studies surrounding such idealized film cooling layers. Because of its high importance and widespread application, research into the many aspects of film cooling has seen a tremendous increase in the last ten to fifteen years. The publications relating directly or indirectly to film cooling deal with the major effects of film hole internal fluid dynamics, interactions with the mainstream gas flow, turbulence and vorticity production, effects of approach flows prior to the hole entry, hole shaping, orientation, and spacing, hole length-to-diameter ratio, density ratio, blowing strength, momentum flux ratio, effects of mainstream turbulence intensity, mainstream acceleration, external surface curvature, and external surface roughness [22].

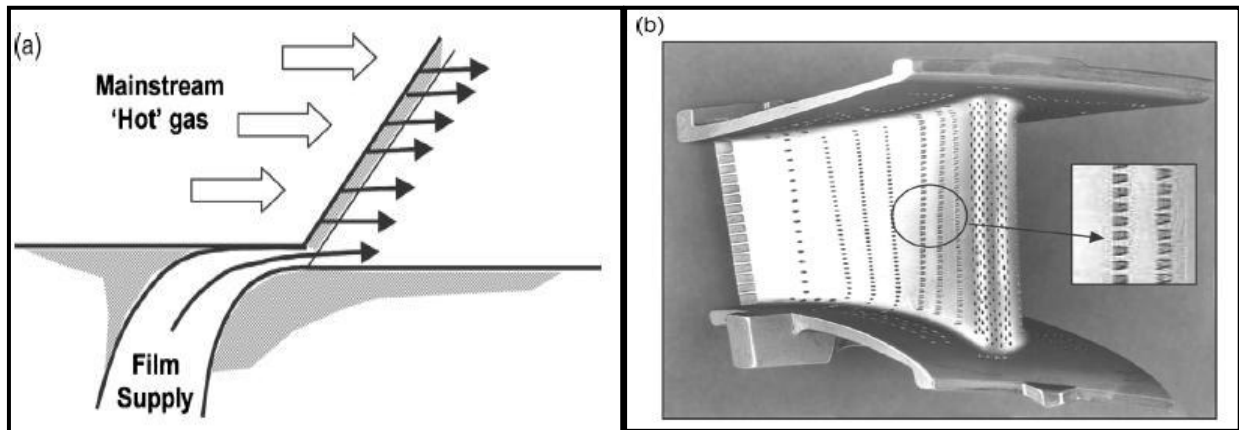


Figure II.18: (a) Idealized two-dimensional film cooling; (b) typical film cooled turbine inlet guide vane.

Conclusion:

The aerodynamics of blades is governed by the fluid mechanics equations such as the mass conservation, momentum conservation and energy conservation, and aerodynamic principles those equations and principles let us better understand the behavior of the fluid and the effect of the fluid upon the solids, all those effects are governed by norms represented by different parameters like the Reynolds number and the Mach number.

to improve the performances of the compressor many techniques of cooling were adopted to decrease the temperature around the compressor blades in order to make it more resistant.

Chapter III

Numerical simulation

I. Introduction

Turbomachinery Aerodynamicists have long realized that the flow within multistage is complex, they wanted to study the effect of the fluid on and around the components of the turbomachinery like the compressor blades in order to find the applied force and moments there in a fast and accurate analysis method called the computational fluid dynamic (CFD)

(CFD) has been made around the early 20th century, it includes the use of applied mathematics, physics and computational software to visualize how a gas or liquid flows as well as how it affects objects as it flows past.

In this chapter, we will see a numerical simulation of the flow behavior around compressor blade with the help of (CFD) and the effect of aerodynamic forces on the blade surface. For this purpose this chapter is decomposed into two main sections: the first section using the Gambit software to design the geometries and the CFD tool software Fluent to study the flow behavior around the blade.

II. The Gambit software:

Gambit is a 2D/3D Geometry and mesh generator to help analysts and designers build and mesh models for computational fluid dynamics (CFD) and other scientific applications use. Gambit software has three main functions:

- Definition of the geometry of the object
- Creation of the Mesh
- Definition of borders (Boundary conditions) and definitions of fields calculations.

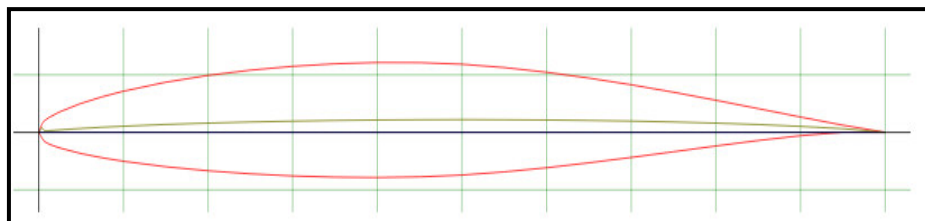
But in this case we only used Gambit software to define the geometry of the blade and the others we will be using Fluent software.

• Geometry Model:

This step consists of drawing the geometry of the compressor blade profile and the surrounding fluid domain around the blade using the Gambit software. For this 2D work we will draw:

- Isolated compressor blade with the coordinates of the blade profile.
- A square fluid domain around the compressor blade.

The profile used is: NACA 65-10% - airfoil



II.1 First step: Isolated compressor blade:

The geometry of the blade profile are done by the gambit software, the first thing we do is to import the blade coordinates into the Gambit software the result will be shown in the Figure II.1:

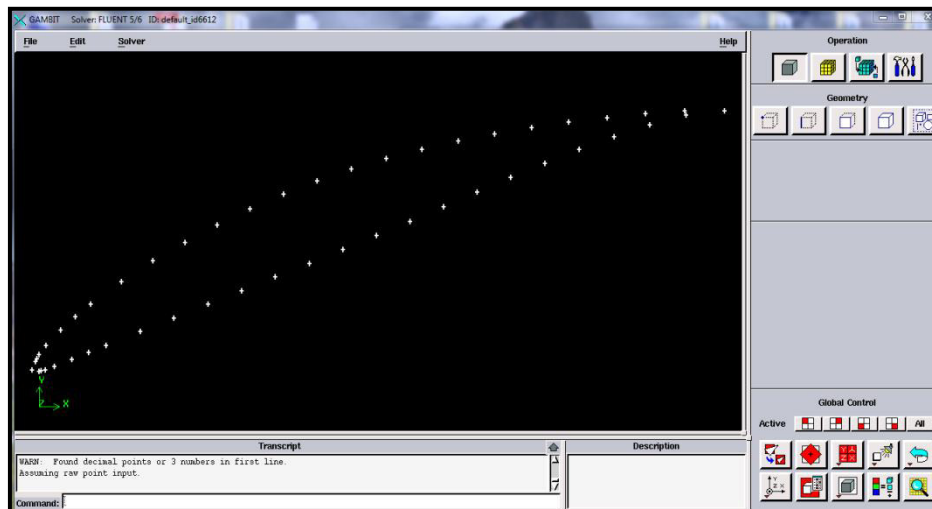


Figure III.1: blade structure with the coordinates.

After importing the blade coordinates we have to draw the blade by creating the edges. after that the geometry of the blade is completed like it's shown in the Figure II.2:

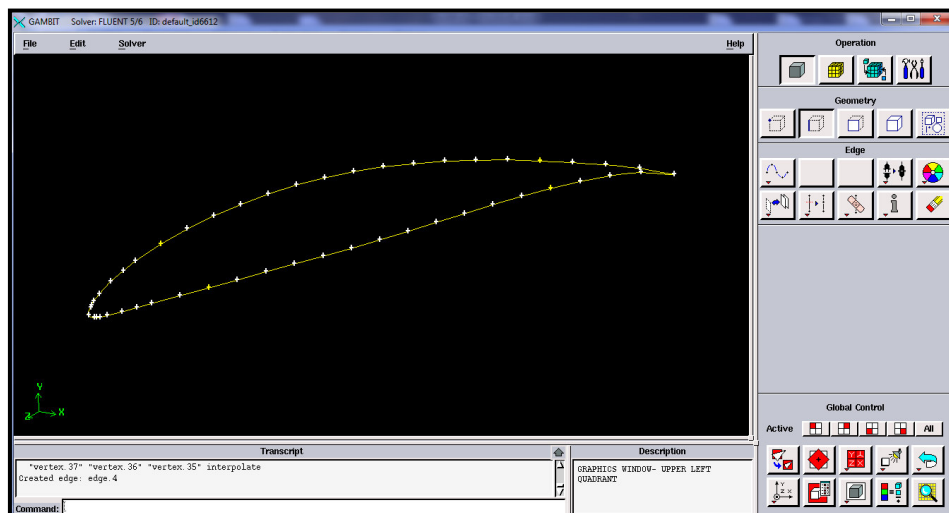


Figure III.2: Blade geometry

II.2 Second step: The fluid domain

To study the fluid flow behavior around the compressor blade, we have to create a fluid domain around the compressor blade, for that we create a square domain following this table:

Vertex (Label)	X (cm)	Y (cm)
A	2.1	-2.1
B	2.1	2.1
C	-2.1	2.1
D	-2.1	-2.1

The points A, B, C, D are created in the axes X and Y because of the 2D geometry of the blade compressor.

After finishing from the domain fluid we have to specify the faces of the geometries that we have and for that we need to create two faces (The blade face and the fluid domain face). And extract the blade face from the fluid zone surface as it is illustrated in the Figure II.4:

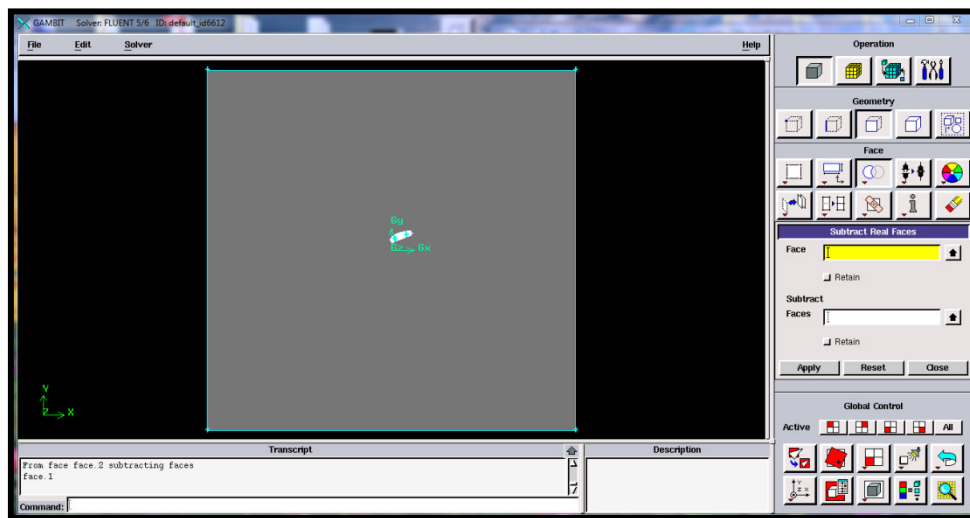


Figure III.3: The fluid zone surface without the blade surface.

Now we have the geometry of the fluid domain and the blade ready to be exported to the ANSYS tool software FLUENT for meshing the blade geometry and its fluid zone.

III. Fluent simulation software:

ANSYS Fluent software is one of the most powerful computational fluid dynamics (CFD) software tools available. It contains the broad physical modeling capabilities needed to model flow turbulence, heat transfer, and reaction for industrial applications ranging from air flow over an aircraft wing to combustion in a furnace and much more.

- **2D simulation:**

III.1 Meshing the Geometry:

After importing the Geometry from Gambit software to ANSYS tool software Fluent, the meshing part is the most important part of this simulation, the extent of accuracy of result depended to a great extent of the fact that how fine the physical domain was meshed.

- Mesh Report :

Table III.1 Mesh information

Domain	Nodes	Elements
Face	9298	4427

Table III.2: Names of the Edges of the Geometry.

Edge	Name
Left	Inlet
Right	Outlet
Above	Upper Wall
Under	Lower Wall

For the 2D modeling geometry the physical model meshed is illustrated in the figure III.1:

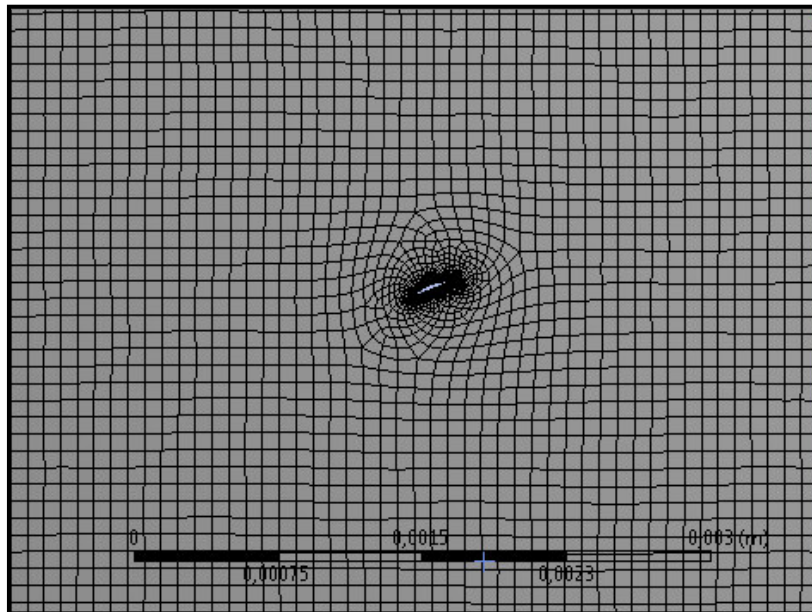


Figure III.4: Geometry meshed.

III.2 Flow properties and Results:

The fluid inside the compressor is the Air so the study was performed in terms of the inlet Mach number and inlet positive flow incidence angles:

- Fluid : Air (Ideal Gas)
- Type: Density Based.
- Time: Steady.
- Energy equation : ON

III.3 Boundary conditions:

The boundary conditions used are as follow:

Table III.3: Boundary conditions of the geometry.

Elements	Boundary conditions
Inlet	Pressure far-field
Outlet	Pressure outlet
Airfoil edges	Wall
Upper and lower edges	Periodic
Table III.4: Input and output conditions for the simulation.	
Flow type	Steady/Viscous(spalart-Allmaras turbulence model)
Inlet pressure	Atmospheric pressure 101300 Pa
Outlet pressure	120560
Temperature	300 K
Mach number	0.6
Angle of attack	45°

III.4 Calculation of drag and lift forces:

From the fluent software, we have the results of lift and drag coefficients for each case. We can calculate the lift and drag forces using the relations shown below.

To calculate the drag force:
$$D = \frac{1}{2} \rho V^2 C_d$$

And the lift force using:
$$L = \frac{1}{2} \rho V^2 C_L$$

The resultant force we can calculate by the relation:

$$R = \sqrt{F_x^2 + F_y^2}$$

With:

- $\rho = 1,225 \text{ kg/m}^3$
- $V = 100 \text{ m/s}$

After running the calculation of our Fluent software we found the drag and the lift coefficient

- The lift coefficient : $-2.1939\text{e-}03$
- The drag coefficient : $1.5106\text{e-}03$

So calculation the lift force: $F_y = \frac{1}{2}\rho V^2 C_L \rightarrow F_y = 12.32 \text{ N}$

And for the drag force: $F_d = \frac{1}{2}\rho V^2 C_d \rightarrow F_D = 8.46 \text{ N}$

The resultant force is: $R = 14,89 \text{ N}$

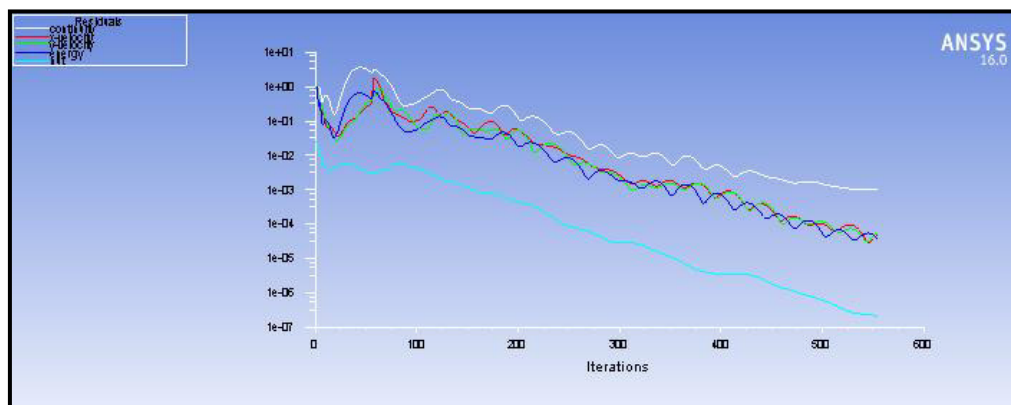


Figure III.5: Scaled residuals.

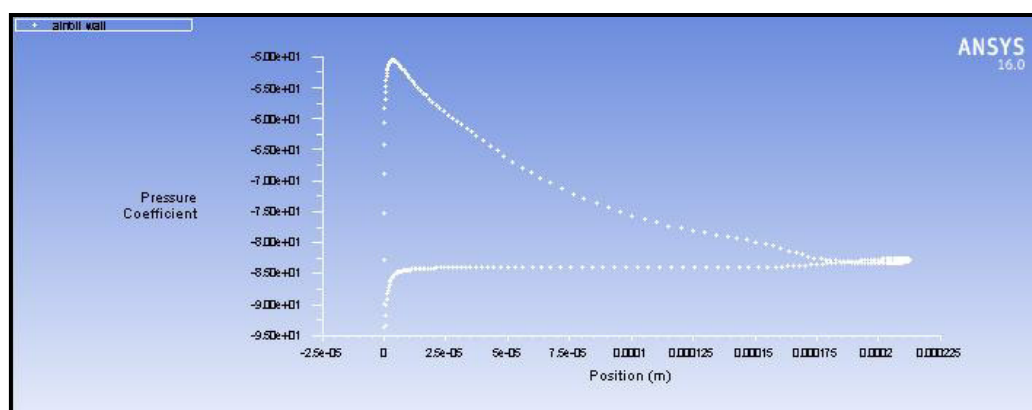


Figure III.6: Pressure coefficient around the profile.

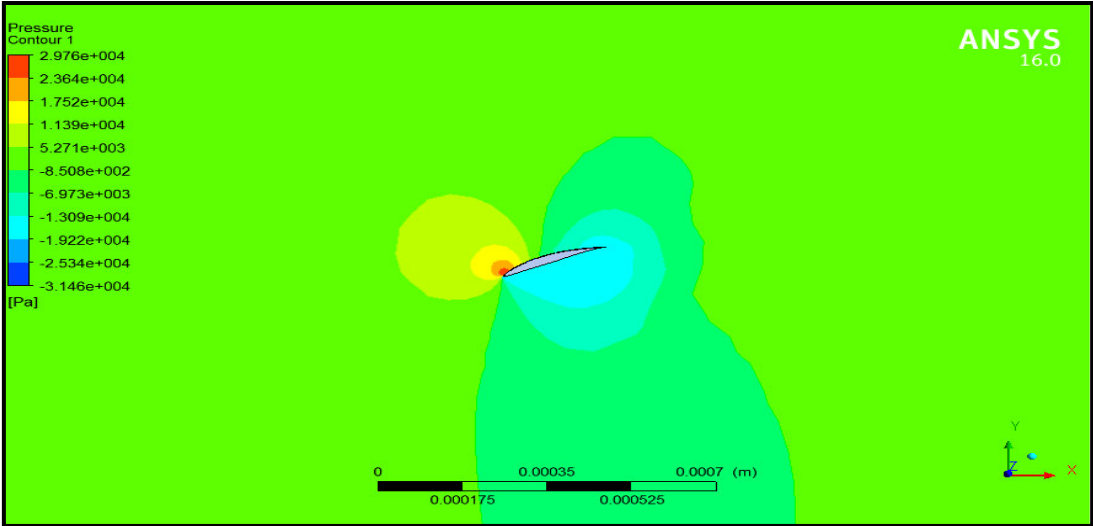


Figure III.7: Pressure contours.

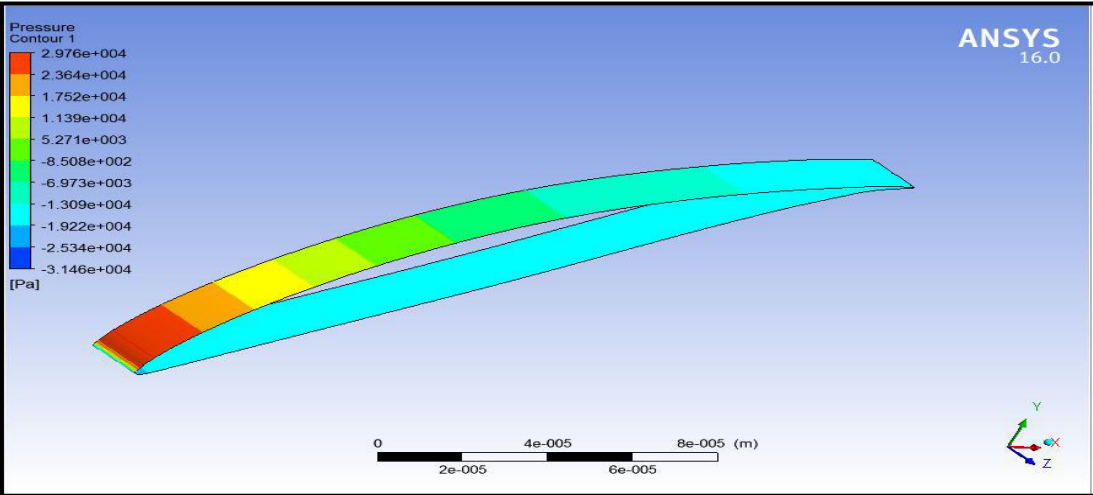


Figure III.8: Pressure contours of the Airfoil wall.

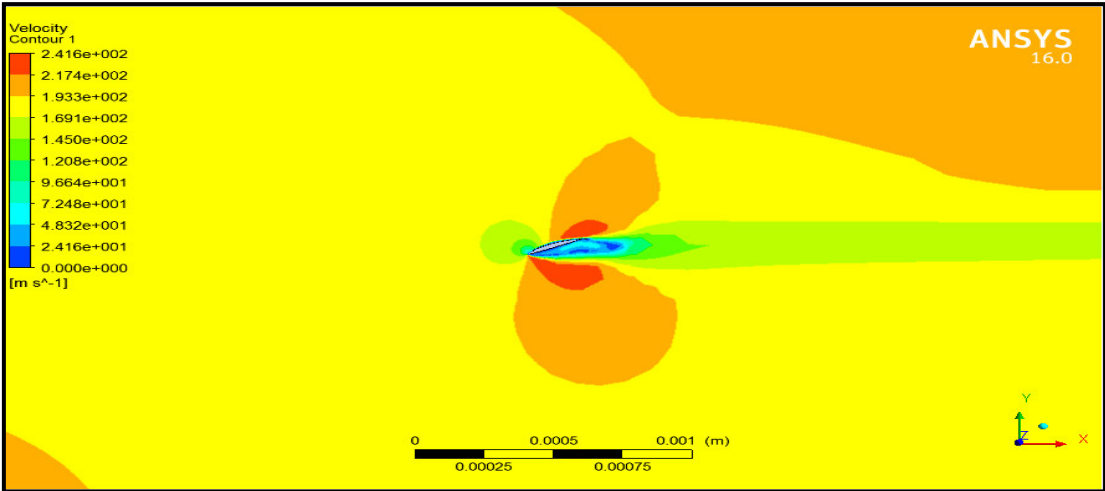


Figure III.9: Velocity contour.

IV. ANSYS simulation Software:

IV.1 SOLIDWORKS Software:

SOLIDWORKS design software is as simple as it is powerful, enabling any company to bring its vision to life and capture global markets.

SOLIDWORKS solutions focus on the way you work every day, with an intuitive integrated 3D design environment that covers all aspects of product development and helps maximize your design and engineering productivity. Over 2 million designers and engineers worldwide use SOLIDWORKS to bring designs to life from the coolest gadgets to innovations for a better tomorrow.

IV.2 Static structure ANSYS Analysis:

A static structural analysis determines the displacements, stresses, strains, and forces in structures or components caused by loads that do not induce significant inertia and damping effects. Steady loading and response conditions are assumed; that is, the loads and the structure's response are assumed to vary slowly with respect to time. A static structural load can be performed using the ANSYS. The types of loading that can be applied in a static analysis include:

- Externally applied forces and pressures
- Steady-state inertial forces (such as gravity or rotational velocity)
- Imposed (nonzero) displacements
- Temperatures (for thermal strain)

In this section, we are interested to find the maximal deformation, Von-Mises stress, strain of the Airfoil when it due to the aerodynamic forces.

- ✓ Boundary conditions used in static structural analysis are the same as the modal analysis but we add the force applied on the airfoil surface.

After creating a 3D design In SOLIDWORKS for the profile we imported it to the Static structural in ANSYS to Analyze and determine the displacements, stresses, strains, and forces in Different kind of structure with different changes on the profile.

IV.3 Structural steel Analysis:

- **Modal analysis:**

In modal analysis, we are interested to find the Total deformation, the Equivalent Von-Mises Strain and the Equivalent Von-Mises stress of the system using ANSYS workbench (Modal) which will serve as a base for us for the complete analysis of the system.

- ✓ Boundary condition used in modal analysis are:

Table III.5: Boundary conditions of the structure.

Fixed support	The side face (A)
The force applied	The upper surface (B)

Importing the geometry to static structural then meshing it to apply the forces on the profile as illustrated in figure IV.1:

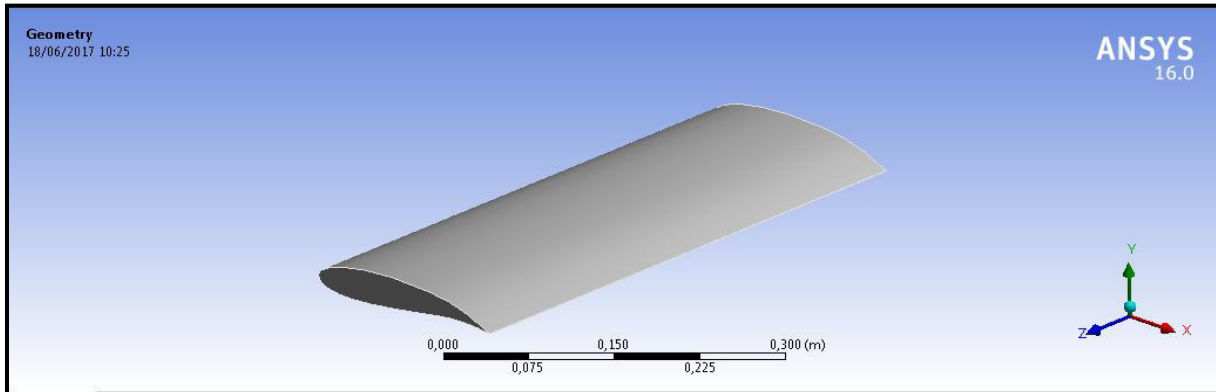


Figure III.10: Importing the geometry of the profile.

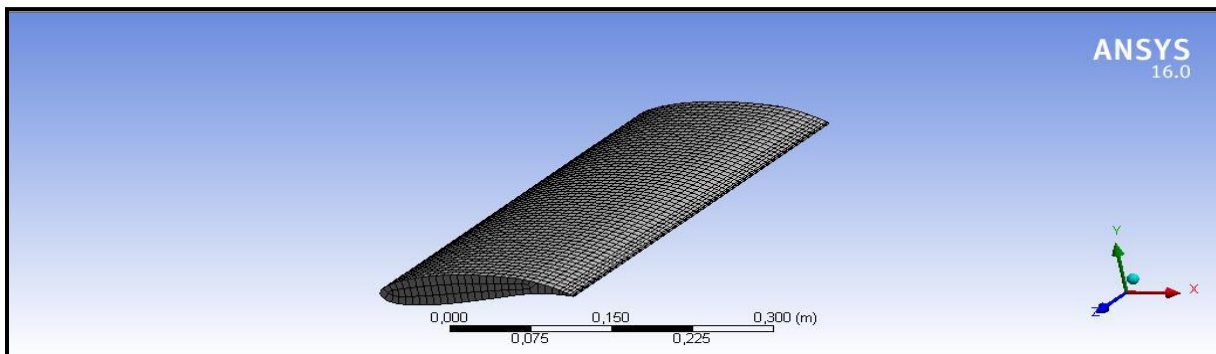


Figure III.11: Meshing the profile.

Then we apply the force on the profile with (A) is the fixed support and the (B) is the force applied on the upper surface.

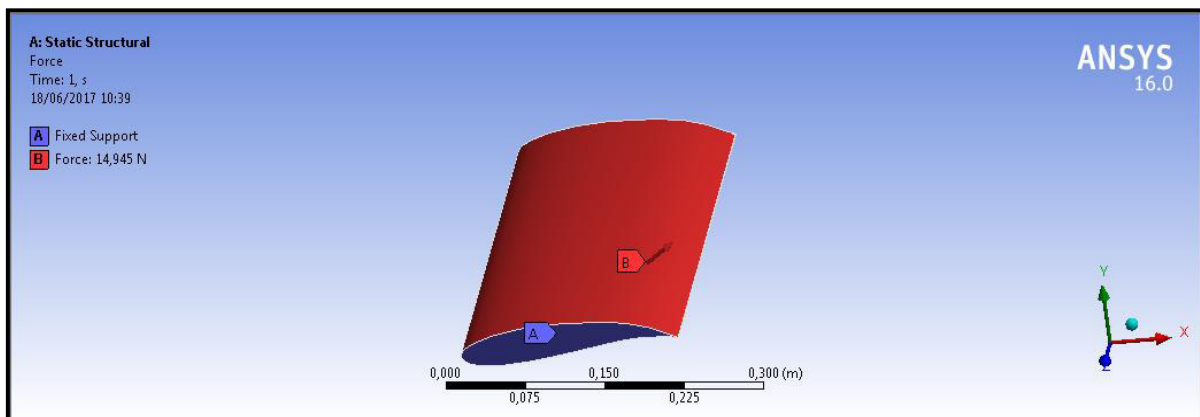


Figure III.12: Fixed support and the force applied.

In the static structure we simulate with three different materials with different properties to see any changes for both of Total deformation and Equivalent Von-Mises stress.

Table III.6: Properties of the three materials.

Materials Properties	Young Modulus (GPa)	Poisson's ratio	Density (Kg/m³)	Tensile Strength (MPa)
Steel	200	0.3	7850	340-490
Aluminum Alloy	70	0.334	2700	180-470
Titanium Alloy	115	0.32	4420	270-500

After different simulation, we have got a total deformation, Von-Mises stress which are depicted below:

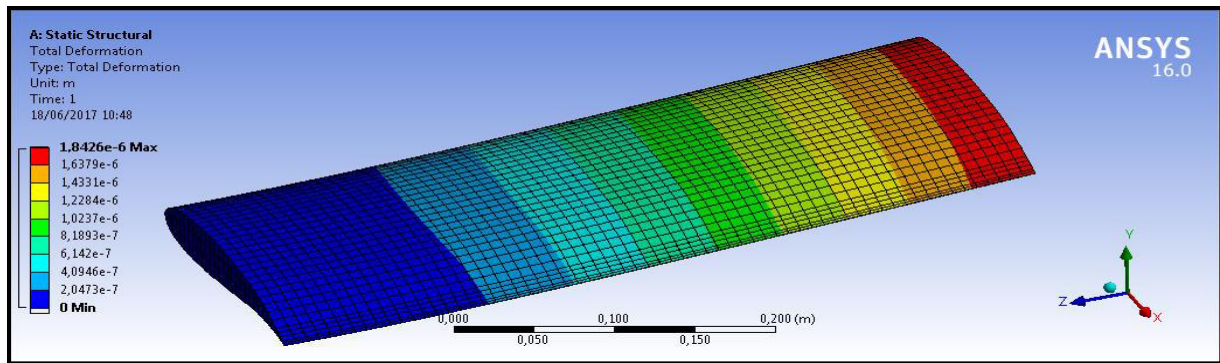
V. The different effects on Blade Materials

V.1 The number of holes effect

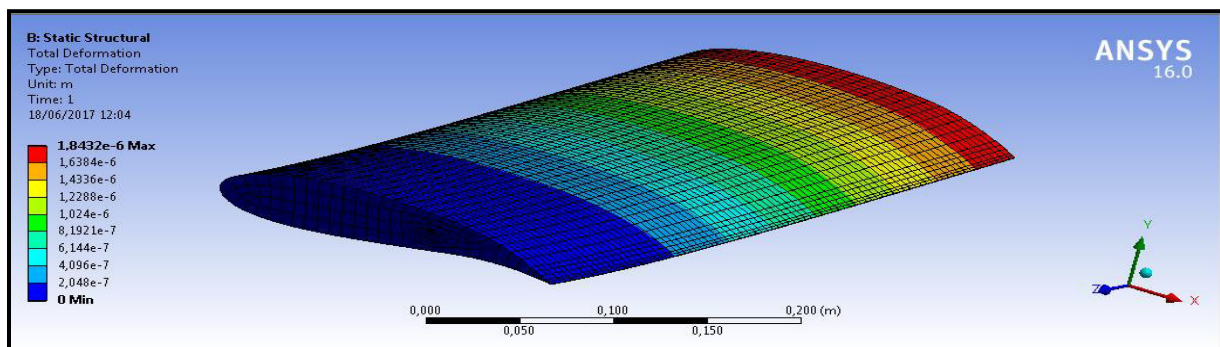
The table below shows the result analysis of the Structural steel for different number of holes done on the body and the total deformation and the Equivalent Von Mises Stress results for each case:

Table III.7 Results of stress, deformation with different number of holes.

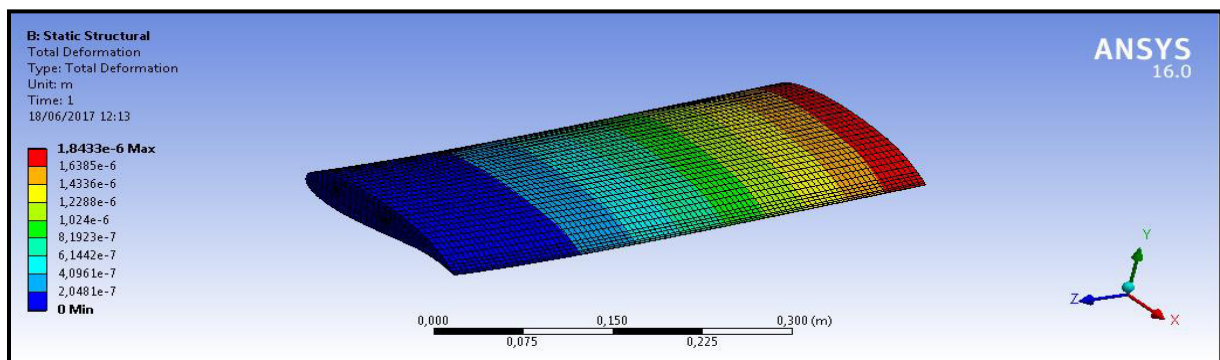
Case	Without hole	one holes	Two holes	Three holes	Five holes
Deformation	$1,8426. 10^{-6}$	$1,8432. 10^{-6}$	$1,8433. 10^{-6}$	$1,8435. 10^{-6}$	$1,8437. 10^{-6}$
Stress (Pa)	$1,0038.10^5$	$1,0142.10^5$	$1,0651.10^5$	$1,0801.10^5$	$1,1428.10^5$



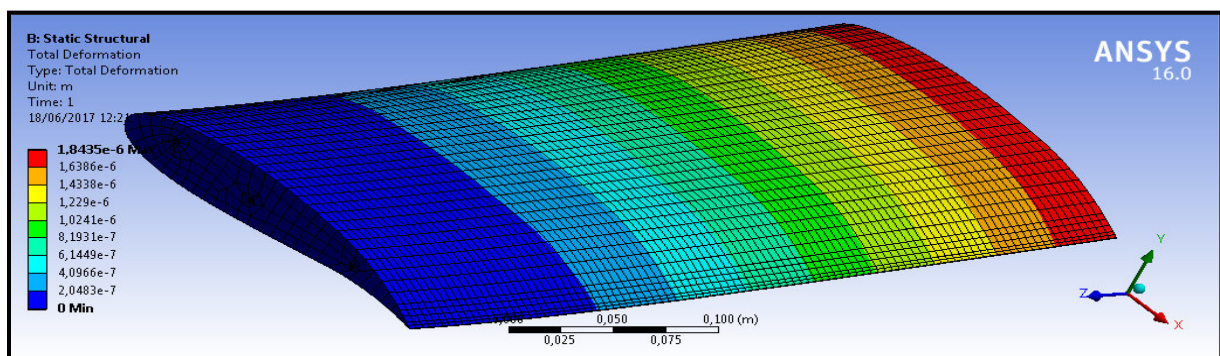
Without holes.



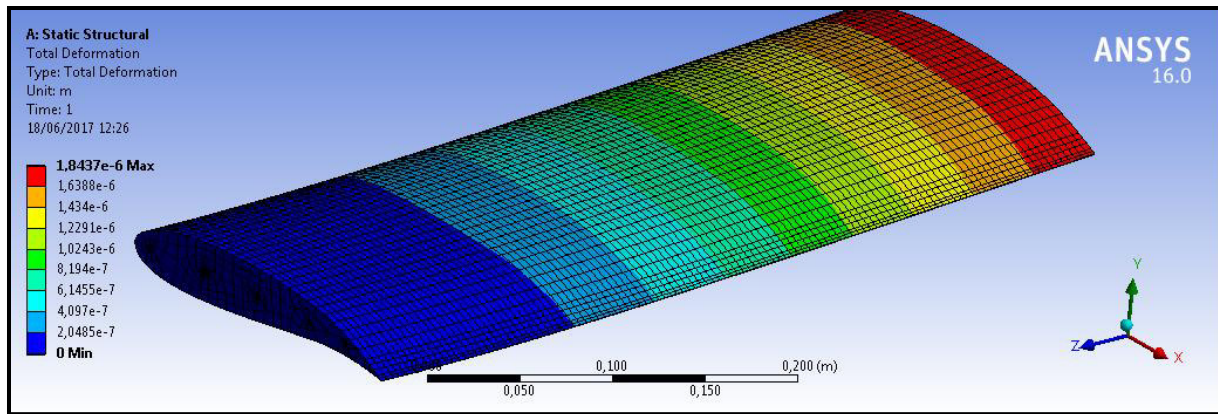
One hole.



Two holes.



Three holes.



Five holes.

Figure III.13: Total deformation for different number of holes.

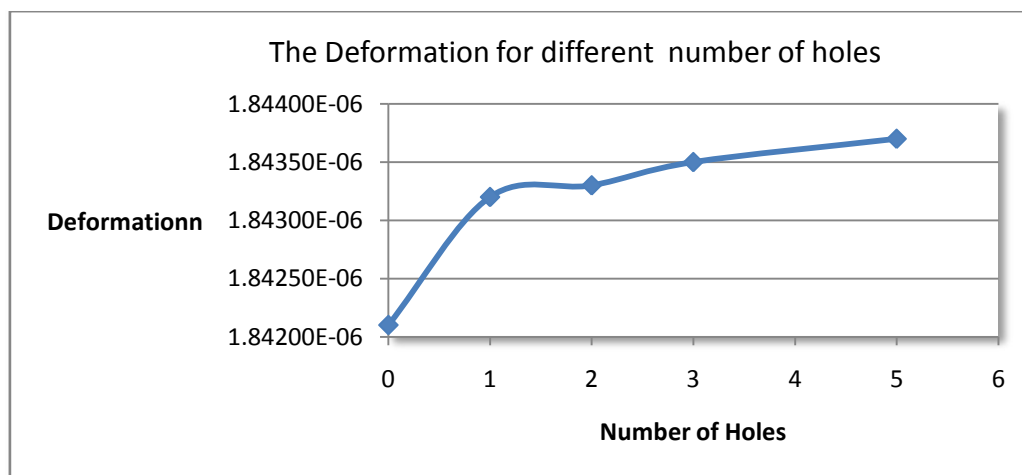
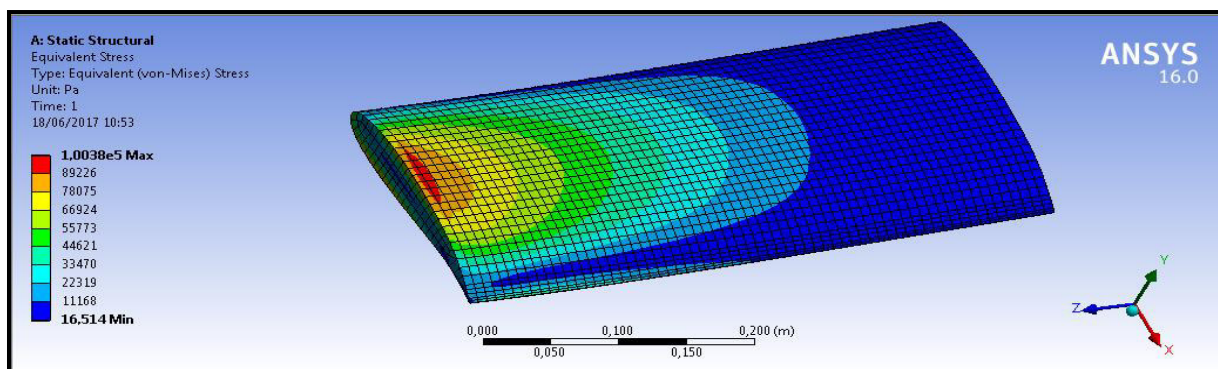
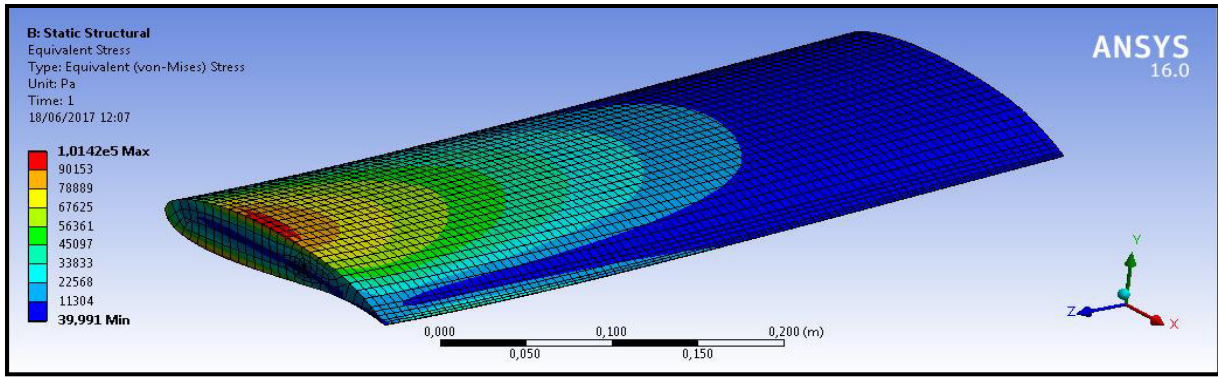


Figure III.14: Total deformation for number of holes on the blade.

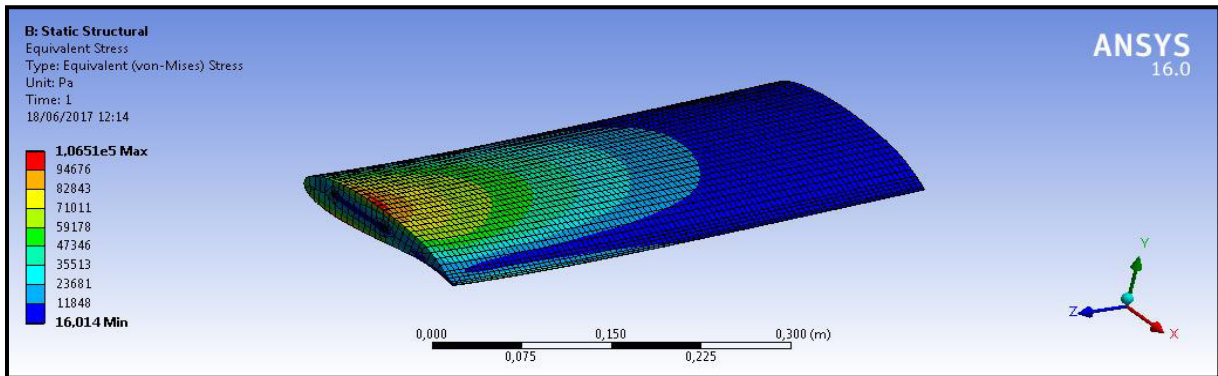
This Figure III.14 illustrates curve of the total deformation values according to the number of holes on the profile with Steel material, we observe from this curve that the total deformation increases when the number of holes increases.



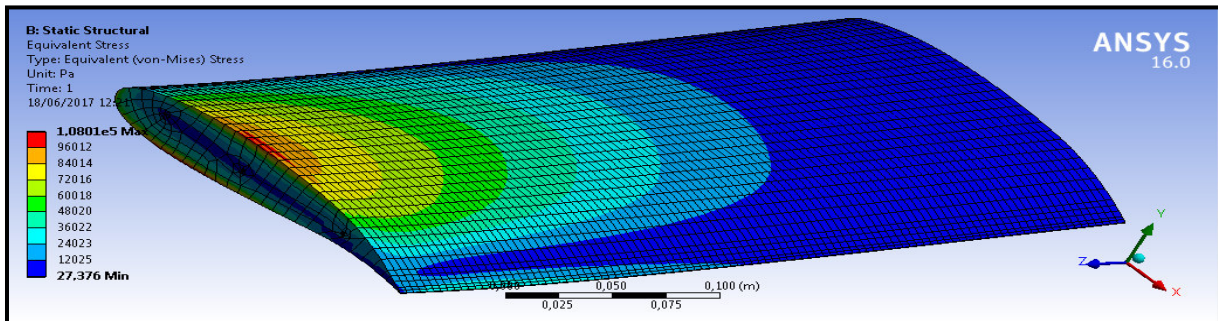
Without Hole



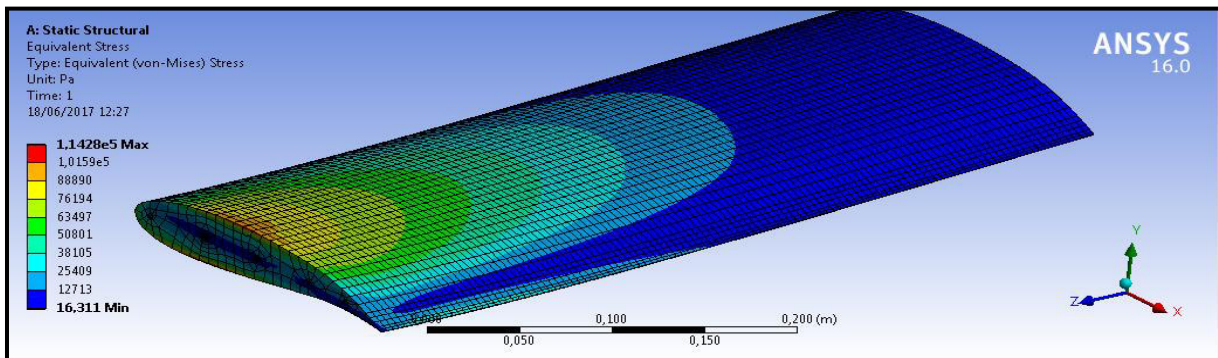
One hole.



Two holes.



Three holes.



Five holes.

Figure III.15: Equivalent Von-Mises stress for Different number of holes.

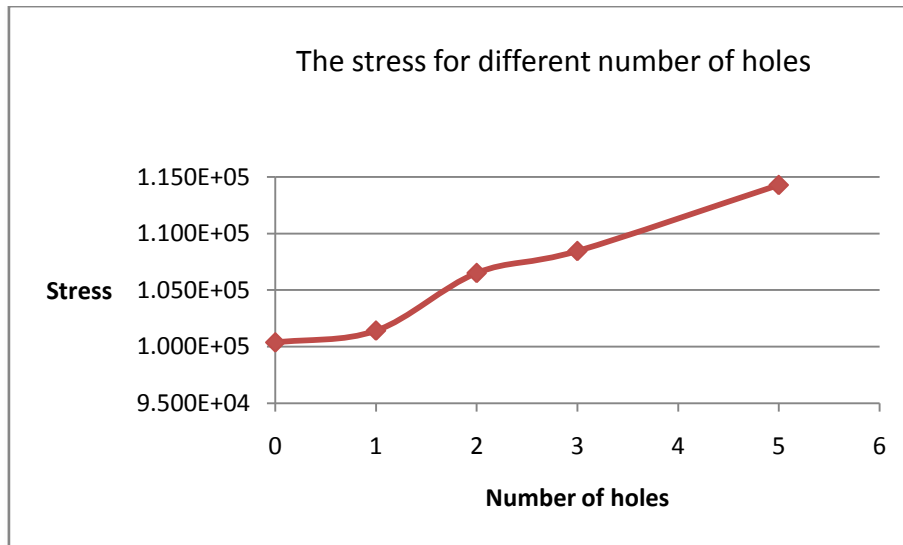


Figure III.16: The Equivalent Von Mises stress for number of holes on the blade.

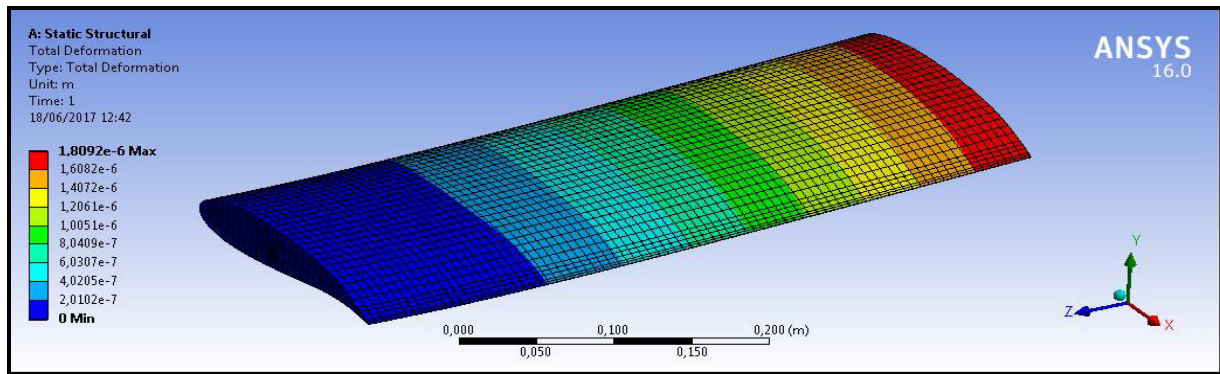
Figure III.16 shows that Equivalent Von-Mises Stress value varies increasingly in function of number of holes, where it goes up from the minimum value of $1,0038.10^5$ at number of holes(1) to reach the maximal value for $1,1428.10^5$ at the hole number (5).

V.2 The diameter of holes effect:

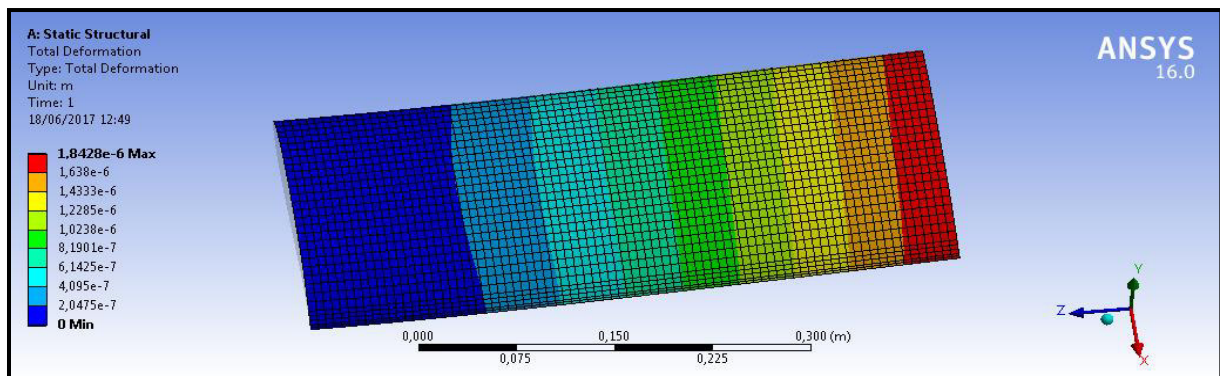
The table below shows the result analysis of the Structural steel for different Diameter of holes done on the body and the total deformation and the Equivalent Von Mises Stress results for each Diameter case:

Table III.8: Results of stress, deformation with different Diameter of holes.

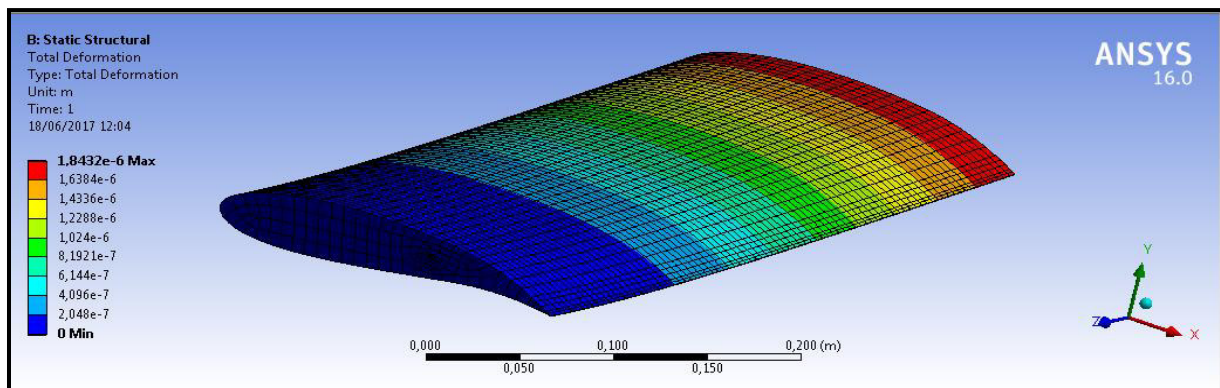
Diameters (mm)	Without hole	(a)	(b)	(c)
Deformation	$1,8092. 10^{-6}$	$1,8326. 10^{-6}$	$1,8435. 10^{-6}$	$1,8459. 10^{-6}$
Stress (Pa)	$1,0038.10^5$	$1,0142.10^5$	$1,0198.10^5$	$1,1470.10^5$



(a)



(b)



(c)

Figure III.17: Total deformation for different Diameters of holes.

Where: $a=0.1\text{mm}$

$b=0.3\text{mm}$

$c=0.6\text{mm}$

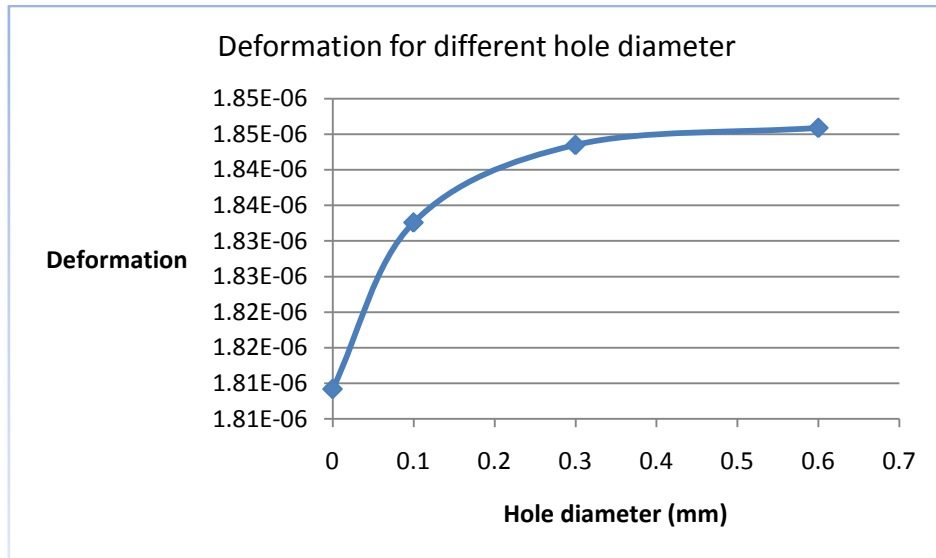
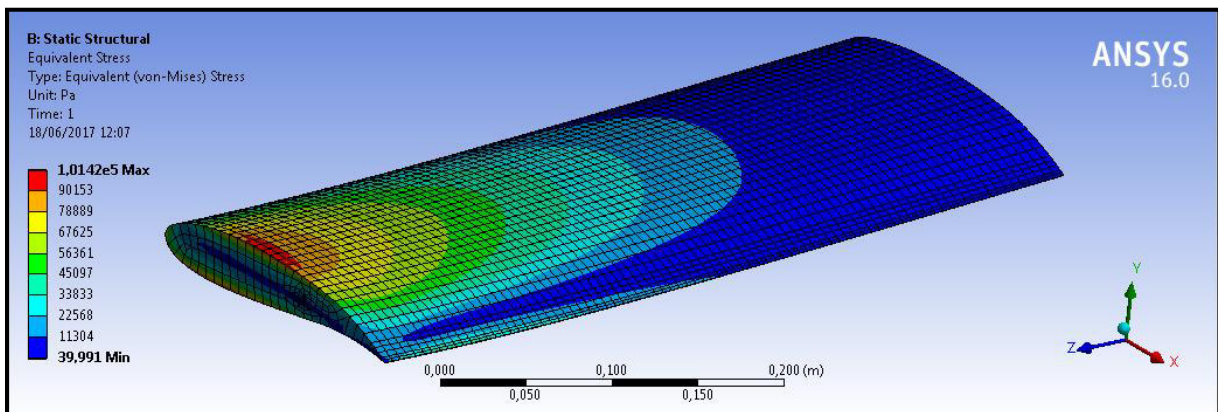
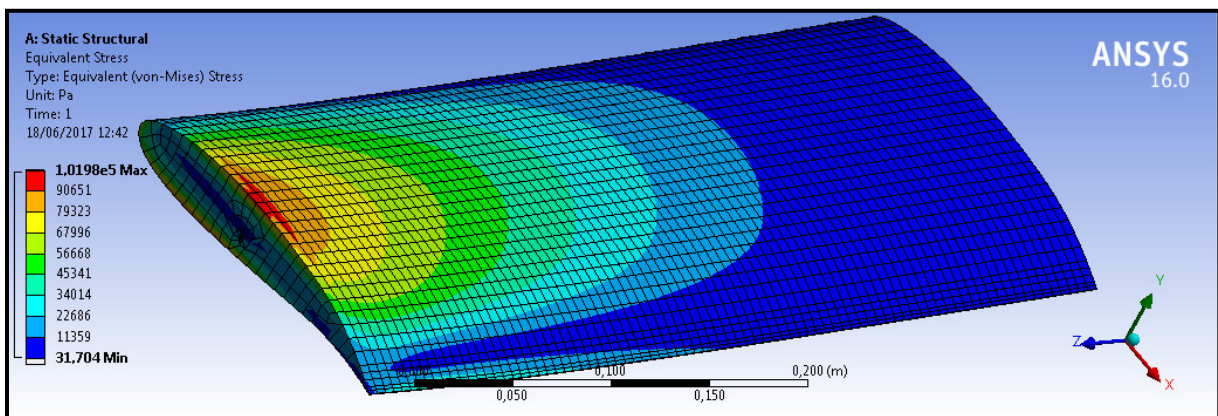


Figure III.18: Total Deformation for holes diameter.

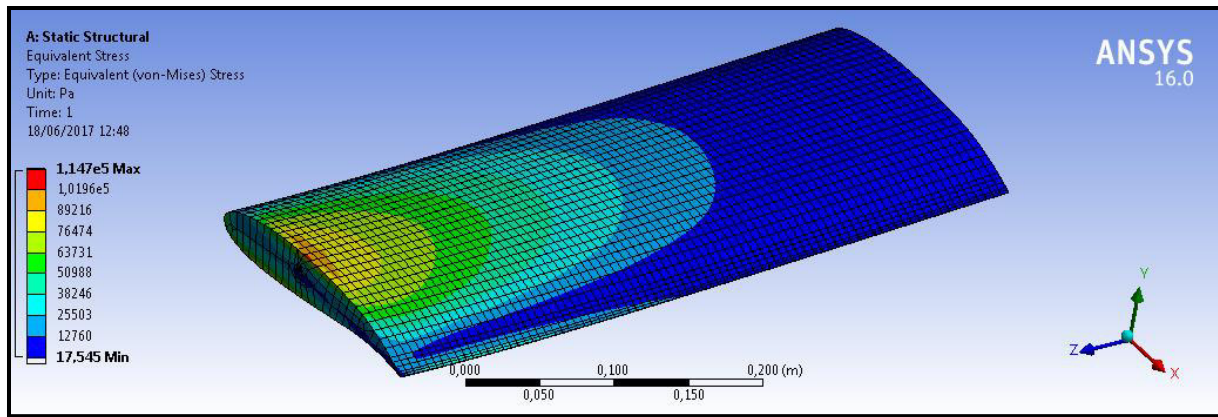
This **Figure III.18** shows the different deformation values for every diameter hole, where we notice that when there is no hole on the profile it reaches the minimum value of deformation of $1,8092 \cdot 10^{-6}$. Then it increases slowly with the changing of the diameter of the holes where it reached the maximum value of the total deformation in the diameter of 0,6mm of $1,8459 \cdot 10^{-6}$.



$\varnothing = 0.1\text{mm}$



$\varnothing = 0.3\text{mm}$



$\varnothing = 0.1\text{mm}$

Figure III.19: Equivalent Von-Mises stress for different diameters of hole.

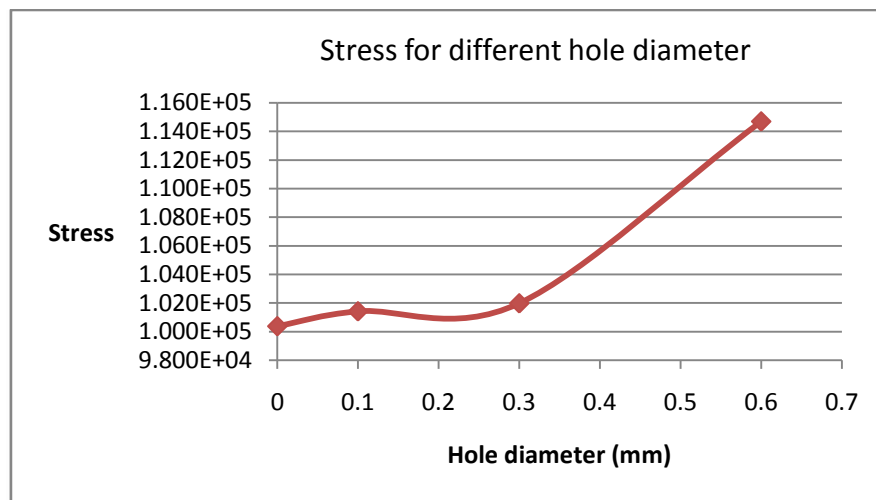


Figure III.20: Equivalent Von Mises Stress for holes diameter.

We have in the **Figure III.20** the curve of Equivalent Von-Mises Stress according to the holes diameters.

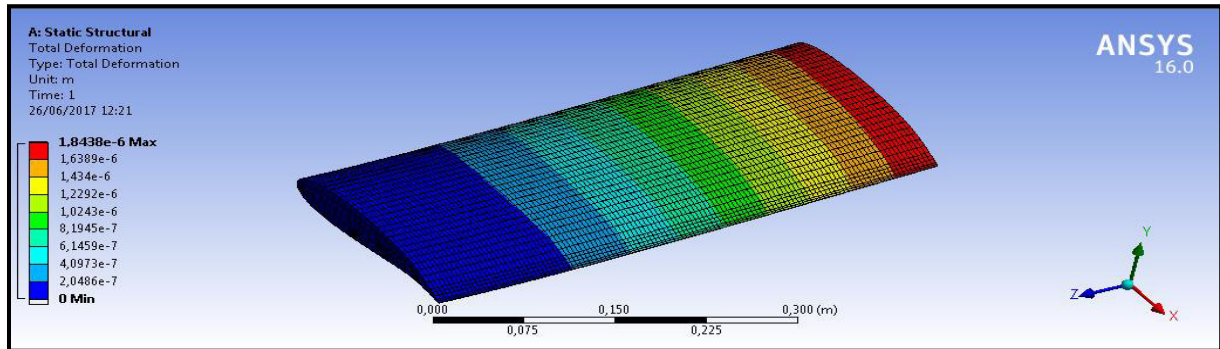
We notice that there is a proportional relationship between this two parameters, when the hole diameter increase from 0,1 to 0,3 then 0,6mm the Equivalent Von-Mises Stress also increases, where it increases smoothly from no hole diameter to 0.1mm diameter and the same thing from the 0.1mm diameter to the 0.3mm then it goes to the maximum value of $1,1470 \cdot 10^5$.

V.3 The Position of the holes effect:

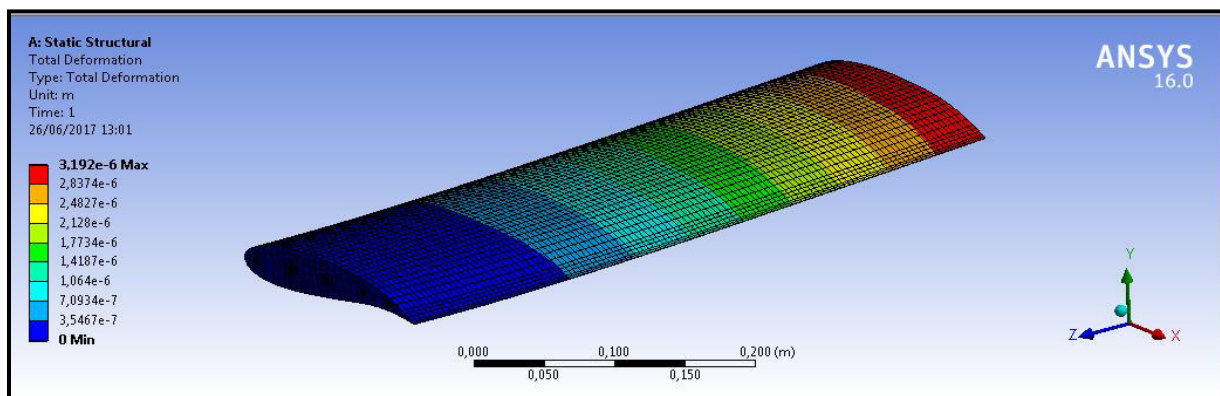
The table below shows the result analysis for different position of holes done on the body and the total deformation and the Equivalent Von Mises Stress results for each position:

Table III.9: Results of stress, deformation with different position of holes.

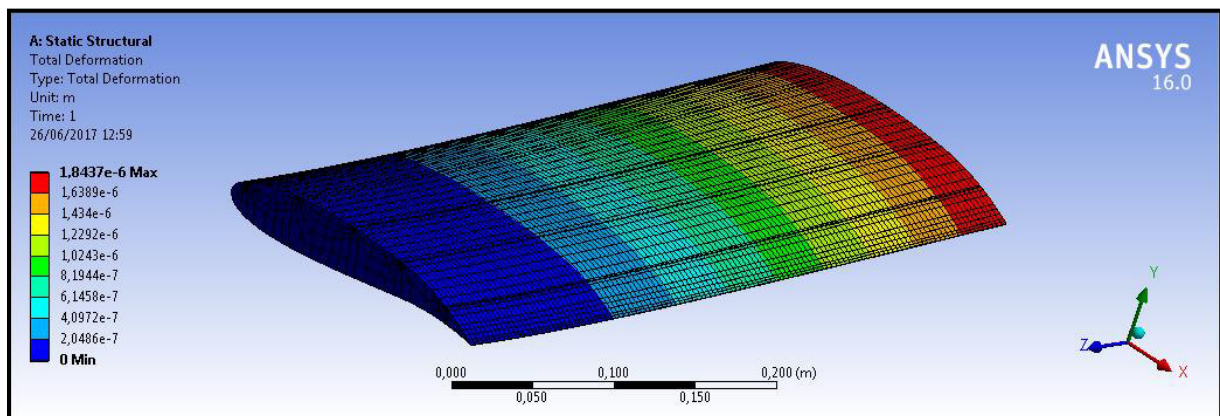
Position	High	Middle	Low
Deformation	$1,8438 \cdot 10^{-6}$	$1,8437 \cdot 10^{-6}$	$1,8437 \cdot 10^{-6}$
Stress (Pa)	$1,973 \cdot 10^5$	$1,1428 \cdot 10^5$	$2,0279 \cdot 10^5$



(A)



(B)



(C)

Figure III.21: Total deformation for the different position of the holes.

Where: A: is the lowest Position

B: is the Middle Position

C: is the Highest Position

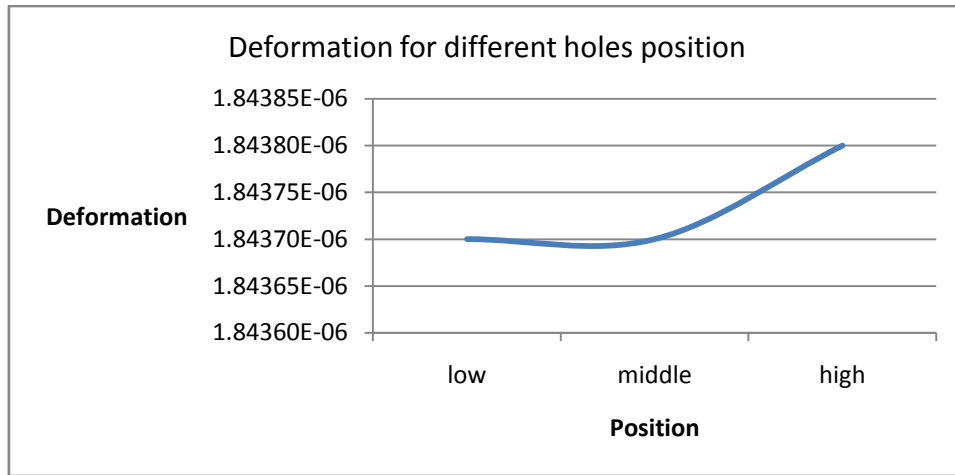
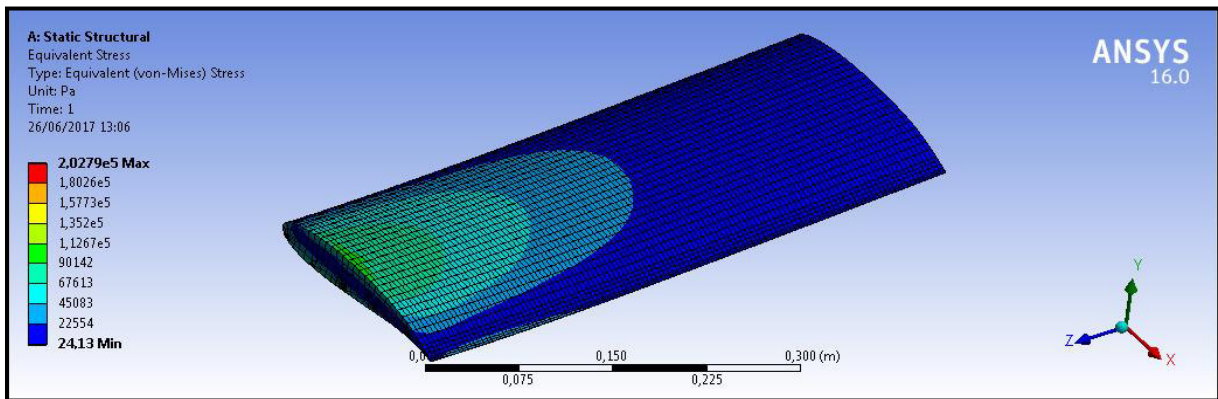
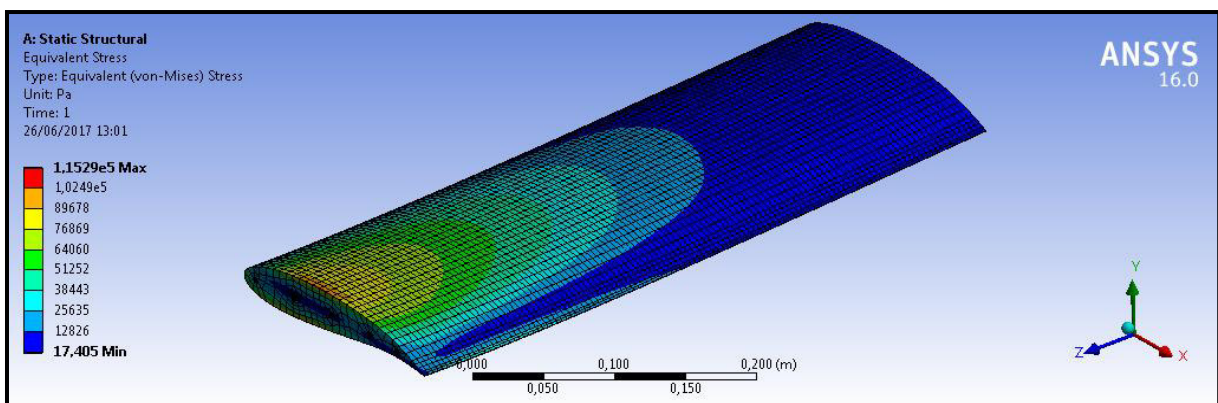


Figure III.22: Total Deformation for holes position on the blade.

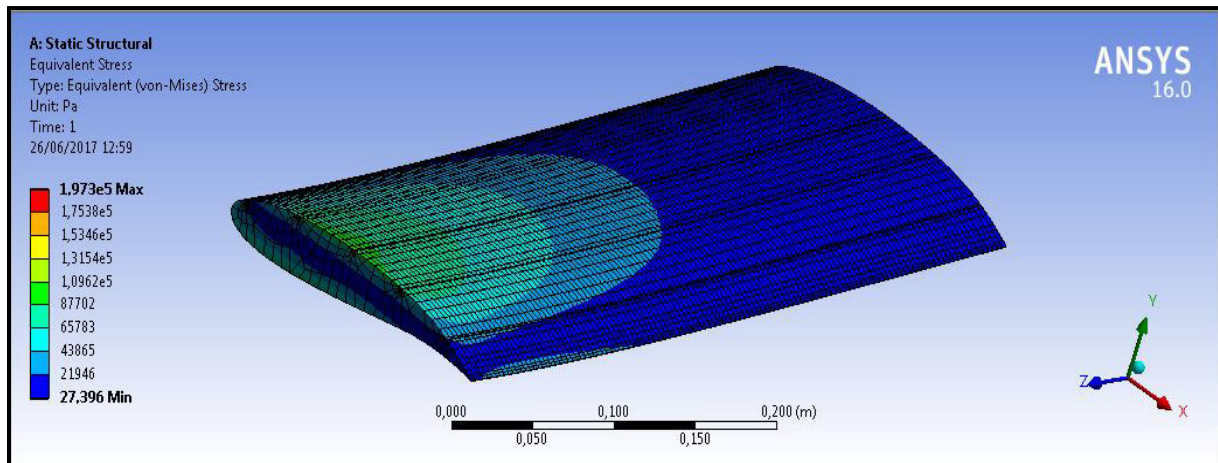
Figure III.23: represents the total deformation for different holes position done in the profile, where the five holes are applied in the high section of the fixed support as well the center of it and the lower section. The deformation in the low and the middle section is almost constant with a value of $1,8437 \cdot 10^{-6}$, then the deformation in the high position of the holes rises to reach the maximum value of $1,8438 \cdot 10^{-6}$.



Lowest position



Middle position.



Highest position.

Figure III.24: Equivalent Von Mises stress for the different position of Holes.

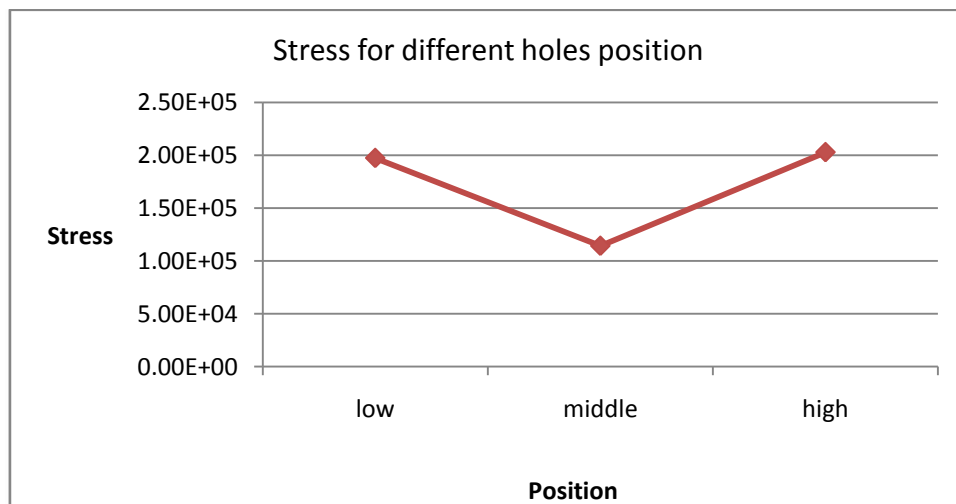


Figure III.24: Equivalent Von Mises **Stress** for holes position on the blade.

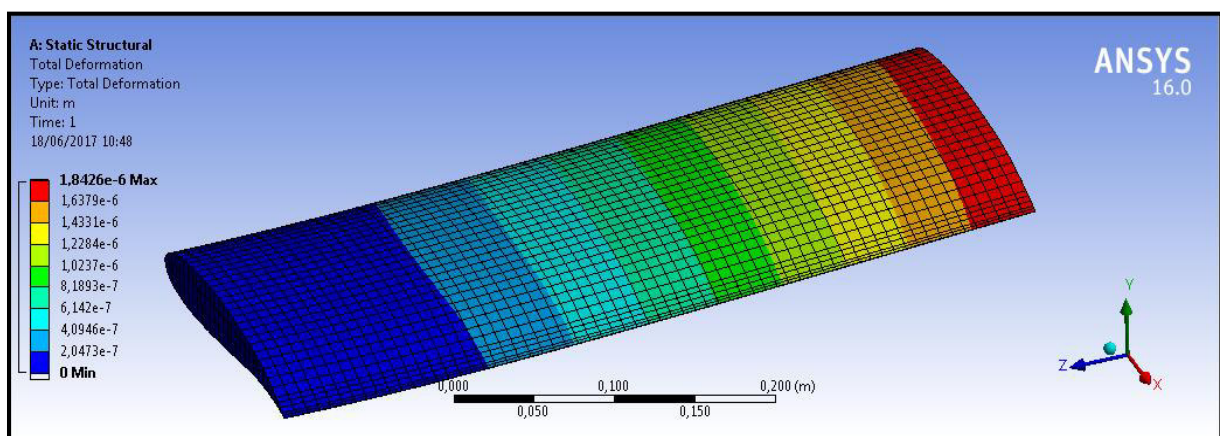
We can see from the **Figure III.24** the Equivalent Von-Mises Stress Values for different three holes position, the stress decreases from the lowest to the middle position with a significant value where it was $2,0279 \cdot 10^5$ MPa to reach the minimum value of $1,1428 \cdot 10^5$ MPa, then increases in the highest position of the holes to reach $1,973 \cdot 10^5$ MPa.

V.4 The effect of the blade materials:

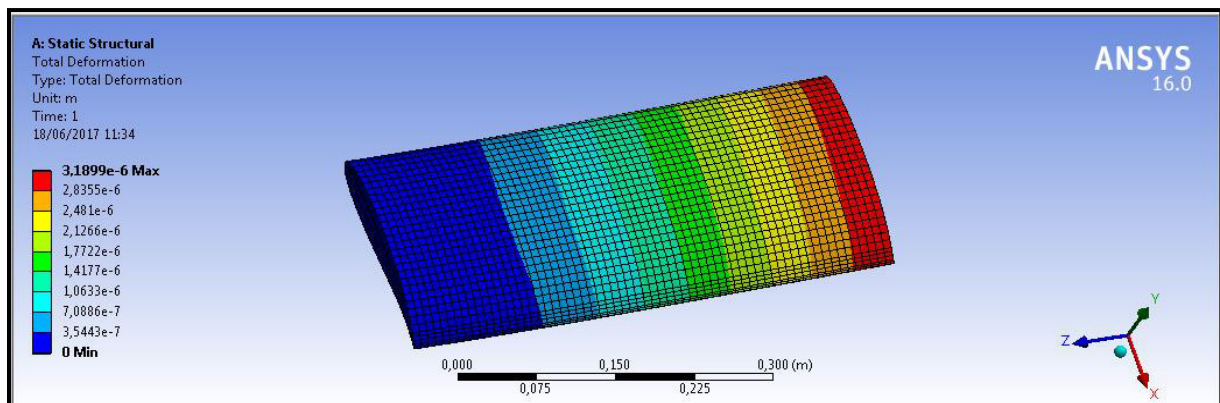
The table below shows the result analysis of the Structural steel, Aluminum Alloy and the Titanium Alloy for the holes done on the body and without them, the total deformation and the Equivalent Von Mises Stress results are shown for each case of Material used for this simulation:

Table III.10: Results of stress, deformation with different Materials.

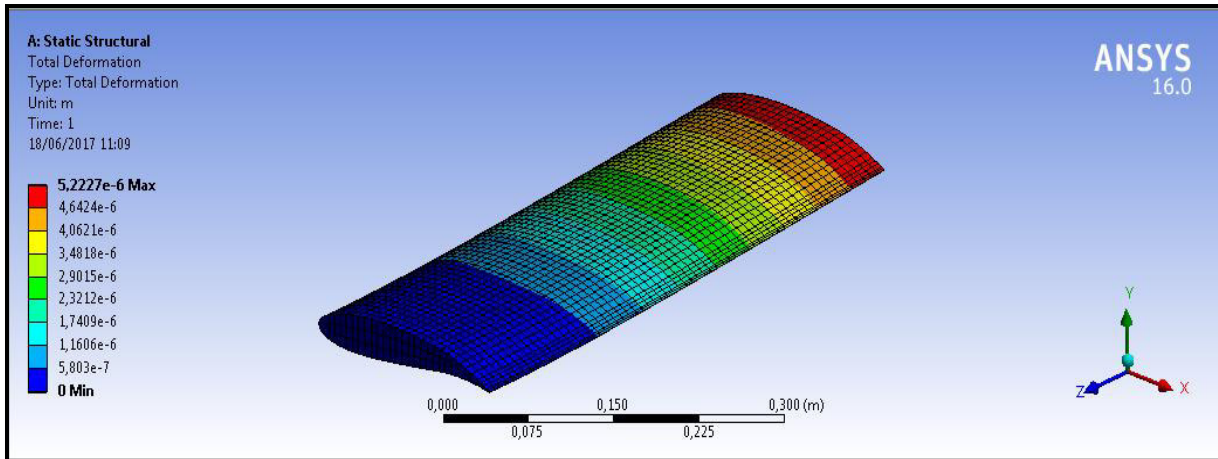
	Structural Steel		Aluminum Alloy		Titanium Alloy	
	With hole	Without hole	With hole	Without hole	With hole	Without hole
Deformation x(10⁻⁶)	1,8437	1,8426	5,2267	5,2227	3,1920	3,1899
Stress X(10⁵)	1,1428	1,0038	1,1616	1,0183	1,1529	1,0119



Steel.



Titanium Alloy.



Aluminum Alloy.

Figure III.25: Total deformation of the three materials Without Holes.

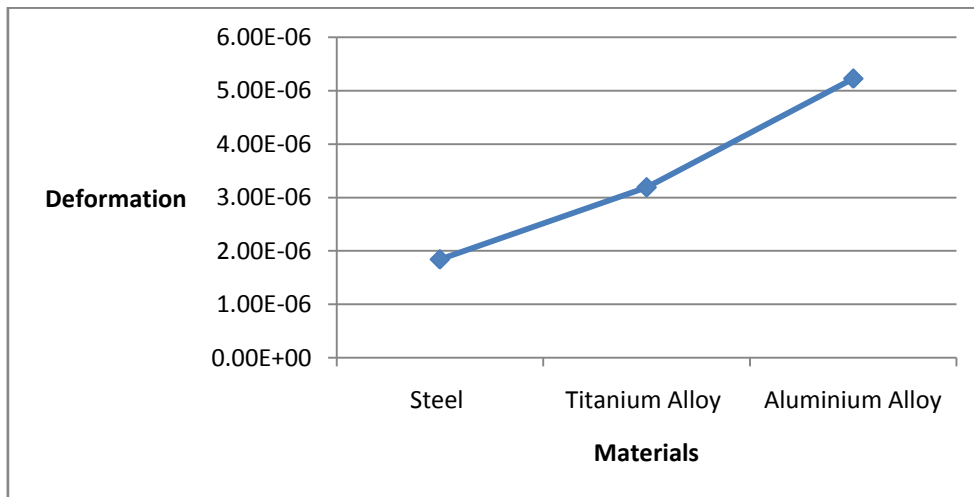
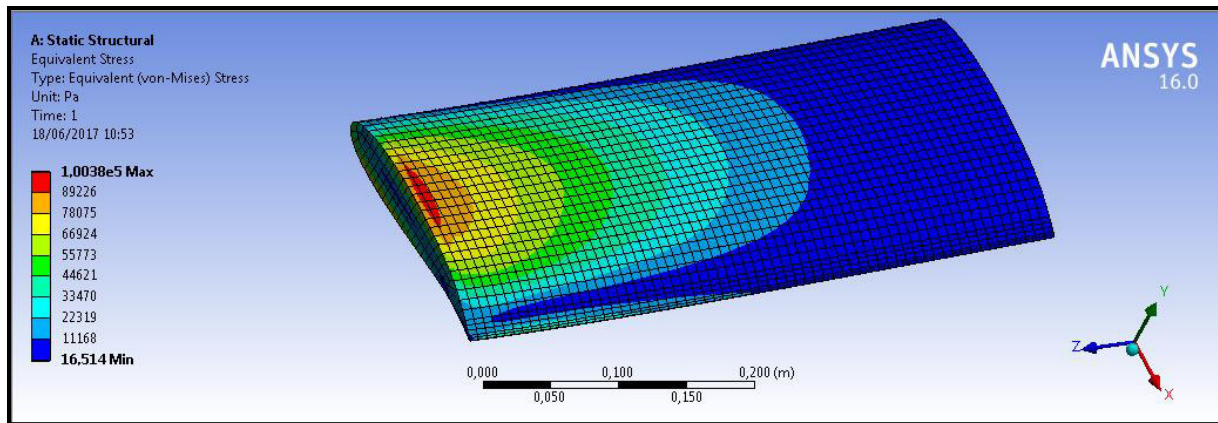
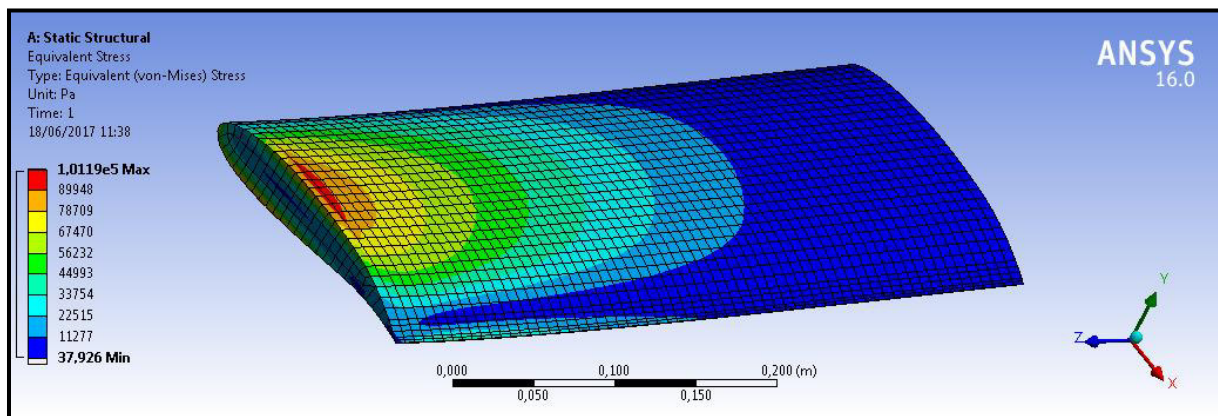


Figure III.26: Total deformation of the three materials Without Holes.

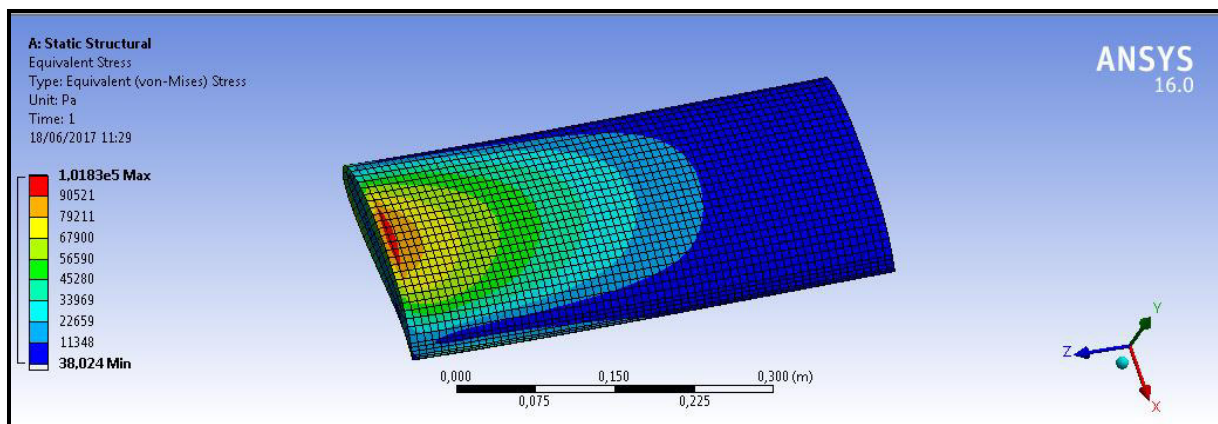
Figure III.26 shows that total deformation values varies with the variation of the Characteristics (density, Young modulus, Possion’s ratio) of each material we have without Any hole on the blade, where we see the minimum value of the deformation is for the Steel material, and for the maximal value reached is for Aluminum Alloy material.



steel.



Titanium alloy.



Aluminum Alloy.

Figure III.27: Equivalent Von Mises Stress of the Three Materials without Holes.

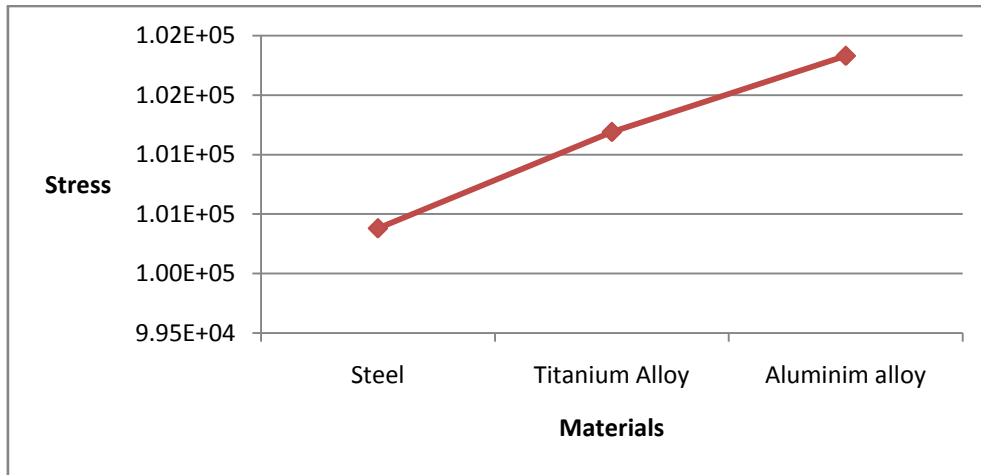


Figure III.28: Equivalent Von Mises Stress for the materials Without Holes.

Figure III.28 represents the Equivalent Von Mises Stress values with the different types the materials, we see that the Stress curve change with the characteristics of each material which the deformation depends on, where the Stress is minimal for the Steel then it goes up for the Titanium Alloy Material because of the resistance of this last is a little bit smaller then the steel, to reach the maximal value for Aluminum Alloy Material which is less resistant.

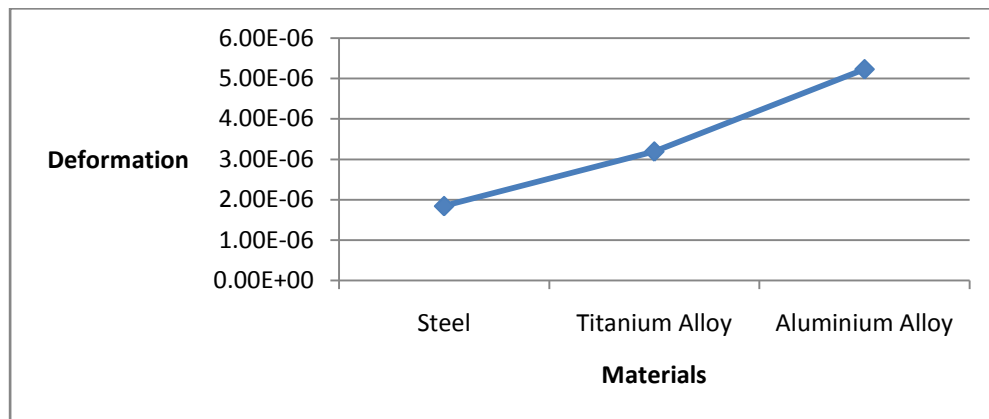


Figure III.29 Total deformation of the three Materials With holes.

Figure III.29 Illustrate the curve of the Total deformation values for the three types of materials With the five holes on the body, where it goes up from the minimum value for the Steel material to reach the maximal value for Aluminum Alloy Material because every material have its own characteristics and resistance and we see that the curve depends on those parameters.

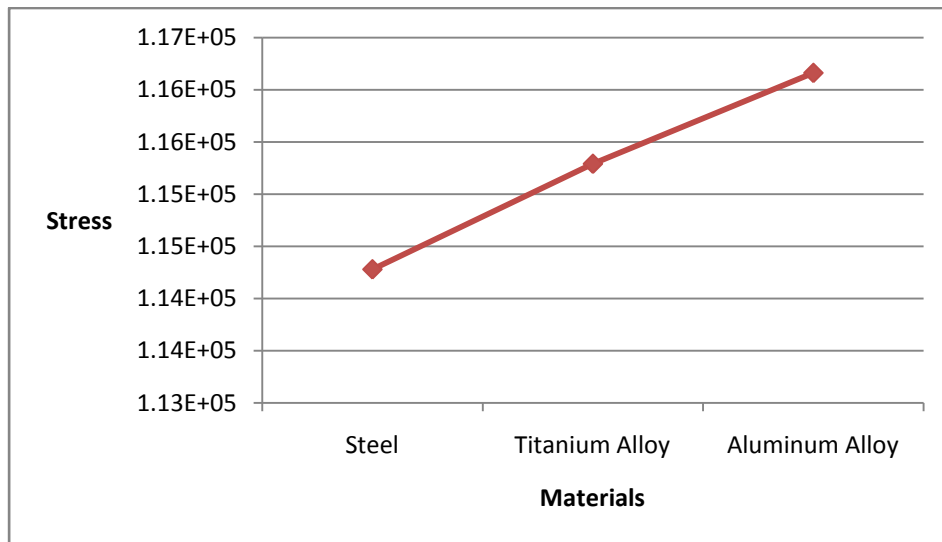
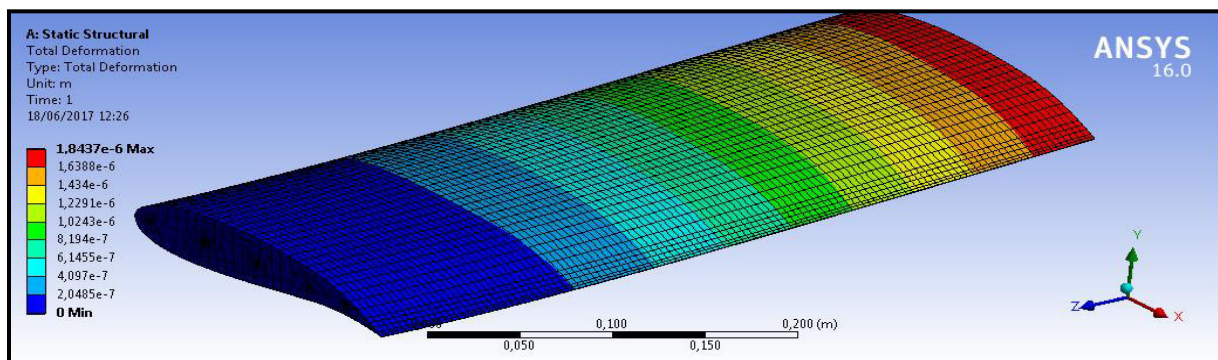
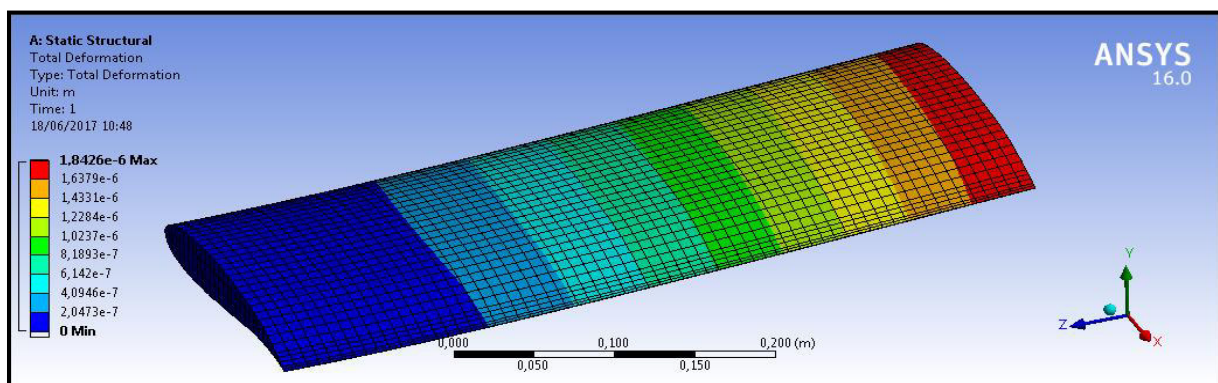


Figure III.30 Equivalent Stress of the three Materials With holes.

Figure III.30 Shows the curve of the Equivalent Von Mises Stress values according to the different characteristics of the three types of materials with the five holes on the Blade, where it goes up from the minimum value for the Steel material to reach the maximal value for Aluminum Alloy Material.



Five holes.



Without holes.

Figure III.31: Total deformation with and without the holes for the steel.

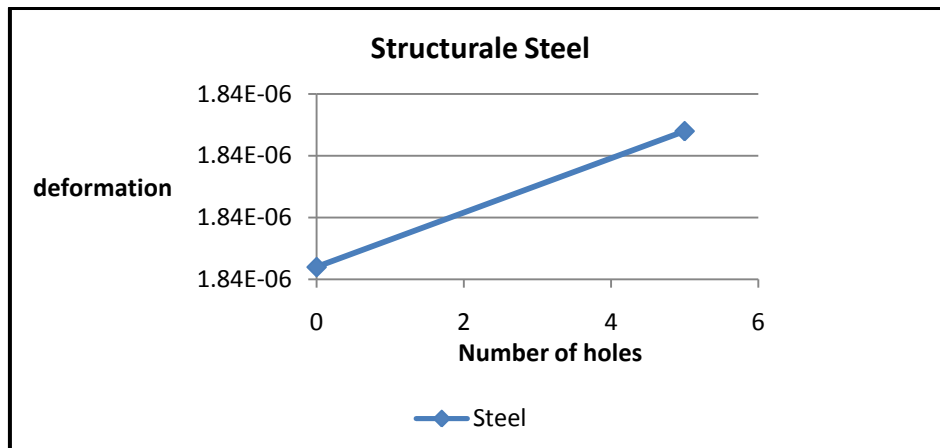
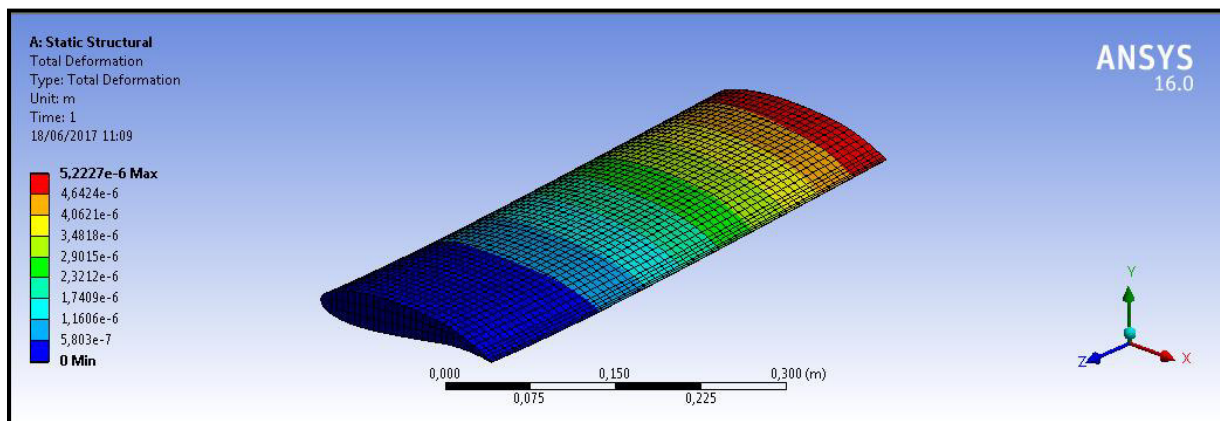
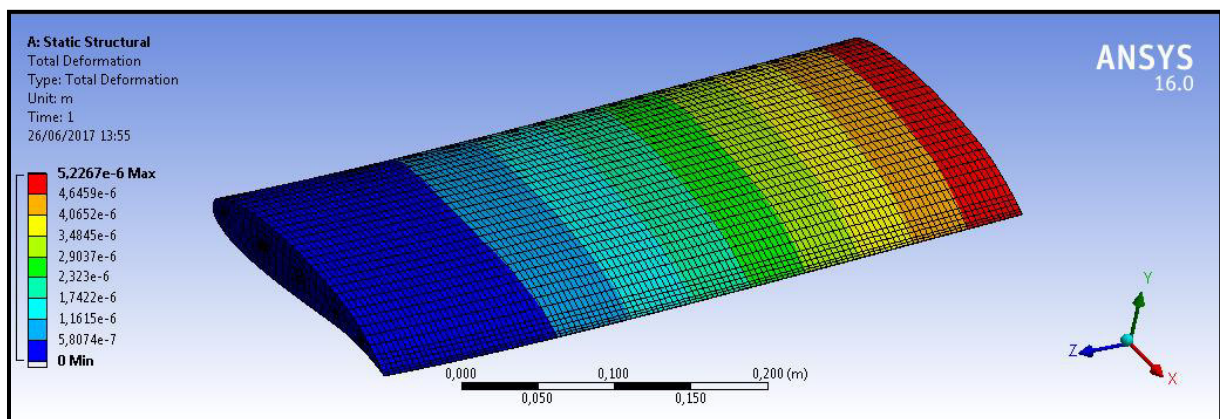


Figure III.32: Deformation for different number of holes of the structural steel.

The Figure III.32: shows the total deformation for the two different cases: with and without the five holes for the structural steel. As we can see that there is a proportional relationship between these two parameters. Where the deformation increases when the there is no holes on the profile from $1,8426 \cdot 10^{-6}$ Mpa to the maximum value of $1,8437 \cdot 10^{-6}$ Mpa for the five holes done on the body.



Without holes



Five holes

Figure III.33: Total deformation with and without holes for the Aluminum Alloy.

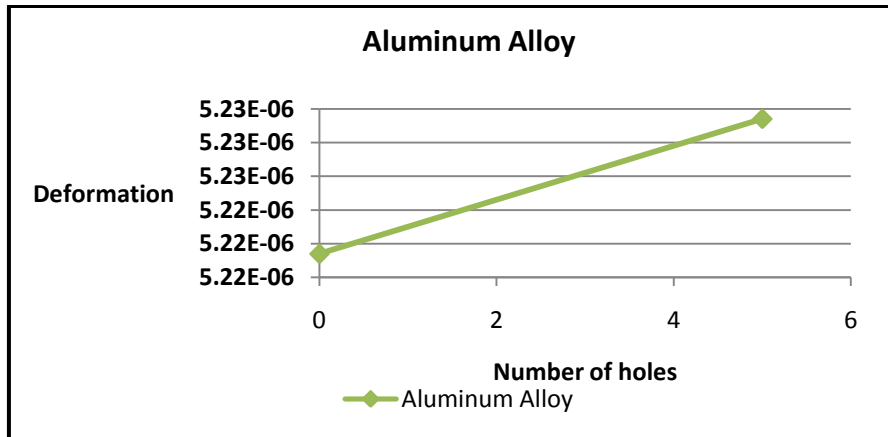
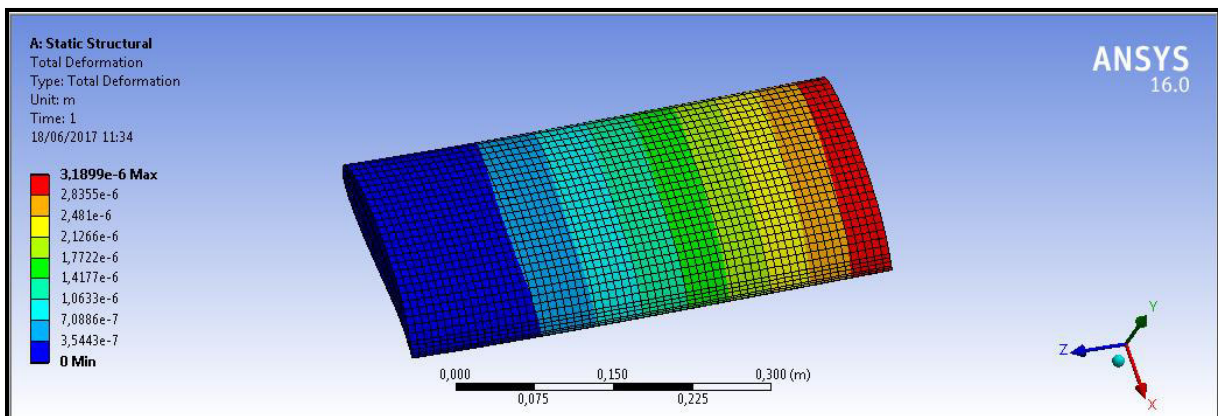
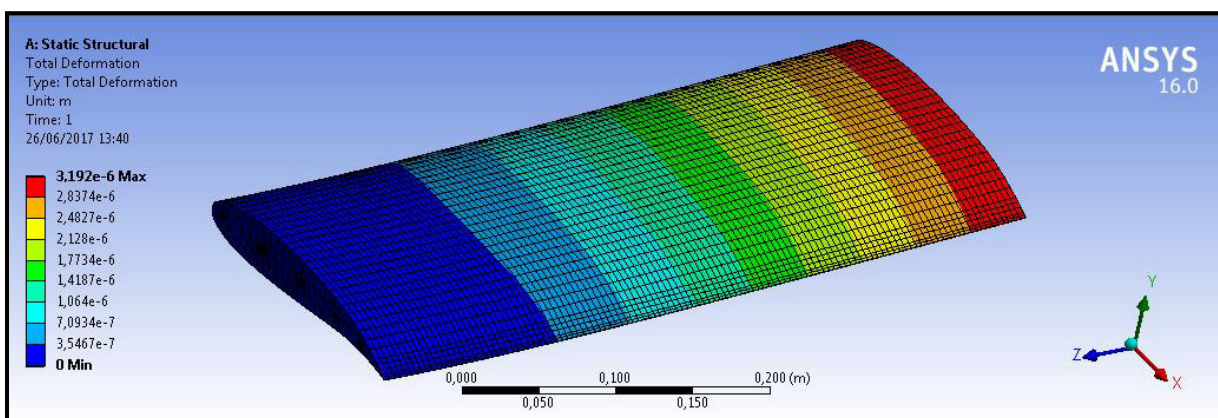


Figure III.34: deformation for different number of holes for the Aluminum Alloy.

Figure III.34: illustrates curve of the total deformation values according to the two cases which are: with and without the holes on the blade profile for the Aluminum Alloy material. We observe that in the case where there are no holes, the deformation value was smaller comparing to the case where there is five holes on the body. Where the curve goes up from the minimal value without holes to reach the maximal value with the holes.



Without holes



Five holes

Figure III.35: Total deformation with and without holes for the Titanium Alloy.

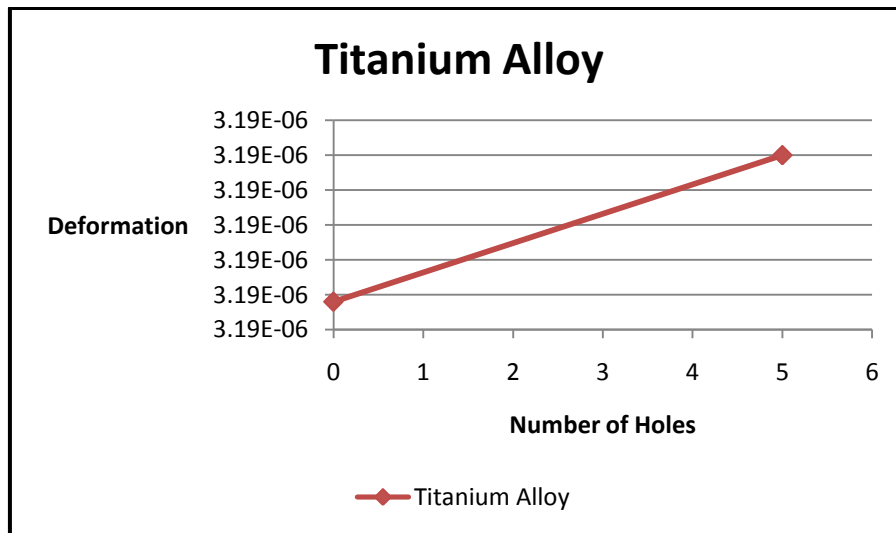


Figure III.36: Deformation for different number of holes of the Titanium Alloy.

Figure III.36 : illustrate the curve of the total deformations for the two cases we have (without and with the five holes) for the Titanium Alloy, we observe that the deformation increases from the first case linearly from $3,189.9 \cdot 10^{-6}$ where it was the minimum value to reach the maximum value of $3,192.0 \cdot 10^{-6}$ for the seconde case.

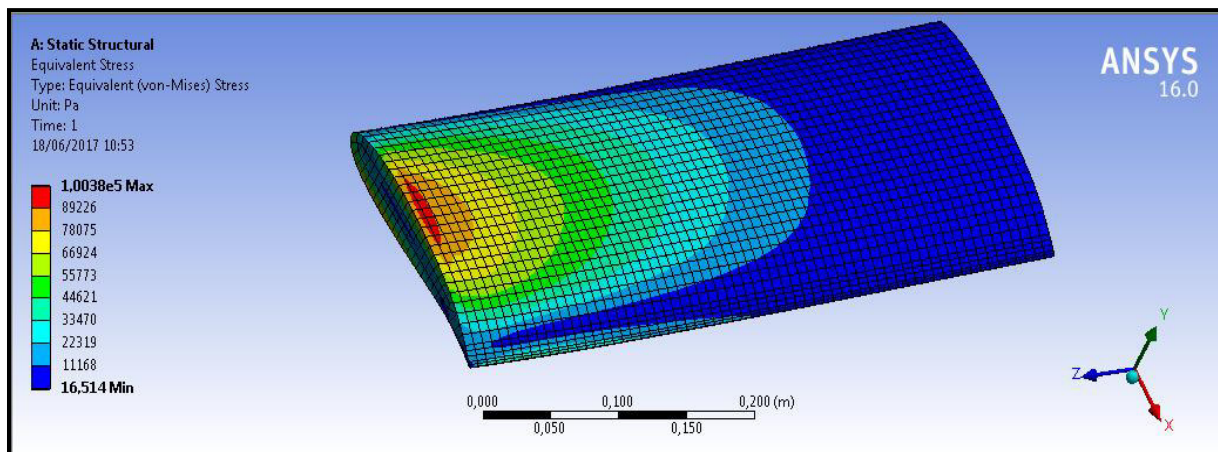


Figure III.37: Equivalent Von Mises Stress of the Steel.

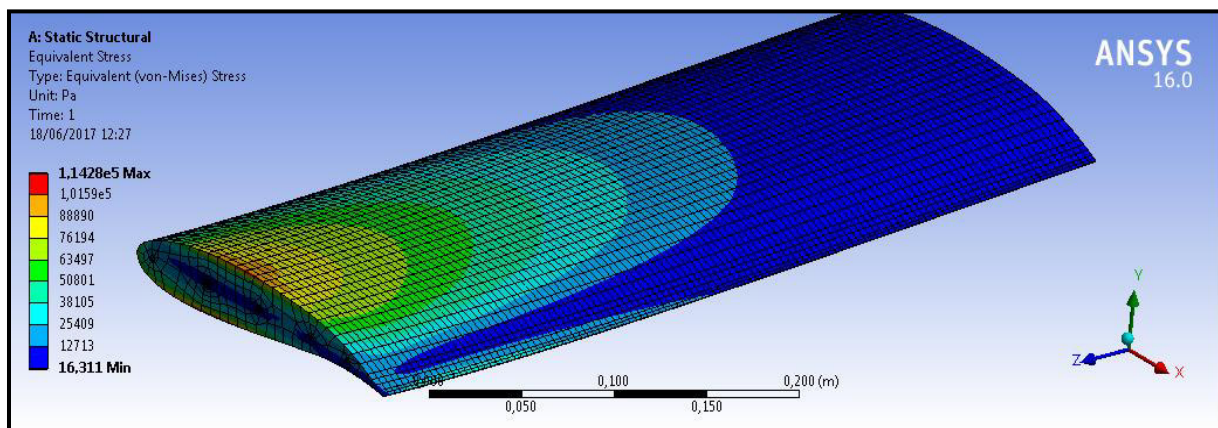


Figure III.38: Equivalent Von Mises Stress of the Steel with five holes.

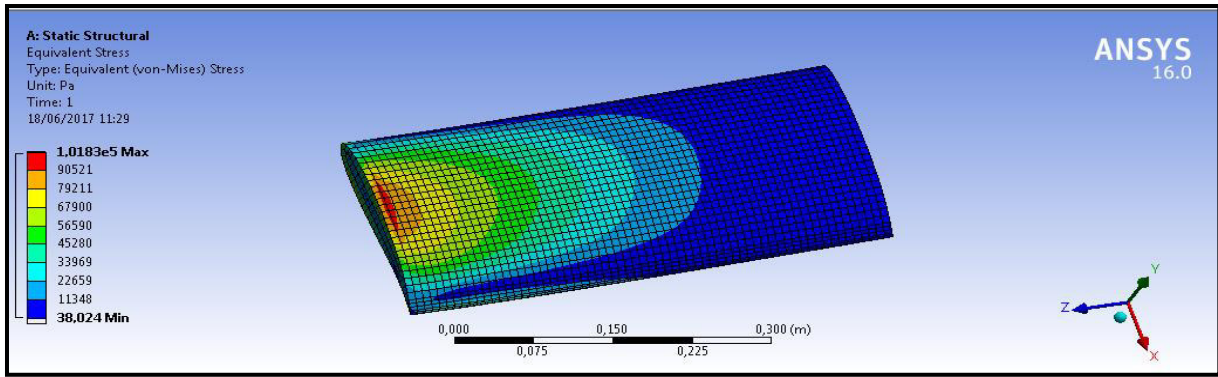


Figure III.39: Equivalent Von Mises Stress of the Aluminum Alloy without holes.

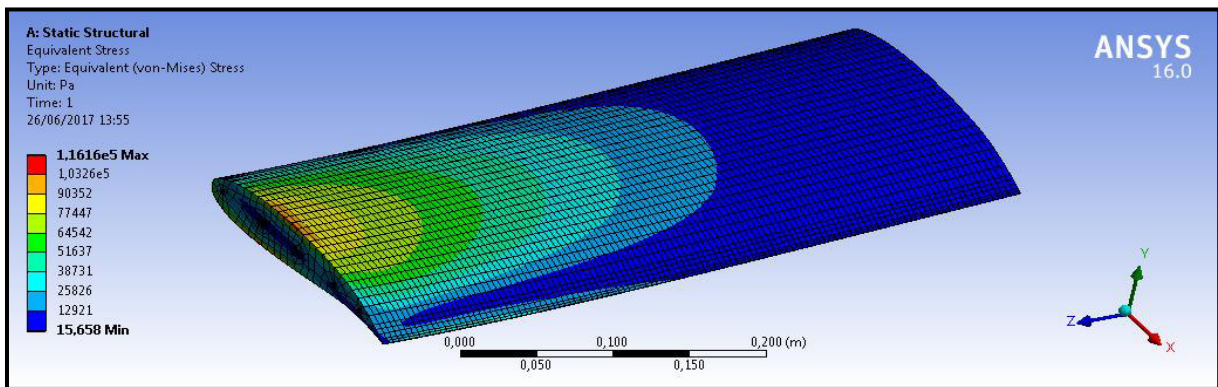


Figure III.40: Equivalent Von Mises Stress of the Aluminum Alloy with five holes.

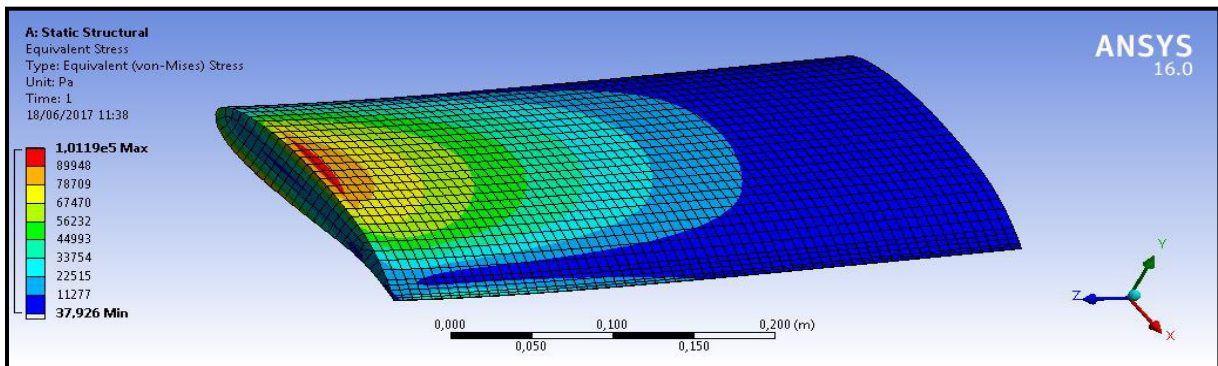


Figure III.41: Equivalent Von Mises Stress of the Titanium Alloy without holes.

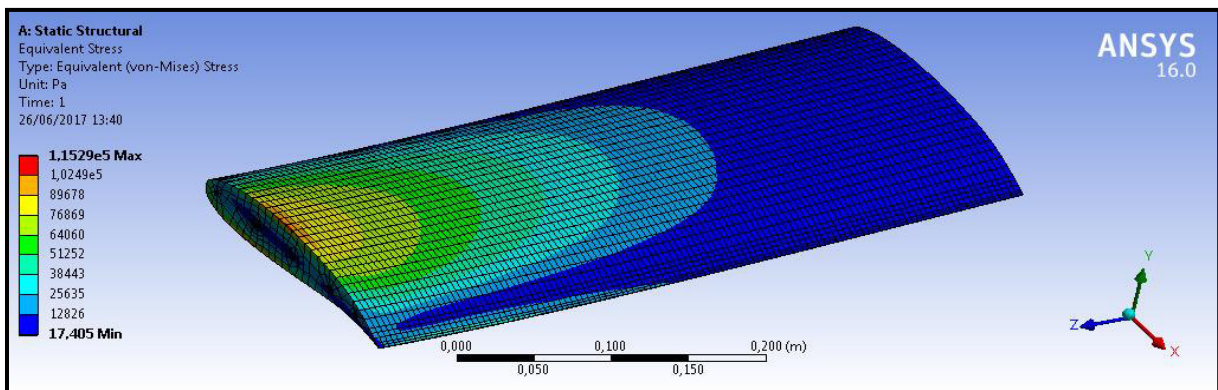


Figure III.42: Equivalent Von Mises Stress of the Titanium Alloy with five holes.

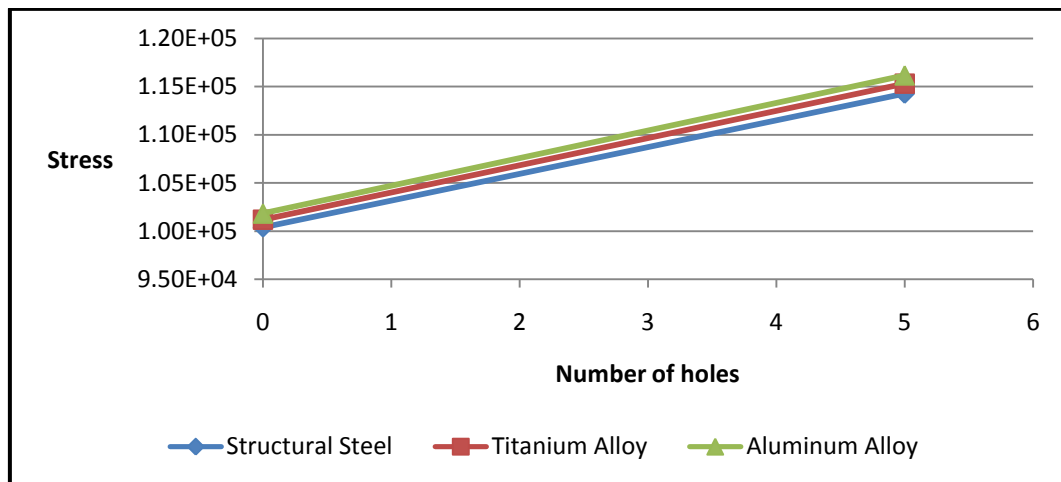


Figure III.43: Stress for different number of holes for each Material.

We see in this curve of the **Figure III.43** the stress results of every material we used in the simulation with and without holes to see any changes, for the Equivalent Von Mises Stress in the case of the body with holes we see that the Aluminum Alloy has the maximum stress value comparing to other two materials, and for the second case where there is no hole on the profile we notice that Aluminum Alloy has also the Maximum value.

The smallest value of the stress we found is in the Structural Steel whether for case of holes or without them

We notice that the total deformation varies on each Material where the smallest deformation value is found in the Structural steel comparing to Titanium Alloy values, and the maximum deformation reached is found in the Aluminum Alloy.

So the best material and the more resistant material for this simulation to use is the STRUCTURAL STEEL.

Conclusion:

In this chapter, we have seen a numerical simulation of 3D compressor blade with different Structural materials and holes number and diameter along the profile, this simulation was done by ANSYS 16.0 software (Static structural Tool)

We had concluded that the response of the materials varies from a material to another with a specific total deformation and Equivalent Von Mises stress values, the less deformation value is smaller for a material with holes around the profile is much better for functioning from that which hasn't holes on the body because of its resistance against the external factors.

General Conclusion

Conclusion

After drawing the geometry, with GAMBIT software, of the NACA 65 10% airfoil commonly used in the compressors we did some simulations with ANSYS FLUENT software to obtain the values of the aerodynamic coefficients and to calculate the resultant aerodynamic force acting on the compressor blade.

We have also drawn the geometry of the same profile but this time with some holes which allowed the blade cooling.

By using ANSYS software we could evaluate the blade response to the aerodynamic forces for the two cases with and without blade cooling. The blade response was represented by the total deformation and the equivalent Von-Mises stress supported by the blade.

From the obtained results we noted that the material removal due to the film cooling system had an influence on the blade strength. The total deformation and the equivalent Von-Mises stress are more important when the blade is cooled. We found also that those two parameters are affected by the variation of the holes characteristics as the number and the diameter. When the number or the diameter increased the total deformation and the Von-Mises stress became more important. We also noted that these parameters are sensible to the position of the holes. We found that the total deformation and the Von-Mises stress were less important when the holes were located in the middle of the profile and they were the same when the holes are located in the lower or in the upper of the profile.

Relatively to the blade material used in our simulations we found that every material has its own behavior and response when it's exposed to the aerodynamic forces, so the total deformation and the equivalent Von-Mises stress values change from a material to another. We also noted that steel was the material which corresponded to a total deformation and an equivalent Von-Mises stress less important.

Finally we can say that further improvements and new techniques may become feasible as materials and systems integration.

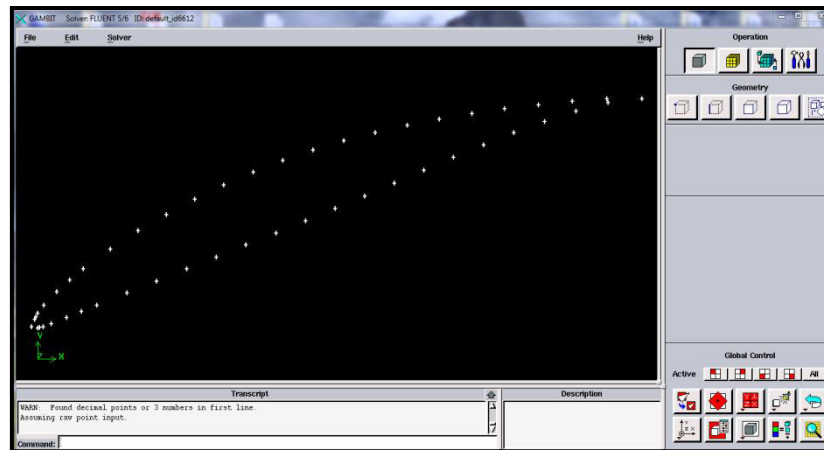
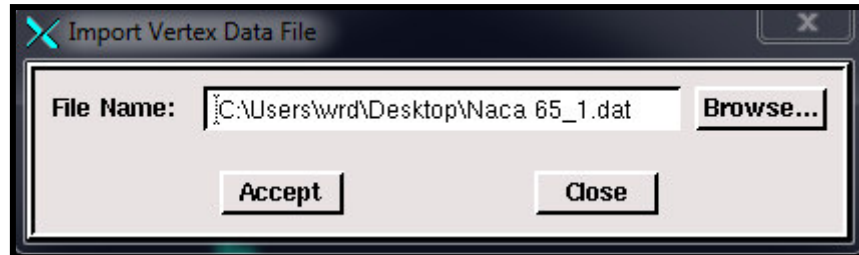
Appendix

Appendix 1: 2D geometry creation steps in gambit.

1) Single compressor blade :

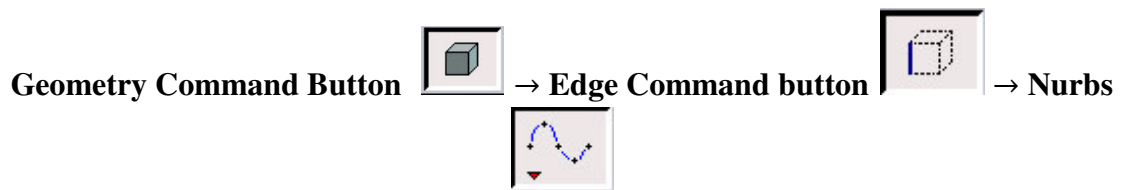
- **Import the data file :**

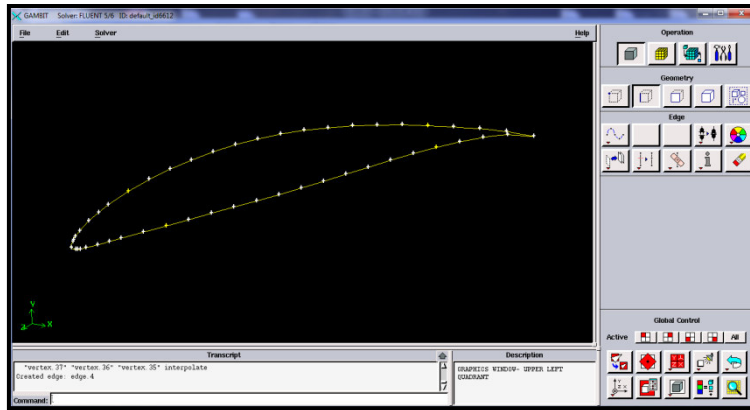
Main menu → File → Import → vertex data



- **Create edges :**

Four edges are created on the blade geometry.

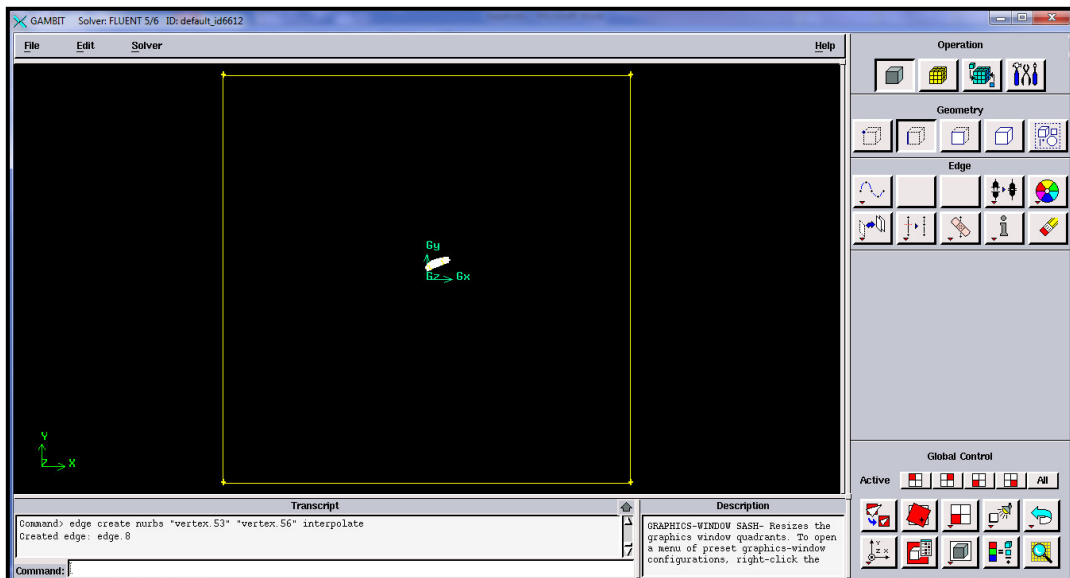




- **Creating the fluid zone :**

We create a square around the compressor blade that we created previously. To create it we have to use the measures below:

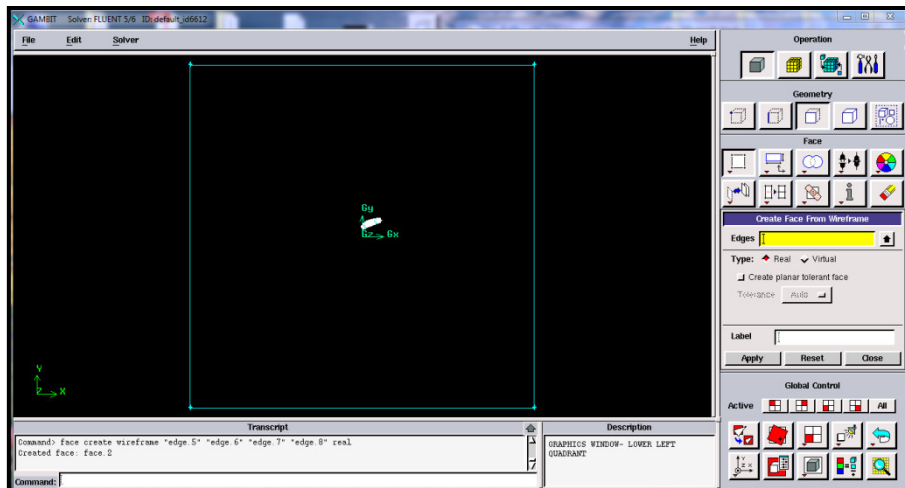
Vertex (Label)	X (cm)	Y (cm)
A	2.1	-2.1
B	2.1	2.1
C	-2.1	2.1
D	-2.1	-2.1



- **Creating the faces :**

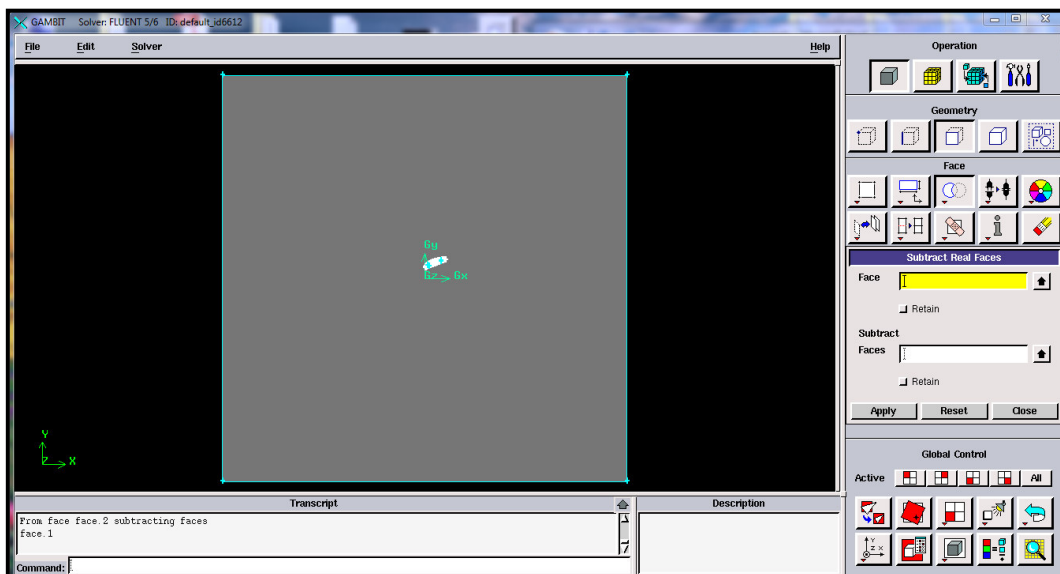
Two faces are created **the blade** and **the fluid zone** (the square):





- **Subtract the blade from the fluid :**

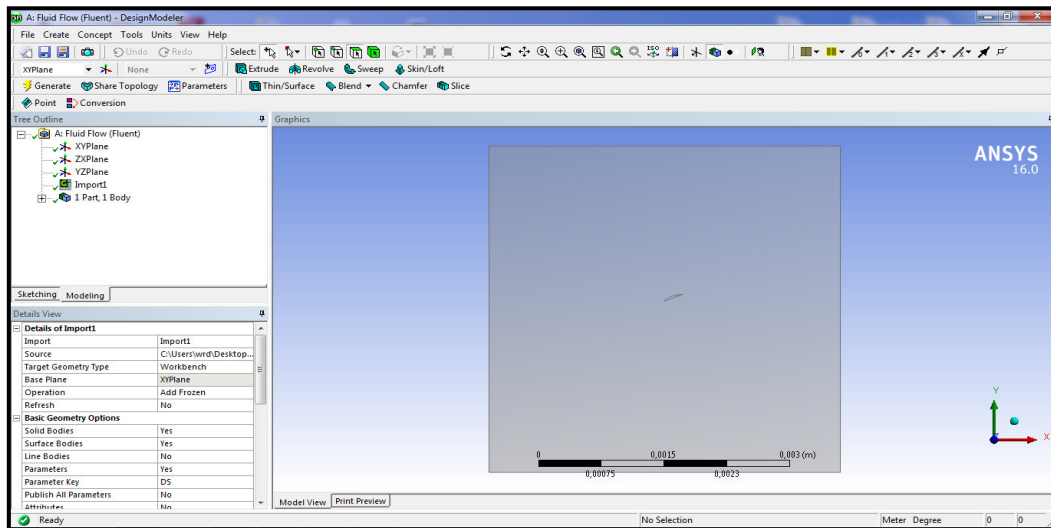
- **Geometry**  → **Face** command button  → **Subtract faces** 



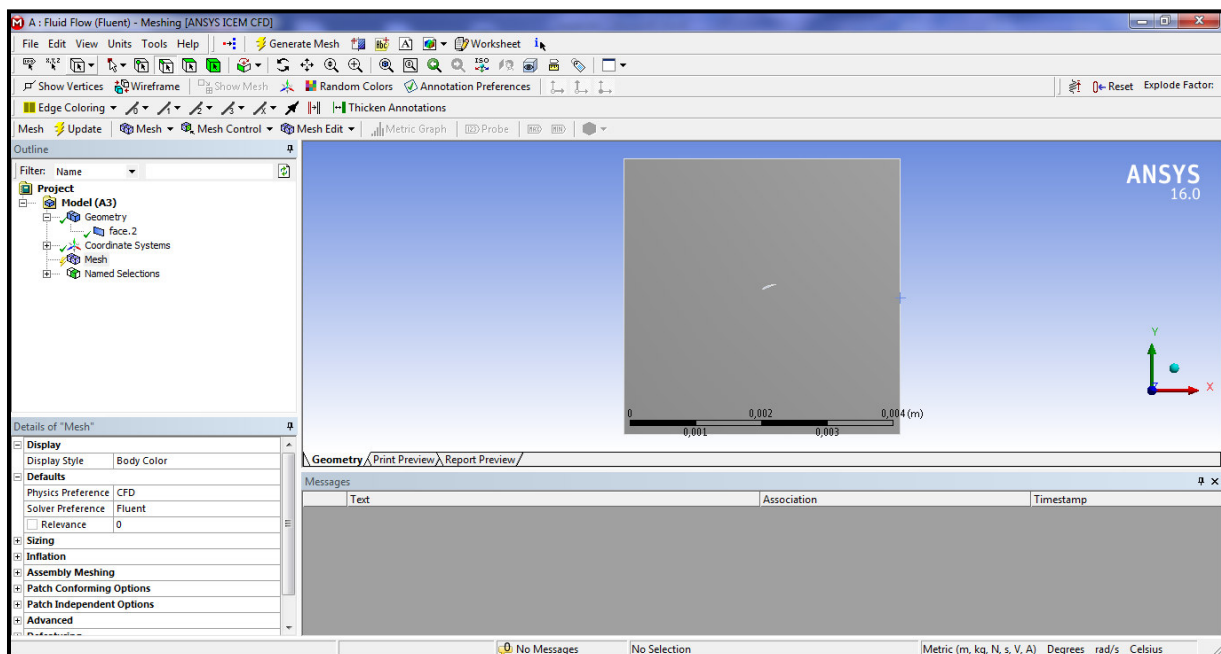
Appendix 2: Fluent steps of work

- **Importing the geometry file :**
- After we've done from the geometry that we did with the Gambit software now we import the Gambit file to ansys Fluent in the Geometry section.

File → import external geometry file → choose the file → Generate



- Now we go to the mesh part of the fluid flow (fluent)



- **Meshing in Fluent steps :**

First of all we name the edges of the fluid zone.

Edge  → Right click on the mouse → create named selection.

Edge	Name
Left	Inlet
Right	Outlet
Above	Upper Wall
Under	Lower Wall

- And we name the airfoil that we have in the fluid zone : **Airfoil**

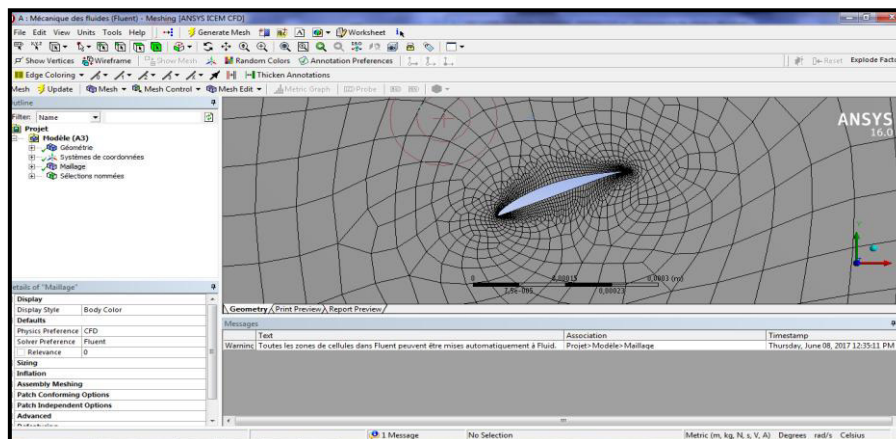
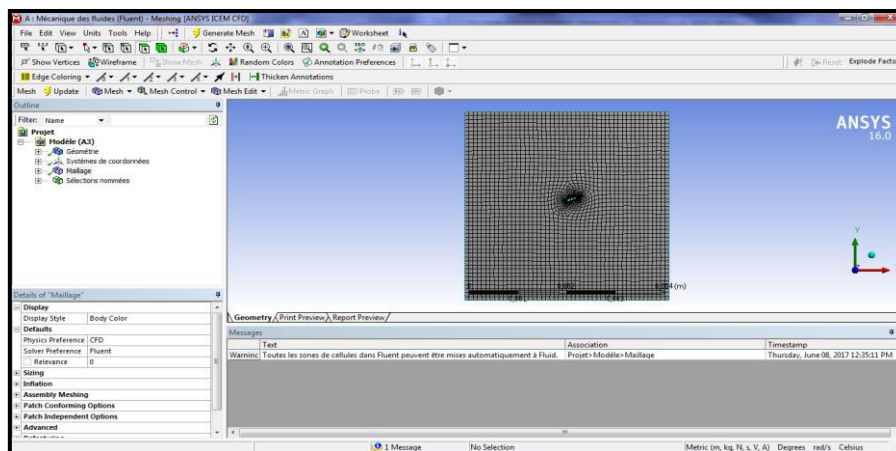
After naming the Edges we have to select an option in the mesh part:

Go to Mesh → Sizing → Relevance center → Fine

Then we go to mesh again to choose refinement to mesh our geometry:

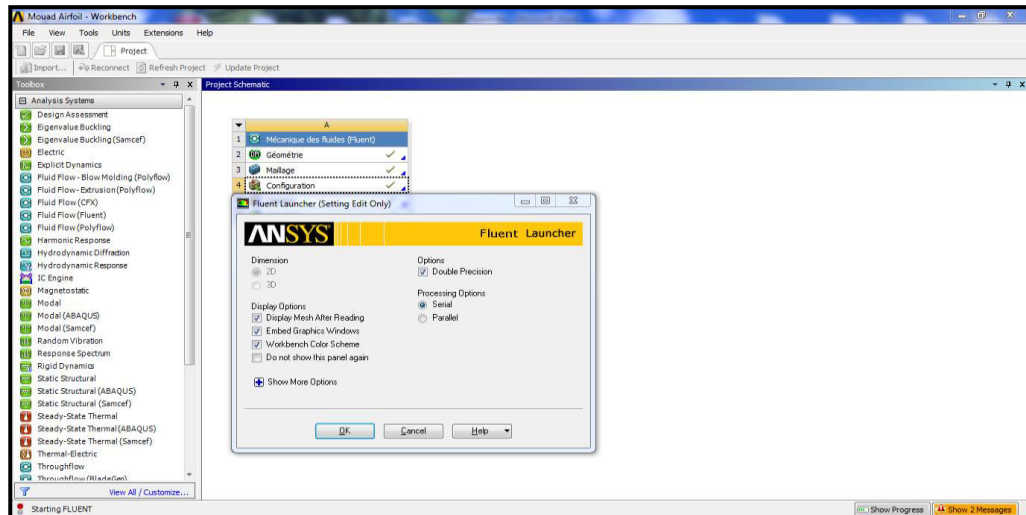
Go to Mesh → Insert → Refinement → CTRL + the shape of the airfoil → generate Mesh.

- The meshing will look like this :



- **Flow properties :**

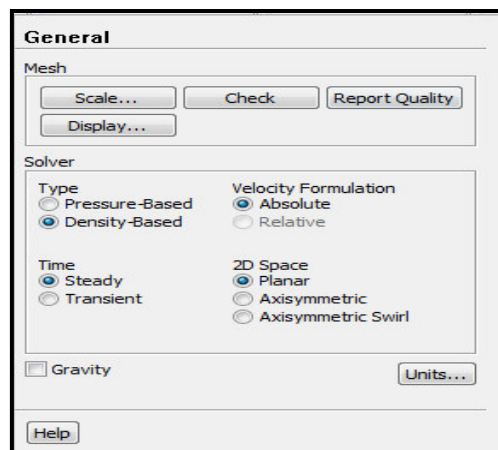
We go to configuration in the workbench to configurate our flow around the blade. In ther Fluent launcher we select the **Double precision**.



- ✓ **Flow type :**

As it is known that the flow around the blade that we have is a time independent flow we must select the steady form:

General → Type: Density based.

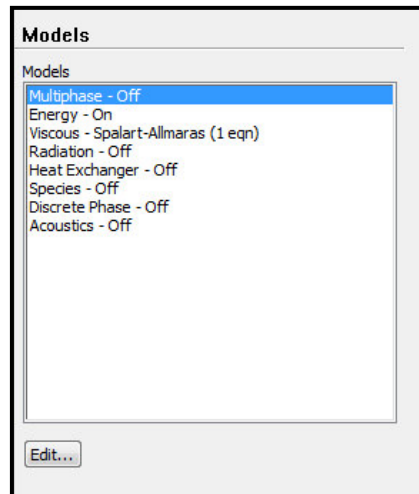


- ✓ **Flow characteristics :**

In the compressor, the environment is viscous:

Models → Energy → ON

Models → viscous → spamlart – Allmaras (1eqn)



✓ **Flow Material property :**

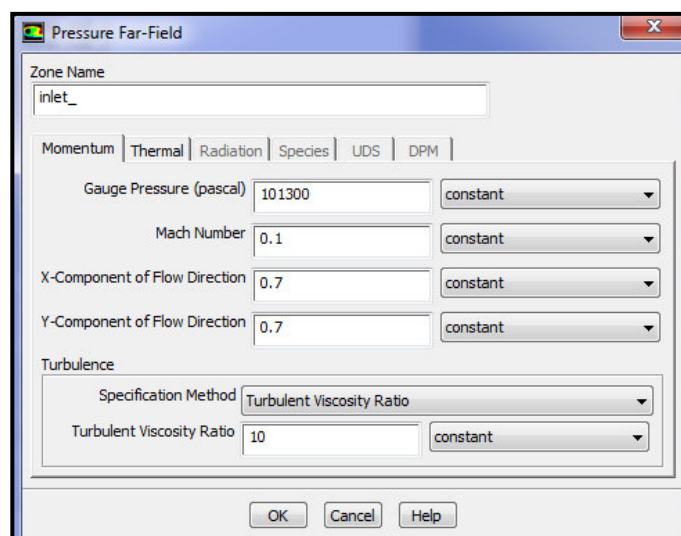
The fluid inside the compressor is the air and the air is taking as an ideal gas :

Materials → fluid →air →density →ideal gas

• **Boundary conditions**

✓ **Inlet :**

- Gauge pressure : Atmospheric pressure **101300 Pa**
- Mach number : [0,1.0,2.0,3.0,4.0,5.0,6.0,7.0,8.0,9]
- **X component of flow direction : cos (angle of attack)**
- **Y component of flow direction : sin (angle of attack)**



✓ **Outlet :**

- Gauge pressure : **121560 Pa (Determined by taking a compression ratio of 1.2)**
-

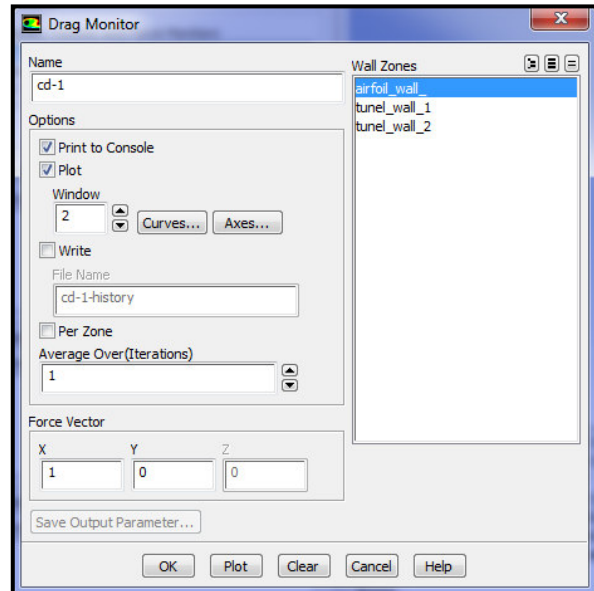
- Turbulence specification method: **Intensity and hydraulic diameter.**
- **Monitor :**

In order to display of the lift, drag and moment historic results, we proceed as the following:

Monitor → Create $\left\{ \begin{array}{l} \text{Lift} \\ \text{Drag} \end{array} \right.$

Then for each one we enable the sub-option :

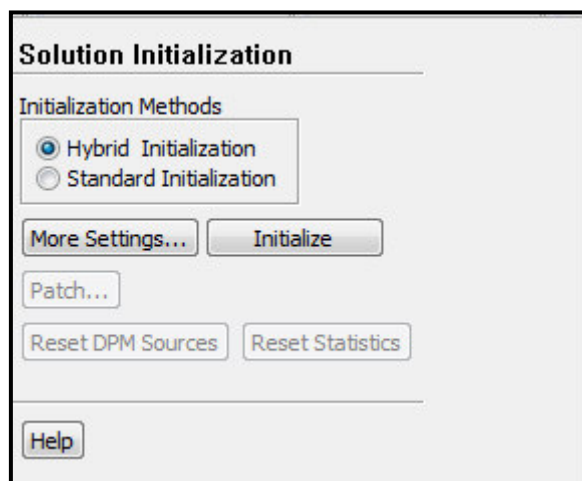
- ✓ Print to consol
- ✓ Plot
- ✓ Write
- ✓ Per zone (in the case of compressor cascade)



- **Solution initialization :**

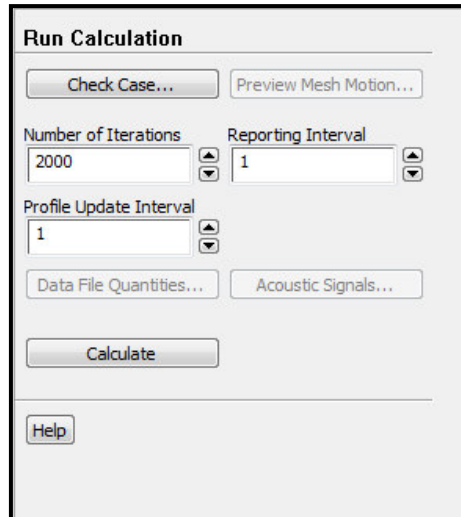
Before the start of every simulation we must initialize the solution from the inlet conditions.

Solution initialization → standard initialization → compute from → inlet → initialize



- **Run the calculation :**

Finally we launch the calculation by clicking on Run calculation options and we set Number of iterations to 2000 for example:



- After completing the calculation we notice that all the solutions are in the window of solutions where we find the coefficients of Drag and lift when **the solution is converged**.

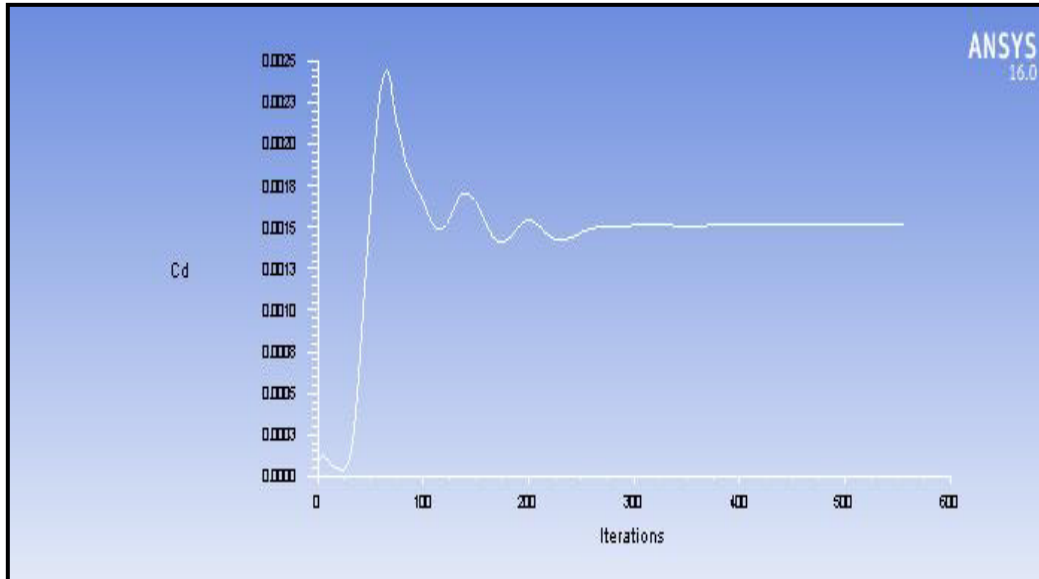


Figure: Fluent Convergence history

References

- [1] Dr. Douglas E. Wolfe, Jet Engines and Thermal Barrier Coatings, 2003, p 73-80.
- [2] Safran Reveals New Turboprop Efforts. Aviation week. 1 May 2013. Retrieved 4 August 2013.
- [3] Pratt and Whitney. Aerobuzz.fr 24 January 2012. Retrieved 4 August 2013.
- [4] Anderson J D (2001). Fundamentals of aerodynamics, McGraw-Hill New York Vol 2.
- [5] Brophy C M, Turbulence Management and flow qualification of the Pennsylvania (1994).
- [6] Bleier F P, Fan handbook : selection, application and design McGraw-Hill ,1998.
- [7] The Jet Engine, Rolls Royce 1986.
- [8] Energy management series 14 for industry commerce and institutions compressors and turbines.
- [9] Burton T, Sharpe D et Al.(2001). Wind energy handbook, closed-loop control : issues and objectives, 2nd Edn, John Wiley & Sons, Ltd, UK, 478.
- [10] KLM technology Group, Practical engineering Guidelines for processing Plant Solutions, Rev 02 By: Viska Mulyandasari (2011.)
- [11] Process Technology Equipment Chapter 7.
- [12] Helicopter aerodynamic, Paul Cantrell.
- [13] The NACA airfoil series PDF.
- [14] IJETAE Exploring Research and Innovations, International Journal of Emerging Technology and Advanced Engineering, Vol 4, Octobre 2014, Sisir Sagar & Sarath Chandra.
- [15] Fluid Mechanics and Thermodynamics of Turbomachinery by Sydney Lawrence Dixon.
- [16] Article 9 in the website [www. totalmateria. com](http://www.totalmateria.com), March 2001.
- [17] Research Memorandum, Altitude performance characteristics of the GE J-79 Turbojet engine By Carl E Campbell and E. William, Lewis flight propulsion laboratory.
- [18] CIVE 1400: Fluid Mechanics Fluid Dynamics: The Momentum and Bernoulli Equations
- [19] 2016 hydrodynamics by Prof. A.H. Techet.
- [20] Fluids – Lecture 3 MIT by Anderson.
- [21] Airfoil Film cooling PDF, David G. Bogard Mechanical Engineering Department University of Texas at Austin.

References

[22] Innovative gas turbine cooling techniques R.S. Bunker, GE Global Research Center, USA.

[23] Doctor of the National school superior Mechanical and of aerotechnics of Poitiers, Daniel THIBAULT.